THE FIRST ORTHOTROPIC SUSPENSION BRIDGE IN NORTH AMERICA

Hon-Keung Wan

A DISSERTATION

IN THE

FACULTY OF ENGINEERING

Presented in Partial Fulfilment of the Requirements for the

Degree of MASTER OF ENGINEERING

at

Sir George Williams University

Montreal, Canada

September, 1972

SIR   GEORGE   WILLIAMS   UNIVERSITY

FACULTY OF ENGINEERING

GRADUATE STUDIES

DISSERTATION

This is to certify that the Dissertation prepared

By _____Hon-Keung Wan_____

Entitled "The first Orthotropic Suspension Bridge in North America"_____

Complies with the regulations of this University and meets the
accepted standards with respect to originality and quality.

For the degree of:

_____Master of Engineering_____

Signed by the examining committee:

_____ Supervisor

_____

_____

_____

_____

Approved, for and on behalf of the Dean of Engineering

_____

Secretary for Engineering Graduate Studies

ABSTRACT

HON KEUNG WAN

THE FIRST ORTHOTROPIC SUSPENSION BRIDGE IN NORTH AMERICA

In the past few decades, considerable progress has been made in the design of long span suspension bridges. With the objective of providing more technical information in the area, the details of design and construction of the A. Murray MacKay Suspension Bridge, built in Halifax in 1970 are covered comprehensively in this report.

This is the first time that a full orthotropic deck truss suspension bridge has been used on this continent. The orthotropic deck acts as the top lateral system and in combination with the stiffening truss and bottom laterals forms a box system. This combination provides high torsional stiffness as well as favourable aerodynamic characteristics.

The behaviour of this bridge under wind action during construction and after completion has been proved satisfactory by wind tunnel tests. A chapter in this report presents the findings of aerodynamic studies made on a full model of the entire bridge under both smooth and turbulent flows, as well as the section model tests.

TO MY PARENTS

ACKNOWLEDGEMENTS

CONTENTS

LIST OF TABLES

LIST OF FIGURES

NOTATIONS 1

The following notations were used in the orthotropic deck and floor truss design[4] in section 7.3

A — area enclosed by one closed rib (in^2)

a — spacing of open ribs; top width of closed ribs

a_o — effective width of plate acting with one open rib, computed under an assumption of equal loading of all ribs

a_o+e_o — effective width of plate acting with one closed rib, computed under an assumption of equal loading of all ribs

D_x, D_y — flexural rigidity of the orthotropic plate in the x- or y-direction, respectively

E — $\doteq 29 \times 10^6$ psi = modulus of elasticity of steel in tension or compression

e — width of deck plate between two closed ribs

F_m — reaction at support m of a continuous beam on rigid supports

F_o — reaction at support m = 0 of a continuous beam on rigid supports; load on floor beam m = 0 due to one lane loaded, computed under an assumption of rigid floor beams

G — $= \dfrac{E}{2(1+\nu)} \doteq 11.2 \times 10^6$ psi = modulus of elasticity of steel in shear

$2g$ — width in the direction perpendicular to ribs of an uniformly distributed wheel load

H — torsional rigidity; effective torsional rigidity of the orthotropic plate representing the actual steel deck

I_F, I_R — moment of inertia of a floor beam, or a rib, respectively, computed with the appropriate effective width of the deck plate

K	section property characterizing torsional resistance
l	floor beam span
l_1	effective floor beam span
M	bending moment (k-in or k-ft); bending moment in the ortho-tropic plate per unit width (k-in/in)
M_c, M_s	benging moment at midspan or at support, respectively, of a continuous beam (k-in or k-ft); bending moment at midspan or at support, respectively, of a continuous orthortopic plate per unit width (k-in/in)
M_R, M_F	bending moment acting on one rib, or one floor beam, respectively
$\Delta M_R, \Delta M_F$	bending moment correction in a rib or a floor beam, respectively, due to floor beam flexibility
P	load; wheel load
p	uniformly distributed load (k/in^2)
Q_o	$= \dfrac{P}{2g}$ = load on deck per unit length in the x-direction of bridge (k/in)
r	radius of gyration
S	section modulus
s	≈ 15 ft. 10 in. = spacing of floor beams
s_o	effective width of plate acting with one floor beam
s_1	$= 0.7\, s$ = effective span of longitudinal ribs, used in computation of a_o
s_2	$= 0.81\, s$ = effective span of longitudinal ribs, used in computation of H
s^x	effective spacing of unequally loaded floor beams
t_p, t_R	thickness of deck plate or rib plate, respectively

u   developed width of one rib plate (in.)

x   ordinate in the transverse direction of bridge

y   ordinate in the longitudinal direction of bridge; distance
along the rib to the nearest support with a smaller number m

z   vertical ordinate; one-half of the wheel spacing in an axle

γ coefficient characterizing the relative flexural rigidity of
the ribs and the floor beams

$\bar{\eta}_{im}$ influence ordinate at support m, for the bending moment at
point i under consideration, of a continuous beam on elastic
supports

$\bar{\eta}_{om}, \bar{\eta}_o$ influence ordinate at support m for reaction F_o at support
m = 0 of a continuous beam on elastic support

μ reduction coefficient, used in determination of the effective
torsional rigidity, H

γ =0.3= Poisson's ratio for steel

NOTATIONS 2

The following notations were used in stiffening truss, main cable and bottom lateral design[7] in sections 7.4; 7.5; and 7.7

EI $=16.465 \times 10^7$ k-ft^2 = bending rigidity of one stiffening truss at main span

EI_1 $=15.217 \times 10^7$ k-ft^2 = bending rigidity of one stiffening truss at side span

F force in each diagonal member of bottom lateral

f $=128$ ft. = cable sag at main span

f_1 $=17.24$ ft. = cable sag at side span

H_w the horizontal component of cable pull due to dead load

k the load length, see Fig. 7.13

L_s total length of cable due to the effect of cable stretch

L_t total length of cable due to the effect of temperature change

l $=1400$ ft. = main span length

l_1 $=513.83$ ft. = side span length

M bending moment in k-ft

N_c factor due to cable stretch

N_s factor due to the effect of side spans

N_t factor due to temperature change

p $=1.0$ kip/ft. = live load per cable

V shear force in kips

w $=2.882$ kip/ft. = dead load per cable

x the location to define see Fig 7.13

α the inclination of the chord in any span and segment of cable

θ slope of the bridge span

η deflection of the bridge span

ϵ $=65 \times 10^{-7}$ = coefficient of expansion

NOTATIONS 3

The following notations were used in the aerodynamic stability study[10,11] [12,13,14,] in Chapter 8

A_D $=8.87$ in^2 = section area of bottom lateral diagonal

A_d $=10.65$ in^2 = section area of stiffening truss diagonal

A_h $= \Sigma A_D \sin^2 \phi_h \cos \phi_h$ in one panel

A_l area of lower chord of stiffening truss

A_u area of upper chord of stiffening truss

A_v $= \Sigma A_d \sin^2 \phi_v \cos \phi_v$ in one panel

a amplitude of vibration

b $=57$ ft. = c. to c. of cable distance (i.e. width of the bridge)

C_w warping modulus

d $=10$ft. = c. to c. of top and bottom lateral distance (i.e. bridge depth)

E modulus of elasticity for stiffening trusses

E_c modulus of elasticity for cables

f $=128$ ft. = cable sag at main span

f_1 $=17.24$ ft. = cable sag at side span

G shear modulus

H horizontal component of cable pull

I_D modulus of torsion

K stiffness factor or spring constant or coefficient of rigidity

K_t coefficient of torsional rigidity

L_s function of cable length

l $=1400$ ft. = main span length

l_1 $=513.83$ ft. = side span length

M moment

m $\quad = \dfrac{W}{g}$ = mass per unit span length

N_c $\quad$ critical flutter frequency

N_t $\quad$ natural frequency of torsional oscillation

N_v $\quad$ natural frequency of vertical oscillation

n $\quad$ modes of oscillation in center span

n_1 $\quad$ mode of oscillation in side span

r $\quad$ the polar radius of gyration

S, S_1 $\quad$ stiffness index

s $\quad = \rho \pi b = 0.426$ = the weight of the air

t_u $\quad = 3/8$ in. = thickness of deck plate

V $\quad$ shear force

v_c $\quad$ critical wind velocity

v_F $\quad$ flutter velocity for coupled oscillations

v_T $\quad$ flutter velocity with pure torsional oscillations

w $\quad$ weight per linear ft. of bridge

Z $\quad = 0.30$ for $k_c = 0.241$

α $\quad$ angle of wind attack

ϕ $\quad$ angular displacement

ϕ_h $\quad$ angle of diagonal and chord intersection of bottom lateral

ϕ_v $\quad$ angle of diagonal and chord intersection of stiffening truss

ω $\quad$ flutter frequency or circular frequency

ω_1, ω_v $\quad$ circular frequency in vertical oscillation

ω_2, ω_T $\quad$ circular frequency in torsional oscillation

$\mathcal{M}$ $\quad$ mass of gyration per unit length

ρ $\quad = 0.00238$ slug = mass density of air

μ $\quad = \dfrac{sb}{2m} = 0.0696$ = mass in the bridge structure compared to the mass in an air cylinder

ν $= \dfrac{8r^2}{b} = 1.138 =$ the mass distribution in the bridge section

ξ longitudinal movement of cable

γ the inclination of the cable-chord

CHAPTER I

INTRODUCTION

1.1 General

The A. Murray Mackay Bridge, located in Halifax (Fig. 1.1), Nova Scotia, Canada, has a 1,400 ft. long steel main span flanked by 514 ft. side spans with approach facilities on either side. For the first time in North America, a full orthotropic deck system is employed in a suspension bridge. The orthotropic deck acts as part of the top chords of the deck type stiffening trusses.

The orthotropic theory of bridge design and construction was developed primarily in Germany following World War II. Due to the shortage of steel and other materials in the post-war years, bridge engineers developed lightweight steel bridge decks that are not only very economical but also possess excellent structural characteristics. The improvement of welding techniques has made possible great progress in the use of orthotropic bridges.

Orthotropic type plate has found wide application as the deck system of suspension bridges in conjunction with stiffening girders. By using an orthotropic deck, the dead weight is likely to be reduced compared with other conventional light-weight deck system. This reduced weight generally affects adversely the aerodynamic stability of a suspension bridge. However, it may be more than offset by the increase of the flexural and torsional rigidity of the stiffening system due to the participation of the deck plate in the stiffening system stresses.

1.2 History of Project

Shortly after 1955, and the opening of the Angus L. Macdonald Bridge which was built by the Halifax-Dartmouth Bridge Commission across Halifax Harbour, the traffic volume grew rapidly. The average daily traffic volume had been tripled by 1962, which indicated an average annual growth rate of 15.6%. This extremely high growth rate could be attributed, in part, to the rapid development of the City of Dartmouth since the opening of the bridge and, in part, to the ready acceptance by the motorists in the Metropolitan area of a toll facility which provided a quick route between Halifax and Dartmouth.

Owing to this fact the Province of Nova Scotia passed an amendment for Chapter VII of the Acts of 1950.

If the Province and either the City, the Town or the County request the Commission to investigate the sufficiency of the means of access to the City provided by the present bridge operated by the Commission or the present or future need of an additional bridge or bridges, the Commission may:

(a) Conduct such investigation and studies as it considers advisable respecting

1. the need or advisability of an additional bridge or bridges across Halifax Harbour or the North West Arm;

2. the proper location of any such bridge or bridges and the approaches thereto;

3. the manner or method of financing and operating any such bridge;

4. the probable cost of acquiring lands for the purposes of

an additional bridge or bridges and the cost of construc-

ting such bridge or bridges;

5. any other matter related to the construction, operation

or financing of an additional bridge or bridges and the

approaches thereto that the Commission considers relevant.

In June, 1962, the Bridge Commission appointed Consulting Engineers

Messrs. H.H. L. Pratley and R.A. Dorton of Montreal (by whose office the

Angus L. Macdonald Bridge was designed) to carry out such a study. The

Consulting Engineers retained the service of a specialist firm in traf-

fic engineering, A.D. Margison and Associates Limited of Toronto. Much

information was obtained from many Government Departments and various

organizations. A report of "Halifax Area Bridge Study 1963" was fur-

nished by the Consulting Engineers to the Bridge Commission covering

all the subjects required by them.

In the report the Consulting Engineers recommended that the bridges

across the harbour at George's Island and at North West Arm should be

built simultaneously. Not only would the financial situation be im-

proved by construction of both bridges at the same time, but these two

bridges would combine very well to provide a through route helping to

complete a ring road around the metropolitan area, without making any

appreciable use of the city street systems. However, for economic rea-

sons, the Bridge Commission adopted a revised scheme across the Narrows.

At present, the North West Arm Bridge is still under study.

1.3 Scope of Report

This multimillion dollar project comprises an orthotropic deck

suspension bridge and approach roads, with two clover-leaf interchanges and several grade separation structures.

Although extensive research work on orthotropic decks in the past has been carried out contributing useful data to designers, only a few papers covering the comprehensive behaviour of such a system applicable to suspension bridges have been published. The system is still in the development stage and the writer feels that there would be much interest in reading a full technical report of this nature. The full report covering the details of the design features, the aerodynamic stability wind tunnel tests, the application of epoxy asphalt surface, the fabrication procedures and the erection stages etc. could be used as a reference for design of similar bridges and also in making any comparative studies of different suspension bridge systems.
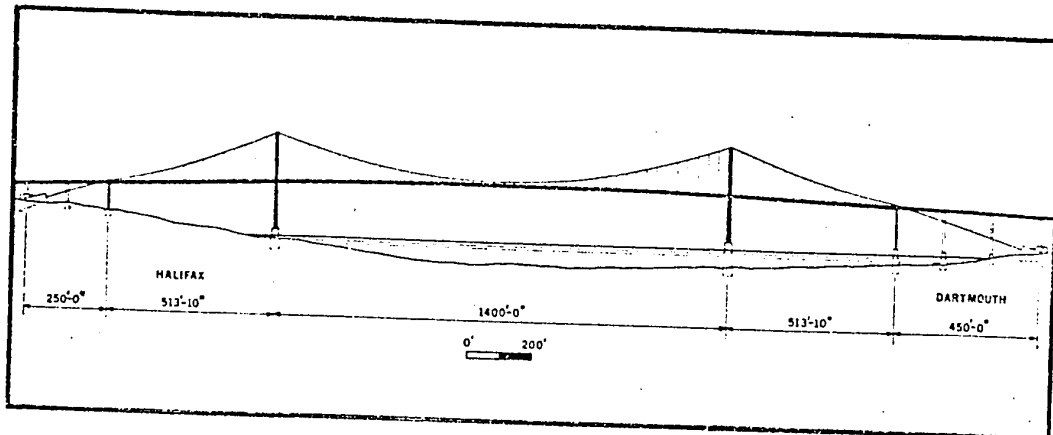
A. THE A MURRAY MACKAY BRIDGE
(NARROWS BRIDGE)
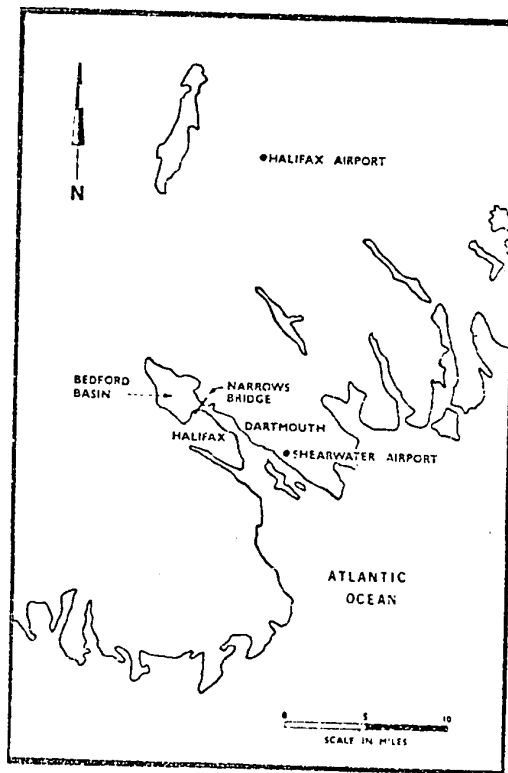
B. LOCATION OF THE BRIDGE

FIG. 1.1 HALIFAX AND ITS VICINITY

CHAPTER 2

TRAFFIC STUDY

2.1 General

A large area including not only the Cities of Dartmouth and Halifax
but also all the suburban area within a radius of several miles have been
studied. This comprises an examination of population growth combined
with the best possible forecasts of the development of suburban areas,
so that an estimate could be made of the likely growth and changes in
traffic patterns.

From traffic patterns one can gauge whether an additional bridge
is required. If so, this leads to more detail study and investigation of
location of sites, site exploration and economics.

The return of revenue is calculated on an escalated traffic growth
over a term period.

2.2 Capacity Analysis

The capacity of any facility is directly related to its width and
alignment and the types of vehicles wishing to utilize it. The existing
Angus L. Macdonald Bridge, 2 lanes and 2 way traffic, has one additional
limit factor, which is the "no passing" regulation which limits the
operating speeds of all vehicles to the speed of the slowest vehicle
using it.

Observation of the traffic movement on the bridge during peak hours
in 1962 indicated an average headway between vehicles of three seconds
during normal operating conditions, with a minimum headway of two to

two and one half seconds. For all practical purposes, a headway of two and one half seconds between vehicles is the lowest which should be considered for safe and efficient movement. This headway gives a practical capacity of 1440 vehicles per hour for one lane for one direction. Compared with the existing high volume of 1,600 vehicles per hour, this indicated that on normal weekdays the bridge was operating at the peak hour at 90% to 110% of practical capacity. While the peak hour would not necessarily increase at the same rate as the twenty-four hour total volume, it could safely be assumed that within two years the normal weekday traffic would regularly produce over-capacity conditions, thus extending the peak hours condition.

Therefore, as the capacity of the bridge could not be economically increased, and the demand to use this facility would continue to increase, consideration should be given to the construction of a new bridge across Halifax Harbour to avoid the serious congestion.

2.3 Existing and Future Population and Development

The development of a rational estimate of future population is depended upon an analysis of past records and the opinions and the prediction for the six major sections of the Halifax Metropolitan Area for the period from 1941 to 2000 had been tabulated in Table 2.1

The population for the entire Metropolitan Area will reach 270,000 by 1980 and 318,000 by 2000. This seems reasonable since the past history of the Province had indicated a gradual increase in the percentage of urban population, as opposed to rural population, and all studies of the economic growth of the Halifax Metropolitan Area indicated that this trend would continue.

TABLE 2.1

EXISTING AND ANTICIPATED POPULATION IN THE HALIFAX METROPOLITAN AREA

AREA	POPULATION						
	1941	% Inc. /Year	1961	% Inc. /Year	1980	% Inc. /Year	2000
City of Halifax	69,000	1½%	92,500	¾%	105,000	¾%	118,000
City of Dartmouth	16,000	5½%	47,000	2½%	75,000	1%	90,000
Herring Cove & Spryfield	3,600	7½%	14,800	3%	26,000	¾%	30,000
Arndale, Dutch Settlement & Fairview	2,300	7½%	10,100	5%	26,000	2%	39,000
Rockingham & Bedford	2,300	7½%	10,300	3¾%	21,000	1½%	28,000
Cole Harbour & Eastern Passage	2,000	7%	7,600	4¼%	17,000	1%	21,000

2.4 Passenger Car Ownership and Usage

Due to the lack of accurate data on passenger car ownership in the Halifax Metropolitan Area, it was decided to utilize the provincial records to establish a trend line for increased ownership. Similar to Table 2.1, the relation between the provincial population and persons per passenger car for the period 1941 to 2000 had been estimated. The ratios showed persons per automobile of 5.1 in 1961, 3.5 in 1980 and 3.2 in 2000 for the Province as a whole, while the Metropolitan Area would probably have a persons per car ratio of about 3.0 by 1980 and 2.5 by 1995, after which it would remain relatively constant.

2.5 Future Traffic Growth Factors

Traffic growth factors had been calculated for each traffic zone in the study area for the period from 1962 to 1980, utilizing the population increase for each zone and passenger car increase for the Province.

Since the available planning data was unable to produce any logical specific zonal population predictions beyond 1980, it was decided to use an average factor for the area. The population increase and reduction of persons per automobile had been combined to produce a traffic increase factor which was 2.5% per year for the period from 1980 to 1994, equivalent to an overall factor of 1.48 for the fourteen years.

The Department of Highways of Nova Scotia used a twenty year expansion factor of 2.0 to adjust its traffic data to the future and this factor was used to adjust some of the data in the traffic study.

CHAPTER 3

FINANCIAL SUPPORT AND REVENUE ESTIMATE

3.1 Financial Study

In 1962, the funded debt of the Commission consisted of two issues. First mortgage serial bonds with an interest rate of 4-1/8 % maturing on the 15th March 1958 to 1977 were sold on the U.S. market in 1952 to finance the construction of the Angus L. Macdonald Bridge. The original amount of this issue was $8,000,000.00 and bonds have been redeemed every year since 1958. So far as the financial study was set in March 1963, the total of the bonds still outstanding amounted to $6,236,000.00. In 1957, the Commission created a new issue of 5% series B debentures maturing 1st September, 1977 in the amount of $2,650,000.00. Both of these issues were guaranteed as to principal and interest by the Province of Nova Scotia and it had been assumed that a similar guarantee would apply to any new issue made to finance new construction.

The Commission had considerable funds available in Reserve Accounts and allocated them for the purchase of outstanding bonds. This amount of money did not help the new project very much. The actual cost of the final project was far beyond that of the preliminary study since the bridge had been widen from a 3 lane to a 4 lane together with additional road works on either side.

3.2 Revenue and Expenditure Estimate

A. Revenue Estimate

The financial prospects were based on the construction of a new

bridge at each of the four sites across Halifax Harbour, to be operated in conjunction with the existing bridge as one combined enterprise. To analyse the revenue of the existing Angus L. Macdonald Bridge, average figures were calculated for each year on the basis of total traffic and also for the traffic divided into two categories. Since passenger automobiles constitute such a large proportion of total traffic, they were seperated out as one category and traffic other than passenger automobiles fell into the second category. It was not felt that this could be done with sufficient accuracy to make it worthwhile for estimating total traffic in future years. However, in forecasting revenue, it could be useful to project established trends, in an effort to foresee what proportion of future traffic might belong to each of the categories considered.

The traffic increase had been very slight in 1961 and 1962, and it seemed unlikely that passenger automobile would ever constitute more than about 88% of the total traffic crossing the harbour. Using this limit of 88% and the assumed stable values for unit tolls in each category, the probable overall average revenue per vehicle could be calculated as 21¢. This average value of 21¢ per vehicle had been assumed to apply to all revenue calculations throughout the 30 year study period.

Other revenue derived from two sources. The Commission received rentals for space occupied by electric power and telephone cables carried on the existing bridge and for the carriage of public transit vehicles. The other source for additional revenue was interested on fund available for investment. The result of the revenue and expenditure in this new suspension bridge was tabulated in table 3.1

B.   Expenditure

The primary item of expenditure would always be interested on funded-debt so long as there were bonds or debentures outstanding. The amount shown in Table 3.1 as Interest Charges was on the existing 5% debentures and First Mortgage bonds, which the rate on the new bond or debenture issue had been taken as $5\frac{1}{2}$%.

The next column in the table represented the costs of operation, maintenance and administration (O.M.A.). It had been assumed for the purposes of these studies that operation, maintenance and administration charges would increase at a steady rate of approximately 2% per annum though the figures shown for any particular year might be far off the mark due to the erratic variations in these charges. The overall trend would certainly be upward and the growth rate indicated would be quite adequate for these calculations.

TABLE 3.1

ESTIMATED REVENUE, CHARGES AND SURPLUS

PRESENT BRIDGE WITH NEW BRIDGE AT SITE NUMBER ONE

(Report from Consulting Engineers in 1963)

1963 To 1984

(Figures in thousands)

YEAR	TOLL REVENUE	OTHER REVENUE	TOTAL REVENUE	INTEREST CHARGES	O.M.A. CHARGES	TOTAL CHARGES	ANNUAL SURPLUS	TOTAL SURPLUS
1963	1,395	106	1,501	852	283	1,135	366	-
1964	1,460	484	1,944	997	278	1,275	669	669
1965	1,522	380	1,902	944	283	1,227	675	1,344
1966	1,590	277	1,867	944	288	1,232	635	1,979
1967	1,656	198	1,854	944	294	1,238	616	2,595
1968	1,814	115	1,929	944	544	1,488	441	3,036
1969	1,876	132	2,008	944	555	1,499	509	3,545
1970	1,961	153	2,114	944	566	1,510	604	4,149
1971	2,076	177	2,253	944	577	1,521	732	4,881
1972	2,200	206	2,406	944	588	1,532	874	5,755
1973	2,316	241	2,557	944	600	1,544	1,013	6,768
1974	2,436	282	2,718	944	612	1,556	1,162	7,930
1975	2,558	293	2,851	944	624	1,568	1,283	6,563
1976	2,683	274	2,957	811	636	1,447	1,510	8,073
1977	2,795	334	3,129	811	646	1,457	1,672	9,745
1978	2,916	401	3,317	811	655	1,466	1,851	11,596
1979	3,044	475	3,519	811	668	1,479	2,040	13,636
1980	3,189	556	3,745	811	681	1,492	2,253	15,889
1981	3,274	647	3,921	811	694	1,505	2,416	18,305
1982	3,368	743	4,111	811	708	1,519	2,592	20,897
1983	3,461	847	4,308	811	722	1,533	2,775	9,060
1984	3,566	373	3,939	-	729	729	3,210	12,270

Amount of New Issue: 14,750   5% Debenture Deficiency   Nil

Capital Surplus   9,060   Grand Total of Deficiencies Nil

CHAPTER 4

SITE SELECTION AND THE PROPOSED BRIDGES

4.1 General

In designing a bridge, site selection is one of the most important factors. This affects the development of cities and their communication. Obviously, bridges on skew alignments are more expensive than on square alignments. The economic justification for a square alignment over a skew alignment increase with the angle of skew proposed for skew alignment.

After preliminary location of the bridge, the site, in general, should be inspected for ground conditions and its surrounding area. For the purpose of navigation, the location of piers and clearance should be carefully considered.

The Consulting Engineers proposed four sites (Fig. 4.1) for a possible additional bridge crossing the Halifax Harbour. It will be seen in the following chapters that each site had been thoroughly studies in order to present to the Commission a feasible report.

4.2 The Natural Condition at Each Site

Site No. 1

The most obvious location of all for a bridge between Halifax and Dartmouth was the narrowest point in the body of water separating the two cities. This seemed to involve the least construction cost. It was significant that the old bridge was not constructed at the narrowest point and it was evident that the distance between the shores was not

the governing factor in this case. A bridge must be built where it would provide at least a measure of convenience to the travelling public. Otherwise traffic and, hence, revenue would be unduly low. The topography of the ground could have a considerable effect upon the overall cost. Sharply rising ground could result in considerably shorter approaches even though possibly the water crossing was somewhat greater. It was such considerations as these that determined the site of the Angus L. Macdonald Bridge. But the crossing at the Narrows was still very tempting and this location had obviously to be considered for the purposes of this study.

Site No. 2

Proceeding down the Harbour to seaward, no other site presented itself north of the old bridge but it was considered desirable to examine the possibility of building a new structure along side the existing one, the combination to be operated basically with east-bound traffic on one bridge and west-bound on the other. Such a site is far from ideal but the operational considerations warranted the study of such a scheme.

Site. No. 3

Possibly, the ideal connection between two adjacent cities would run from center of one city to the center of the other. It was considered desirable to study a scheme of this nature, though once again, the site was not very attractive for various other reasons. The prominence of the Citadel in Halifax and the very steep general slope of the land between the Citadel and the water front, combined to force this scheme to land on Halifax side either to the north or to the south of Citadel Hill.

Site No. 4

Further to the south, there was a natural obstruction to shipping in the form of George's Island. This provided an opportunity for a bridge pier which would not add significently to the difficulties of navigation. On the other side there was the end of the Dartmouth Circumferential Highway which could obviously serve as an eminently satisfactory feeder road.

On the Halifax side this site presented two serious problems. One difficulty consisted of the formidable array of existing structures. The other unfortunate circumstance was the fact that, in contrast with the situation at the other sites considered, the land rose comparatively slowly toward the west. This made it necessary to build a relatively long approach structure if excessively steep grade were to be avoided. However, a structure at this site would offer excellent possibilities of connecting with a bridge across the North West Arm to provide a through road across much of the study area. These possibilities, combined with the advantages at both George's Island and Dartmouth, warranted the study of this site.

4.3 Vertical and Horizontal Clearances

At Site No. 1, it would obviously not be necessary to provide a greater vertical clearance than already existed on the Angus L. Macdonald Bridge. On the other hand, it was unlikely that any less clearance would be acceptable to shipping interests. It was significent that the power transmission line at the Narrows, had maintained this vertical clearance which was nominally 165 feet above low water.

Horizontal clearance, which also determined largely by the needs
of shipping, was not governed so much by physical dimensions of the
vessels as by navigation conditions and manoeuvreability. At Site No.
1, the direction of travel of most of the ships passing through the
Narrows would not be at right-angles to the center line of the bridge.
The configuration of the shore line, especially on the Dartmouth side,
was such as to make it logical to offset the main span of the proposed
bridge towards the Halifax side. There existed towards the Dartmouth
shore a comparatively shallow spot which constituted a menace to the
larger ships. Construction of a pier should benefit from the shallow
water and would not create an additional hazard to shipping, but would,
in fact, convert the existing hidden hazard into a much more obvious one
which could be clearly marked by flood lighting of the pier. It seemed
evident that the next pier to the west should not be located any where
in the water where it would obstruct shipping. The horizontal clearance
thus determined resulted in a span of about 1,300 feet which, due to the
skew, would provide a navigational clearance with an effective width of
about 1,100 feet. This was no less than existed somewhat further seaward
where a jetty jutted out from the Dartmouth shore.

A bridge constructed at Site No. 2 would obviously require clearance
almost identical to those of the old bridge. The vertical clearance would
be exactly the same but the slight widening of the Harbour in the short
distance between the two bridges suggested a slightly greater horizontal
clearance. The physical characteristics of the site, which governed the
locations of piers and anchorages, also led to an increase in the horizon-
tal clearance. The length of the main span would be 1,500 feet vs. 1,447

feet of the old bridge.

At Site No. 3, the bridge would be located on the seaward side of several important wharves which could be used by ships unable to pass under the Angus L. Macdonald Bridge. Consequently, it had been assumed that somewhat more vertical clearance should be provided than existed at the old bridge. At this location in the Harbour there was considerable manoeuvring of vessels approaching and leaving their berths. One main pier had been located at the tip of an existing jetting so as to cause the absolute minimum of difficulty to shipping. The other main pier had been located by considering, in combination, the questions of minimum horizontal clearance, desirable vertical clearances, suitable bridge profile, and depth of water at the pier site. The resulting layout yielded a horizontal clearance in excess of 2,100 feet, minimum vertical clearance at the center of 180 feet above high water. At the same time, a minimum vertical clearance, also above high water, of 165 feet had been maintained at the entrance to the wharves on the Halifax side.

At Site No. 4, the bridge was located quite close to the entrance to the Harbour. Virtually, every ship entering the Harbour would have to pass underneath it. In addition, the bridge passed directly over the Ocean Terminals where the largest passenger vessels were occasionally berthed and consideration must be given to this fact. The profile of the main span to the east of George's Island had been made identical to that of the west of George's Island so that ships might enter the Harbour through one channel and leave through the other. This had maintained a generous clearance right over to Dartmouth shore, making provision for

the movement of oil tanker to that area.

4.4 Traffic Feature and Roadway Width

The basic factor entering into the determination of the number of
lanes is obviously the intensity of traffic. There, consideration must
be given to the various traffic patterns that occur at different times
during the day. Experience on the Angus L. Macdonald Bridge had been
that the traffic at the morning rush hour was nearly twice as dense
west-bound as east-bound. Exactly the reverse was the case at the late
afternoon peak. The distribution between the two directions was quite
well balanced in between these peaks and in the evening hours. The
actual density in either direction during the off-peak hours was always
less than the peak-hour traffic in the less heavier direction. Therefore,
only the rush hour traffic should be considered in determining the number
of lanes on the new structure.

Experience showed that the traffic in the busiest 60 minutes of the
peak period was very close to 10% of the total traffic for the day. Fore-
casted for average daily traffic in 1994 for the four sites considered
range from 56,000 to 69,000 vehicles per day which was equivalent to a
range of 5,600 to 6,900 during the peak hour. Since the peak hour traffic
was approximately twice as heavy in one direction as in the other, it
could be expected that in 1994 the total peak hour traffic in the more
heavily travelled direction might range from 3,700 to 4,600 vehicles
depending on the site of the new bridge; similarly, traffic in the less
heavily travelled direction might range from about 1,900 vehicles to
2,300 vehicles. While it was often considered that no lane should be

required to carry more than 1,440 vehicles per hour, it was a fact that the Angus L. Macdonald Bridge had already experienced a rate as high as 1,600 vehicles per hour without any serious congestion on the bridge itself.

If a total of three lanes were to be provided for traffic in the more heavily travelled direction, the peak rate in 1994 might be expected to be between 1,233 and 1,533 vehicles per hour. The upper end of this range was quite acceptable while the lower end indicated that there would be appreciable unused capacity. It could thus be seen that during the peak hour any new structure must provide, in combination with the old bridge, at least three lanes in one direction and two in the other. Since the old bridge could not carry more than two lanes of traffic, another two laned structure would not result in a combined capacity sufficient to meet the need. The fact that three lanes would be required west-bound in the morning and also east-bound at night immediately suggests that two additional lanes should be provided in each direction.

The Consulting Engineers suggested that a new bridge with three traffic lanes would thus meet the predicted need and would cost appreciably less to build than would a four lane bridge. However, the Bridge Commission preferred a four lane bridge with the same lanes of approach roadway throughout the whole project. This certainly would minimize the traffic congestion and gave the driver a comfortable driveway. It was also easier in design and convenient in the traffic control and management.

4.5 Proposed Bridge Spans at Each Site

The original design proposed by the Engineers for the two shorter schemes at Site Nos. 1 and 2, a bridge of the through type, which had the roadway set down between the two stiffening trusses as on the Angus L. Macdonald Bridge, had been selected. However, for the longer span at Site Nos. 3 and 4, the deck type, with the stiffening trusses entirely below the roadway had been chosen. This made possible the use of two planes of lateral bracing which would greatly improve the torsional stiffness.

The approach spans for each scheme, with the exception of one or two of the longest spans adjacent to the suspension bridge, had all been estimated as steel plate girder. There had been a marked trend in recent years towards using girders for longer spans and trusses had only been shown either where the spans are exceptionally long or where the appearance was improved by their use. Again the good foundation conditions were expected to permit the use of continuous spans such as existed on both approaches to the existing bridge. The span lengths and layout of the approaches had been determined as far as possible by an economic relationship to pier heights. Although steel girders had been assumed for preliminary purpose, the possible use of prestressed concrete should be thoroughly studied before proceeding with a final design since this type of construction might well prove to be competitive in cost.

In all cases the approach spans would be supported by slender concrete piers of graceful proportions to provide both good economy and pleasing appearance. A Toll Plaza of suitable dimensions together with Administration and Maintenance facilities had been assumed at each site except that at Site No. 2 where enlargement of the existing Administration Building and Maintenance Garage would undoubtedly suffice.

Site No. 1

At this location, the preliminary proposed length of the main span is 1,303 feet and the side spans each had a length of 489 feet. On the Halifax side, due to the steeply rising ground, the approach consisted of only three spans of 150 feet, 100 feet and 75 feet respectively. The anchorage was located high up the slope and carried on it the first approach pier. On the Dartmouth side, the anchorage was located on low ground near the shore. And the profile of the ground was such that there were eight approach spans of 150 feet and one of 100 feet between the end of the suspension bridge and the abutment at the beginning of the Toll Plaza. East of the Plaza, it was necessary for the approach road to rise sufficiently to cross over the C.N.R. tracks and a partial clover leaf had been indicated for the connection to Windmill Road.

Site No. 2

At this site the new structure would be paralled to existing bridge for much of its length and some 250 feet to the south. Any attempt to make the second structure identical to the first to improve the appearance from either side was doomed to failure right from the start. It was because the space between the two would always make it impossible to line up more than any one feature of the two structure from any given position.

The span length chosen was 1,580 feet and in this case the two side spans each had a length of 593 feet. Again the steep profile on the Halifax side resulted in a shorter approach than was required in Dartmouth although the new layout did not come down to ground level as soon as did the old bridge. The approach consisted of a 165 feet span from the end of the suspension bridge to a pier on top of the anchorage followed

by a 100 feet span crossing Barrington street and six 700 foot spans, the last of which crossed Brunswick street. On the Dartmouth side both the cable bent and the first approach pier were located in the water and the second approach pier was on top of the anchorage which, as with the existing bridge, was located on the bluff just above the railway tracks. The first three spans were each 165 feet long and these were followed by three more each 140 feet long and a final set of five, each 75 feet long. Starting at the abutment, road spreaded out very rapidly to join the existing Plaza and a new loop road had been added for traffic turning right off the bridge.

Site No. 3

This scheme called for a very long main span of 2,245 feet with identical side span each 962.5 feet long. The symmetry was prolonged by the use of three 260 feet truss span on each side beyond which the two approaches differ. On the Halifax side it was necessary to splay the roadway very early in order to fit in a toll plaza for which no satisfactory site could be found on the Dartmouth side. Splaying of the roadway was carried out on the last five approach spans, four of which were each 100 feet long while the fifth, which crossed Gottingen street, had a length of 75 feet. On the Dartmouth side the anchorage was located in shallow water quite near the shore and once again it carried an approach pier since this extra load was always advantageous. Beyond the three truss spans there were twelve plate girder spans each 150 feet long loading to an abutment beyond which the road spreaded out and divided to connect up with existing streets.

Site No. 4

The scheme proposed at this site is quite unusual and had some similarity to the San Francisco-Oakland Bay Bridge in that there were two suspension bridges with a common anchorage at the center. In this case, the spans were not so great and it was intended that the main cables should be continuous from one end to the other. Each main span had a length of 1,703 feet and four side spans were 851.5 feet long. For the purpose of anchoring the cables at the center to resist any out of balance force, it had been necessary to introduce a gap of 70 feet between the ends of the two side spans and this portion of roadway would actually be on the anchorage itself. Consideration was given to omitting the central anchorage which would result in a strucutre with three main spans. However, the great flexibility of such a structure would require either exceptionally heavy stiffening trusses or cable tied between the tops of the towers and these alternatives were discarded in favour of the scheme illustrated.

As in Site No. 3, the symmetry extended part way down the approaches. In this case there were two 200 feet truss span on each side, in each case ending on a pier supported on the cable anchorage. Beyond the truss spans the Halifax approach consisted of nine girder spans of 150 feet each, three girder spans of 125 feet each, and eight girder spans of 100 feet each, terminating at an abutment just west of Wellington Street beyond which the road divided for connection to the city streets. The great length of this approach was dictated partly by the large vertical clearance required over the water and partly by the topography of the city in this area. On the Dartmouth side, the truss spans were followed by

eight girder spans of 150 feet and one of 125 feet. Beyond these spans were the toll plaza and an interchange providing smooth connection with the Dartmouth Circumferential Highway in both direction.

4.6 Cost Estimate of the Proposed Bridges

To establish estimate of the cost of construction of each scheme, it was necessary to make preliminary designs. Due to the magnitude of the proposals, it had to be carried out in detail in order to obtain sufficient accuracy.

The design of the substructure had been based upon rock levels established largely by familiarity with the area and by considerable local enquiry. In many cases, rock could be seen outcropping from the ground and its presence and quality could be reliably established

In all preliminary design work, the live loading in general use for bridge design throughout North America was used, which was the same as that Angus L. Macdonald was design to carry. Because the approach spans were all of comparatively common types, it was unnecessary to accumulate similar lengths to establish quantities of materials for these spans. Approximate designs were made and the results compared with quantities calculated on many other bridges.

Table 4.1 shows the cost estimate of the four proposals recommended. The cost was originally estimated for a three laned bridge and approach roads.

The Bridge Commission selected Site No. 1 of the four proposals recommended due to economic and mainly immediate development of industry

on completion of the project. After the Angus L. Macdonald Bridge was opened to traffic, the downtown area of Dartmouth city was fully developed. There was lack of space to design an expressway and the interchange in the heart of both cities. In addition this final choice was dictated largely by that studies indicated tnis location as the most desirable with respect to approaches, grades and street connections, thus utilizing less expensive property and offering the minimum of interference to local development, and, at the same time, giving maximum accessibility to the business district and to the principal traffic arteries conveying in this locality.

TABLE 4.1

COST ESTIMATES

HARBOUR BRIDGE PROPOSALS

	Site 1 THE NARROWS	Site 2 HMC DOCKYARD	Site 3 PIER NO. 2	Site 4 GEORGE'S ISLAND
Suspension Spans Substructure	$1,113,000	$1,735,000	$2,935,000	$5,356,000
Approach Spans Substructure	213,000	153,000	433,000	437,000
Suspension Spans Superstructure	4,660,000	6,389,000	14,300,000	17,000,000
Approach Spans Superstructure	749,000	846,000	1,950,000	1,963,000
Overpass Structure	628,000	-	61,000	198,000
Approach Roads	950,000	225,000	525,000	775,000
Electrical Work	195,000	85,000	134,000	279,000
Building and Toll Booths	300,000	50,000	300,000	300,000
Physical Cost	$8,808,000	$9,483,000	$20,638,000	$26,308,000
Engineering	573,000	616,000	1,341,000	1,710,000
Land	550,000	800,000	2,250,000	2,300,000
Total	$9,931,000	$10,899,000	$24,229,000	$30,318,000
Contingencies	497,000	545,000	1,211,000	1,516,000
Total Estimated Cost	$10,428,000	$11,444,000	$25,440,000	$31,834,000
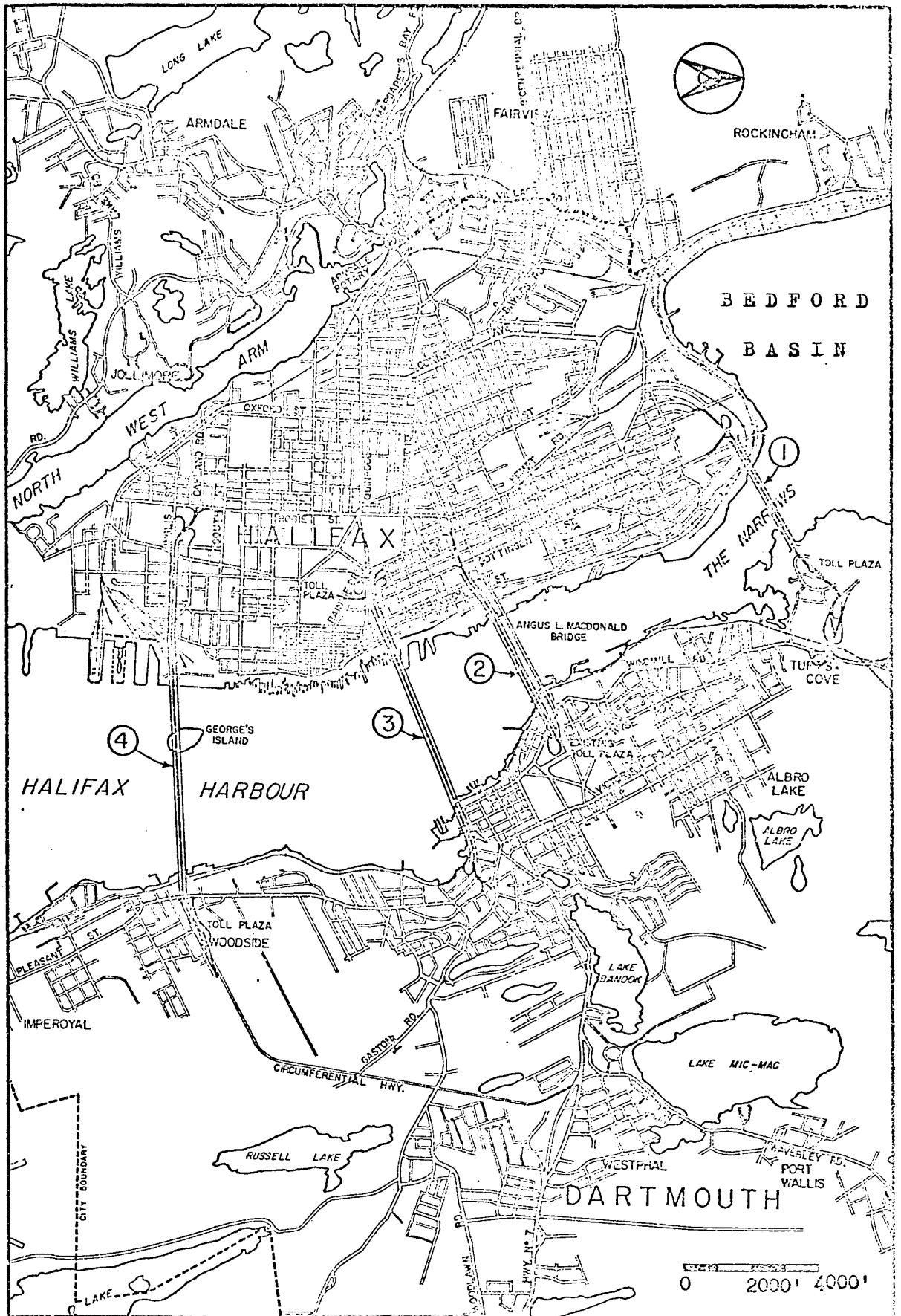
FIG. 4. 1 ALTERNATE HARBOUR BRIDGE SITES

CHAPTER 5

THE NEW APPROACH FACILITIES

5.1 General

For an essential part of the highest type of expressway, grade separations and interchanges are preferrable[1]. The advantages in employing these modern designs are as follows:

1. The capacity of the through travel ways within the interchange can be made to approach or equal that outside the interchange.

2. Increased safety is provided for through and left turning traffic.

3. Stops and speed change are eliminated for through traffic.

Based on the above advantages, the City of Dartmouth and the Nova Scotia Highway Department agreed with following new facilities.

5.2 Approach Facilities and Clover Leaf Interchange at Dartmouth

Not far beyond the Dartmouth approach abutment follows a Toll Plaza with the connection to the existing Princess Margaret Boulvard. Access is available to the Beford Institute of Oceanography and the Northern district of the city. About half mile to the east of the Plaza, there is a full Clover-Leaf Interchange "B" (Fig. 5.1) which runs into downtown Dartmouth. Due east the expressway passes north of Albro Lake, a second semidirect connection Clover-Leaf "C" placed between Lake Banook and Lake Mic-Mac. On the Halifax side a three level interchange and two railway over-passes were constructed.

Due to the lakes so ideally situated, many drainage problems were

solved, thus preventing a high cost for an alternated drainage system.

On the other hand, motorists enjoy a scenic drive from interchange "B" to interchange "C". The hilly country side sprayed with pine and beech trees together with Albro Lake attracts pleasure trips for tourists and local inhabitants.

5.2.1 Toll Plaza

About 2,000 feet to the north of the abutment is the location of the Toll Plaza (Fig. 5.1). It flares out from 52 ft. to 205 ft. gutter to gutter, this width constant for 300 ft., and then converges to a four lanes expressway divided by a four feet median. In order to minimize the possible congestion, the toll station itself consists of seven-lanes on either side. Two 2-lane ramps blend with the existing Princess Margaret Boulvard, from which an exit is connected with Bedford Institute of Oceanography.

On the south side of the Plaza stands the administration building which, together with its maintenance space accomodation, cover an area of 45 ft. by 215 ft. Between this building and the ramp, a paved parking lot is available which, together with an auxiliary lane, are privileges used by the employees.

5.2.2 Clover-Leaf Interchange

2,000 ft. east of the Toll Plaza lies interchange "B" servicing two freeways. (Fig. 5.1) The outer connection of the Clover-leaf are on tangents with curves at the ends. This favors high speed merging and diverging for freeway traffic to and from the outer connections. The

weaving sections of approximately 500 ft. on both freeways, appear adequate to accommodate the high weaving volumes of 1050 vph on both freeways.

Due to the undulating terrain, the south-west outer connection was designed with an 8% upgrade in 1,400 ft. A climbing lane of the same length was provided, since loaded trucks reduce speed unduly.

The two north loops have constant radius of 150 ft., while the south-east loops have minimum radii of 90 ft. This permits an average speed of 25 to 30 mph, while the outer connections are designed for speed as high as 40 mph. All these ramps are single lane, 18 ft. wide with 7ft. wide shoulder on either side, this in turn provides easier manoeuvrability and safety.

The south and north legs of interchange "B" link the business center of Dartmouth to the Industrial Park on highway No. 7 which will help stimulate industrial development.

5.2.3 Semidirect Connection Clover-Leaf Interchange

Interchange "C" (Fig. 5.1) is a partial cloverleaf with a semidirect connection. Loop ramps are provided in two quadrants, while the semi-directional ramp projects from the west outer connection. The predominant turning movements are accommodated on direct connections which form a separate highway to one side of a partial cloverleaf. In this type of interchange, an additional structure is required, but a weaving section is eliminated on each of the intersecting freeways.

The minimum radius of the loop is 170 feet. This permits a ramp speed between 25 to 30 mph. The width of the loops and the outer con-

nection is 18 ft. with 7 ft. shoulder on either side.

The distance between two interchanges is about one and a quarter miles, a median of 14 ft. from gutter to gutter is inserted. The south end of the underpass freeway blends with Woodland Ave., while the north joins the new Lakeview Drive. This provides rapid access from both downtown areas to the Halifax International Airport.

5.3 Three Level Interchange and New Facilities at Halifax Approach

The Halifax approaches encountered congested site conditions due to the existing C.N. Railway, public utilities and narrow land access in parts. This lead to the choice of a three level interchange (Fig. 5.1) which solved the crossing of the railway tracks. However, a railway bridge was unavoidable as the approach, directly from the main bridge was continued west to join the distributed roads linking to the city streets. This location demanded many high retaining walls along Robie street and the Railway Tracks.

The approaches to the bridge were located north of the city of Halifax, so traffic was distributed by three main arteries into the metropolitan area. On the east, Barrington street was linked, another leg extended to the south, which blended with Robie Street, leading to the proposed North-West Arm Bridge, and the third fed the industrial areas via Bicentennial Drive at Fairview.

The existing Angus L. Macdonald Bridge located $1\frac{1}{2}$ miles south would be relieved of traffic from outlying areas which have been growing in population at a rapid rate.

North West Arm

Kempt Rd.

Windsor St.

B E D F O R D

B A S I N

3 Levels
Interchange

Roble St.

H A L I F A X

A. Murray MacKay
Bridge

Barrington St.

THE NARROWS

Angus L. Macdonald
Bridge

HALIFAX
HARBOUR

Toll Plaza

Windmill
Rd.

D A R T M O U T H

Victoria Rd.

Highway No. 7

Interchange
'B'

Woodland
Ave.

Albro
Lake

Lake
Banook

Martin
Lake

Circumferential
Highway

Frenchman
Lake

Interchange
'C'

Lake Mic - Mac

1000'   3000'

0   2000'

FIG. 5.1 THE BRIDGE AND ITS APPROACH ROADS AT BOTH CITIES

CHAPTER 6

CHOICE OF ORTHOTROPIC DECK SYSTEM

6.1 The Economy of Steel Plate Deck Construction

The Orthotropic Deck System has resulted in substantial reduction
of dead weight for long-span bridges, and more recently has found appli-
cations in the design of medium and short-span bridges. A greater saving
is expected for longer spans where the reduction of dead weight would
be a more important factor. Even for short-spans, the price differential
between a reinforced concrete deck and a thin wearing surface for ortho-
tropic plate construction may result in a net saving, in addition to a
considerable saving in the substructure cost. Experience shows that
highway bridge spans of less than 100 ft., the weight of an orthotropic
plate bridge is about one-third of the weight of composite construction
of reinforced and steel.[2] However, the savings in cost are smaller than
the savings in weight, since the cost per pound of erected steel is
higher for steel plate deck bridges than for conventional girder bridges.
It is found that the fabrication of the orthotropic deck generally requires
more man-hours. This offsets the economy gain in weight savings. How-
ever, a reasonable net cost saving is still in favor. It should be
noted that in European and Asiatic countries, labour cost is much cheaper
than here, and, in most case the material saving alone decides the choice
of the design.

6.2 Advantages of the Orthotropic Deck System

There are many advantages to employ an orthotropic plate in various
types of bridges.[3][4] The salient points are as follows:

1. Steel Weight Saving

    The Steel Weight Saving is about one third of the conventional

design for short or medium spans. It becomes remarkable as the bridge

spans increase. Literature shows that (a) the Duesseldorf-Neuss Bridge

(b) the Save River Bridge and (c) the Cologne-Muetheim Bridge were

destroyed during the war. All these old conventionally designed bridges

have been replaced by orthotropic deck types which give steel weight

savings of (a) 25%, (b) 44%, (c) 55% respectively.

2. Cost Saving

    Experience indicates that, on the average, 15% to 20% more man-hours

per ton of fabricated and erected steel are needed for a steel plate deck

bridge than for a girder bridge of conventional construction. This can

be compensated by the favorable steel weight saving. Therefore, a reasonable

figure for net saving in cost is about 15%.

3. Depth Reduction on Saving

    The depth of structure reduction reduces the cost of the approaches

to high-level bridges and allows flatter approach grades. The slenderness

of the spans attributes an aesthetic appearance to the structure.

4. Bridge Deck Savings

    The direct savings in the cost of structural steel is obtained by

replacement of a reinforced concrete deck by a less expensive wearing

surface. Generally the cost of the usual 7" reinforced concrete deck

slab is almost two to four times higher than the 2" wearing surface to

the top of steel deck.

5. Full Utilization of Materials

The orthotropic deck plate serves several structural functions, such as the upper flange of the longitudinal stiffening ribs, the transverse floorbeams, and the main girders. This reduces further dead weight of the supporting members.

6. Increased Factor of Safety

The safety of an orthotropic deck system against failure due to a concentrated load is considerably greater than that of a conventional bridge floor, since a local overload on a steel plate deck causes an elastic and, eventually, plastic stress redistribution to the adjoining elements rather than an immediate failure of the member. If the local load be further increased beyond the critical limits, the eventual failure would be a local one, affecting only one out of the many ribs in the deck, without destroying the overall usefulness of the deck.

7. Erection Efficiency

Most of the steel components were prefabricated and assembled at site. This is a remarkable time saver and increases the efficiency in the erection procedure. The other important factor is the concrete construction confined to one operation instead of two for foundation work and for pouring of the deck after completion of the steel framework. Elimination of one concrete operation tends to shorten the erection period.

8. Substructure Savings

The dead weight of the orthotropic super-structure is almost half to one-third of the weight of conventional bridge superstructure, this in turn obviously reduces substructure size. Records show a saving of

10% to 15% on substructure work can be achieved by the use of an ortho-
tropic deck.

In addition, the appearance of an orthotropic bridge is pleasing.
Therefore, the design of these bridges was governed not only by financial,
practical and technical requirements but also to a great extent by aesthe-
tical and architectural consideration.

6.3 Choice of Structural System

The choice of structural system depends on the foundation conditions
and the navigation requirements. A minimum center span length of 1,400 ft.
due to the final adjustment of the alignment, was set by the Consulting
Engineers at Site No. 1. As the cable anchorage could be placed out of
the water on both sides and all the substructure could be founded on
rock, the site conditions were ideal for a suspension bridge. In recent
years, the cable stayed bridge has been increasingly chosen in the span
range of about 600 ft. up to 1,100 ft. or even more. At the time of
design, suspension bridges were the economic and efficient choice.

In order to obtain an optimum design, three different types of
suspended structure were chosen to carry out prelinimary designs[5]:

Type 1. The standard type with a concrete filled steel grid deck.
(Fig. 6.1)

Type 2. The truss type with orthotropic deck acting with the trusses
in bending (Fig. 6.2) as finally adopted.

Type 3. The single orthotropic box type (Fig. 6.3)

For the reason of comparison the same vertical bending stiffness

was employed for each type, thus giving similar moments, shears and deflections for each. The truss depth of Type 1 was 14 ft. while the orthotropic deck of Type 2 was merely 9 ft. 6 in. For the single orthotropic box girder of Type 3, the depth was 7 ft. which possessed the same stiffness value as the previous two types. The floor beam diaphragms of Type 2 and Type 3 were spaced 15 ft. 10 in., while they were spaced at 31 ft. 8 in. in the standard deck of Type 1.

Complete cost studies of Type 1 and 2 showed an approximate saving of 15% in favor of Type 2, and the total dead load was 21% lesser than Type 1. Cost studies of Type 3 were not completed but the suspended steel weight was found to be 16% in excess of Type 2.
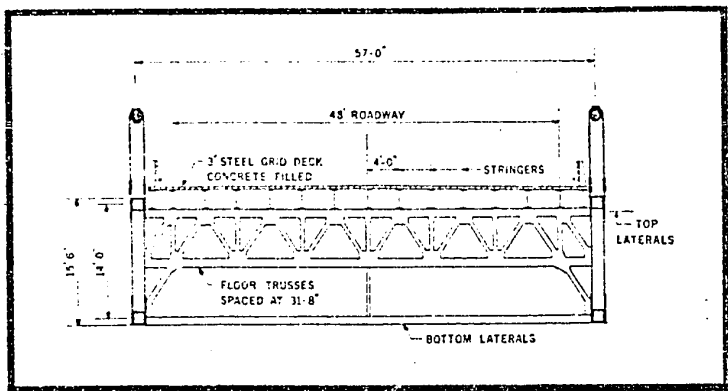
FIG. 6.1 TYPE 1. THE STANDARD TYPE
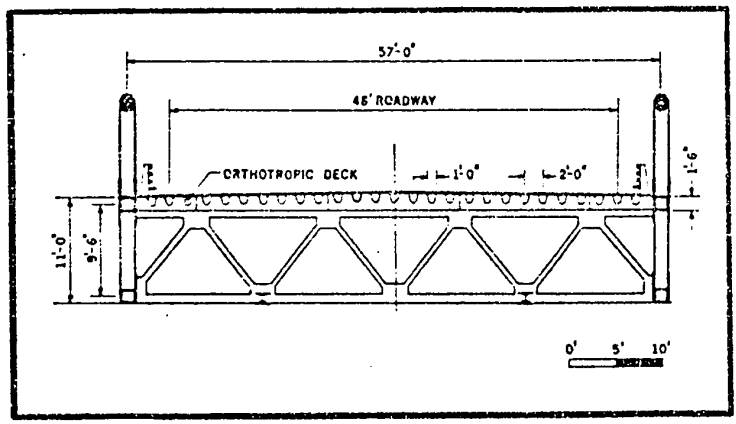
FIG. 6.2 TYPE 2. THE TRUSS TYPE WITH ORTHOTROPIC DECK
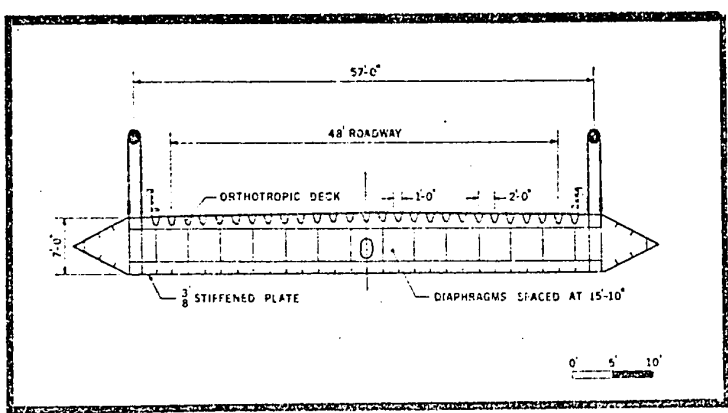
FIG. 6.3 TYPE 3. THE SINGLE ORTHOTROPIC BOX TYPE

CHAPTER 7

SUPERSTRUCTURE DESIGN

7.1 Geometrics of the Bridge

The four-lane new suspension bridge has a 1,400 ft. long steel main span flanked by 513 ft. 10 in. side spans. (Fig. 7.1) There are four 125 ft. spans and five 150 ft. spans on the Dartmouth approach, and three 125 ft. spans on the Halifax approach. The main span provides a 165 ft. vertical clearance from Low Water Level which is -3.79 ft. on the geodetic datum. The main cables are 57 ft. apart with a 48 ft. roadway throughout the bridge. The deck surface is specially treated to protect it from corrosion, and is topped with a 2 in. epoxy asphalt surface.

The final roadway elevation center-span was derived as follows:

Elevation at Low Water Level	-3.79 ft.
Vertical Clearance	165.00
Calculated maximum deflection	8.49
Vertical distance from crown of roadway to bottom of stiffening truss	11.51
Elevation of crown of road at centerline	181.21

For the deck profile of a suspension bridge, the common procedure is to provide a constant side-span gradient, with a parabolic transition across the central span. However, in this case a 1,800 ft. parabolic vertical curve was extended 200 ft. onto both of the side spans. Beyond this point a 4% gradient was employed. The maximum angular rotation of

the truss at the towers due to uniform live loading and temperature gives
a change in grade of 2% which is acceptable in suspension bridge design.

The roadway-profile having thus been settled, that of the cable was
established therefrom. The relation of span to sag for the central span
varies from 1/9.5 to 1/11.5 without serious effect upon either economy
or appearance. A sag of 128 ft. was adopted, and the consequent span to
sag ratio of 10.94, closed to the optimum ratio of 11. With this ratio,
the rigidity of the cable would increase to favourable result.

Depending on the cable diameter, the shortest practicable length of
a suspender-rope, and the depths of truss and floor beam, the elevation
of the center-line of the cable at the mid-point of the central span was
established at 187.0 ft. above datum; and the elevation of the intersection
of cable-tangents at the main saddle became accordingly 315.0 ft. The
top of the tower was then fixed at Elevation 311.0 ft.

The elevation of the cable-intersection at both cable-bents, also
established at the lowest practicable level, were 153.0 ft. The side-
span sag, depending upon the central span sag and upon the relations of
dead loads and spans, was approximately 17.24 ft.

7.2 Suspension Bridge Loading

The design live loading selected for this bridge was the H20-S16
truck load and an uniform live load of 500 pounds per linear ft. per
lane was considered. Truss design was governed by all four lanes load,
giving a design live loading of 1,000 pounds per linear ft. per truss
with no reduction factors for multiple lane loading.

Impact was applied to all superstructure elements of the crossing except the cables, anchorages and towers. No impact was applied to the substructure and to the uniform live loading.

Wind loading is based on the National Building Code of Canada, Supplement No. 1 and No. 3 of 1965. In Halifax, the maximum wind gust speed for a 30 year return period is 88 mph. With the height factor of 1.4 at the deck elevation, this gives a wind gust speed of 105 mph. For the stiffening truss design, the exposed area is 6.02 sq. ft. per foot of bridge, and the total lateral wind load on trusses, deck and fence is 460 plf., compared to the minimum value of 450 plf. as given in C.S.A. -S6 - 1966. Wind on live loading is 100 plf., and on main cables is 53 plf. horizontally.

The bridge was designed for a normal temperature of 55 °F. The effect range of this temperature varied from +105°F. to -20°F.

7.3 Orthotropic Deck and Floor Truss Design

7.3.1 General

An orthotropic bridge deck generally consists of steel plates stiffened at the bottom by welded stringers and floorbeams spaced uniformly in the longitudinal and transverse directions. Since the stiffeners have different geometrical properties in two mutually perpendicular directions and are not symmetrical with respect to the middle surface of the deck plate, the monolithic unit is sometimes called an orthotropic plate with eccentric stiffeners. There are two basic types of stiffeners for orthotropic plates commonly known as torsionally soft ribs i.e. open ribs and torsionally stiff ribs i.e. closed ribs. The former offers little resistance to

torsion, while the latter provides considerable torsional resistance.

In analysing an orthotropic deck system, the basic equations describing the stresses and deformations can be formulated directly in accordance with the linear theory of elasticity. However, they are not used in design because of the mathematical difficulties involved in the solutions. An alternate approach is to assume that the orthotropic plate may be replaced by an anisotropic plate having elastic properties symmetrical with respect to the middle surface of the plate. This is known as Huber's equation, a fourth order differential equation. Even this approach involves a great deal of mathematical and numerical operations. From a practical point of view, approximate methods are acceptable for design purposes so long as the errors are small.

A simplified design procedure had been developed by eliminating some parameters in Huber's equation which were believed to be unimportant in design. Thus, the deck plate with longitudinal ribs was treated as a continuous orthotropic plate supported on rigid main girders and elastic floorbeams. The design computation was broken upon into two steps: (1) The moment in the continuous plate supported on rigid floor beams; and (2) effects of the elastic flexibility of the floorbeams were determined.

In 1963, AISC published the "Design Manual for Orthotropic Steel Plate Deck Bridges," which prompted great interest for this construction on this continent. The manual recommended a simplified design method developed by Pelikan and Esslinger.[6] The method avoided the need to solve the eighth order differential equations based on the exact theory or the fourth order differential equation based on Huber's theory for anisotropic

plates. This manual also provided design charts as well as shortcut design formulas to facilitate numerical computations. This important development enabled engineers to apply optimum design methods to obtain economic light weight structures.

7.3.2 Dimensions and Section Properties

A. Dimensions

The design and analysis of the orthotropic deck in this Bridge followed the recommendations of the AISC design manual and charts from this manual are referred to in the text. The general layout and the typical cross section of the bridge are shown in Fig. 7.2 and Fig. 7.3 respectively.

The closed ribs were rounded at the bottom and inclined at both sides. They were $\frac{1}{4}$ in. thick and 11 in. deep at 2 ft. centers. All ribs were sealed with 5/16 in. vertical diaphragm plates at both ends of each panel in order to prevent corrosion of the inside of the ribs.

The thickness of the deck plate was determined with the equation $t_p \gtrsim 0.07\ a\ \sqrt[3]{p} = 0.34$ in. A thickness of 3/8 in. was chosen, by limiting the plate deflection to 1/300 of the plate span under the action of an H20-S16 track wheel with 30% impact.

The floor trusses were located at suspender points and mid-way between them, giving an economic span of 15 ft. 10 in. for an orthotropic deck with closed ribs.

B. Section Properties

1. Closed Ribs

The section properties were computed with the effective width of the deck plate. Each rib was designed for one wheel line loading.

1. The values of I_R and S_R

Effective Floor beam spacing

$$s_1 = 0.7 \ s = 133 \text{ in.}$$

$$\frac{a}{s_1} = \frac{e}{s_1} = 0.0902$$

where $\qquad a = e = 12 \text{ in.}$

From Chart 1.

$$\frac{a_o}{a} = \frac{e_o}{e} = 1.08$$

The effective width of deck plate acting with one rib.

$$a_o + e_o = \frac{a_o}{a} a + \frac{e_o}{e} e = 25.92 \text{ in.}$$

The section properties of the ribs were:

$$I_R = 238 \text{ in}^4 \ ; \quad S_{RT} = 85.8 \text{ in}^3 \ ; \quad S_{RB} = 27.6 \text{ in}^3 \ .$$

The Section Modulus for top lateral system, consisting of truss chords, deck plate and ribs was 7250 $\text{in}^2- \text{ft}^2$.

2. The torsional rigidity

$$GK = G \ \frac{4A^2}{(u/t_R) + (a/t_P)} = 2.89 \times 10^6 \text{ k-in}^2$$

$$\frac{1}{\mu} = 1 + \frac{GK}{EI_P} \left(\frac{a^3 r^2}{2A^2} \right) \left(\frac{\pi}{s_2} \right)^2 (J + L + M + N) = 4.61$$

where $\qquad A = h \left(\frac{a+j}{2} \right) + r^2 \left(\beta - \frac{j}{2r} \cos \beta \right) = 95.15$

$$J = \left(\frac{A}{ar}\right)^2 \left(\frac{1}{24}\right) = 0.204$$

$$L = \frac{1}{24} (\lambda - B)^2$$

in which
$$\lambda = \frac{B + C}{1 + D} = 0.652$$

$$B = \frac{A}{ar} - \frac{h}{r} - (1 - \cos\beta) = -0.874$$

$$C = \frac{24}{\rho} \left(\frac{r}{a}\right)^3 \left[\frac{i}{2r} \left(1 + \frac{1}{2}\cos\beta\right) - \beta \left(\frac{1}{2} + \cos\beta\right) + \frac{h'(a + j)}{4 \, r^2} \cdot\right.$$

$$\left. (\beta - \frac{i}{2r}) + \frac{h'^2(2a + j)}{12 \, r^3} (1 - \cos\beta)\right] = 8.2$$

where
$$\rho = \left(\frac{t_R}{t_p}\right)^3 = 0.296$$

$$D = \frac{24}{\rho} \left(\frac{r}{a}\right)^3 \left[\frac{1}{2} \left(\beta - \frac{i}{2r}\cos\beta\right) + \frac{h'(a^2 + aj + j^2)}{12 \, r^3}\right] = 10.214$$

$$L = \frac{1}{24} (\lambda - B)^2 = 0.097$$

$$M = \frac{1}{\rho} \left(\frac{r}{a}\right)^3 \left[\frac{\beta^3}{3} - 2(1 + \lambda)\left(\frac{i}{2r} - \beta\cos\beta\right) + \frac{(1+\lambda)^2}{2} \cdot\right.$$

$$\left. \left(\beta - \frac{i}{2r}\cos\beta\right)\right] = -0.01034$$

$$EI_p = \frac{Et_p^3}{12(1 - \nu^2)} = \frac{Et_p^3}{10.92} = 140 \; {}^{k\text{-}in}/_{in.}$$

The effective rib span used in the computation of the torsional rigidity

$$s_2 = 0.81s = 154 \text{ in.}$$

$$N = \frac{1}{\rho} \left(\frac{r^2 h'}{a^3}\right) \left(c_1^2 + c_1 c_2 + \frac{c_2^2}{3}\right) = 0.0358$$

$$c_1 = \beta - \frac{i}{2r}(1 + \lambda) = -0.42$$

$$C_2 = \frac{h'}{r} (1 - \cos\beta) - \lambda\left(\frac{a-j}{2r}\right) = 1.273$$

The effective torsional rigidity, H, of the deck is

$$H = \frac{1}{2}\left(\frac{\mu G K}{a + e}\right) = \frac{1}{2}\left(\frac{2.89 \times 10^6}{4.61 \ (12+12)}\right) = 13,070 \ ^{k\text{-}in^2}/_{in.}$$

II. Floor Beams

The effective spacing of unequally loaded floor beams:

$$s^* = s = 15 \ ft. \ 10 \ in. = 190 \ in.$$

The floor beam system in this orthotropic bridge consisted of a top beam supported by Warren Truss, Fig. 7.4. This kind of composite revealed a five spans continuous beam. Different stages of design were considered.

1. Floor beam only:

The floor beam located above the floor truss was designed as a five span continuous beam with interior spans of 14 ft. between floor truss panel points. The effective floor beam span was:

$$l_1 = 0.8 \ l = 134.2 \ in.$$

then

$$\frac{s^*}{l_1} = \frac{190}{134.2} = 1.42$$

From Chart I $s_o / s^* = 0.33$

The effective width of deck plate acting with one floor beam was:

$$s_o = 0.33 \ s^* = 64.5 \ in.$$

The moment of inertia and section modulus of floor beam were:

$$I_F = 1,319 \ in.^4 \ ; \quad S_{Ft} = 384.0 \ in^3 \ ; \quad S_{Fb} = 82.1 \ in^3$$

2. Combined floor beam and top cnord of floor truss:

The effective floor beam span l_1 and effective width of deck plate were the same as above.

The moment of inertia and section modulus of the combined floor beam and the top chord of floor truss were:

$$I_F = 4,190.9 \text{ in}^4 \; ; \; S_{Ft} = 520.0 \text{ in}^3 \; ; \; S_{Fb} = 236.0 \text{ in}^3$$

3. Combined floor beam and floor truss as a whole

$$l_1 = l = 57 \text{ ft.} = 683 \text{ in.}$$

$$\frac{s^{\ast}}{l_1} = \frac{190}{683} = 0.278$$

$$\frac{s_o}{s^{\ast}} = 0.93$$

The effective width of deck plate acting with one floor truss was:

$$s_o = 0.93 \quad s^{\ast} = 177 \text{ in.}$$

The moment of inertia and section modulus of floor beam and the floor truss were:

$$I = 158,300 \text{ in}^4 \; ; \; S_{Ft} = 8,800 \text{ in}^3 \; ; \; S_{Fb} = 1,375 \text{ in}^3$$

4. Floor truss only

The moment of inertia and section modulus of the floor truss were:

$$I = 63,906 \text{ in}^4 \; ; \; S_{Ft} = 1,151 \text{ in}^3 \; ; \; S_{Fb} = 1,102 \text{ in}^3$$

C. Relative Rigidity Coefficients

I. Ratio of H/D_y

The relative rigidity ratio:

$$H/D_y = 0.0453$$

Where D_y was the deck rigidity in the longitudinal direction:

$$D_y = \frac{EI_R}{a + e} = 288,000 \ \text{k-in}^2/\text{in.}$$

II. Relative Rigidity Coefficient

The relative rigidity coefficient γ was calculated in three different

cases:

    1. Consider the floor beam as a continuous beam with a span of 14 ft.

between panel points acting above the top chord of the floor truss.

$$\gamma_1 = \frac{l^4 I_R}{(a+e)s^3 \pi^4 I_F} = 0.00365$$

    2. Consider the floor beam and top chord acting together as a contin-

uous beam with a span of 14 ft. between floor truss panel points.

$$\gamma_2 = 0.00115$$

    3. Consider the floor beam and floor truss a whole unit with a span

of 57 ft.

$$\gamma_3 = 0.02055$$

7.3.3 Design of the Orthotropic Deck by Charts for H20-S16 Loads

A. Bending Moment in a System with Rigid Floor Beams

I. Live Load Moments in Ribs

1. Moment at Mid-Span:

The wheel load of 16 kips with 30% impact, which gave 20.8 kips was

adopted in the design criteria.

For loading c, the moment was obtained from Chart 10.

$$M_c = 17.0 \ \text{k-in/in.} = 408 \ \text{k-in/rib}$$

For loading c_1, the moment was obtained from Chart 12

$$M_{c1} = 17.4 \text{ k.in/in.} = 418 \text{ k.in/rib}$$

Hence, loading c_1 governed the design. Due to additional wheels in the transverse direction of the bridge, an increase in the bending moments of approximately 1% to 3% resulted.

2. Moment at Support

From Chart 13, loading e, the moment at support was obtained.

$$M_s = -20.2 \text{ k-in/in.}$$

$$M_{Rs} = -M_s \ (a+e) = -485 \text{ k-in/rib}$$

II. Dead Load Moment in Ribs

The dead load for the designed ribs was 104 lbs/ft., which consisted of 3/8 in. steel deck plate, $\frac{1}{4}$ in. rib plate, 2 in. wearing surface, paint, weld etc. The rib was considered as a continuous beam under uniform distributed load. The dead load moment, at mid-span $M_D = \dfrac{Ws^2}{24} = 13.03$ k-in/rib, and at support $M_D = \dfrac{Ws^2}{12} = 26.06$ k-in/rib, was calculated by the conventional method. In the case of a longitudinal splice, an additional weight of 30 lbs/ft. was considered. An the dead load moment at mid-span and at support were 16.8 k-in/rib and 33.6 k-in/rib respectively.

III. Live load and Dead load Moments in Floor Beams

There are no available chart or table in the manual for the continuous beam as in this case. Structure analysis in this stage was quite complicated.

The impact factor for the floor beam design was 0.275, the H20-S16 truck wheel load with impact P = 16 x 1.275 = 20.4 kips. Two kinds of

loading, case A and B were considered, and the location of trucks which gave the maximum loading to the floor truss is shown in Fig. 7.5. The maximum floor beam reaction F_o on ribs were computed by:

For load in panel 0 -1 and

$$\frac{F_o}{P} = 1 - 2.1962 \left(\frac{Y}{s} \right)^2 + 1.1962 \left(\frac{Y}{s} \right)^3$$

For load other than panel 0 -1

$$\frac{F_o}{P} = \left[-0.8038 \frac{Y}{s} + 1.3923 \left(\frac{Y}{s} \right)^2 - 0.5885 \left(\frac{Y}{s} \right)^3 \right] (-0.2676)^{m-1}$$

The maximum reaction:

$$F_o = 53.6 \text{ kips (or 26.8 kips per wheel line loading).}$$

Three lanes loaded was the worst case, Fig. 7.6, and the maximum L.L. Moment occurred at 30 ft. 6 in. from either edge, with a value of 1428.0k-ft.

The floor truss was analysed in the conventional method. The diagonal live load force was -114 kips, and the dead load force was -35 kips, and a W 31 was provided. The bottom chord of the floor truss was in a square box form with 5/16 in. plates. The maximum live load in the bottom chord was 155 kips and the dead load was 48 kips.

The forces in the top chord of floor truss and floor beam were combined together. The maximum live load was -148 kips and the dead load was -49 kips with the superimposed dead load of -18 kips. In accordance with CSA-S6 specification, all the live load in the floor truss had been multiplied by a reduction factor of 0.9 for three lanes loading.

The erection dead load moment was 258 k-ft., and the superimposed dead load moment due to wearing surface and railings was 162 k-ft. At the

erection stage tne direct stress in the top cnord was 2.63 ksi while the bottom chord stress was 2.49 ksi.

B. Effects of Floor Beam Flexibility

I. Additional Moment at Mid-Span of Ribs

The loading used in computation of the bending moment increment, ΔM_R, due to floor beam flexibility is shown in Fig. 7.7. The worst case was when four lanes were fully loaded with a whole truck on each lane, even with 25% reduction. In accordance with CSA - S6 specification, the maximum moment occurred at the critical rib being 30 ft. 6 in. away from the edge. As mentioned before, 16 kips wheel load with 30% impace had been adopted. Then the additional moment at mid-span of ribs should be:

$$\Delta M_R = Q_o s \, (a+e) \, \frac{Q_{1x}}{Q_o} \sum \frac{F_m}{P} \cdot \frac{\bar{\eta}_{im}}{s}$$

where
$$Q_o = \frac{P}{2g} = \frac{16 \times 1.3}{26} = 0.800 \text{ k/in.}$$

$$s = 15 \text{ ft. } 10 \text{ in. } = 190 \text{ in.}$$

$$(a+e) = (12 + 12) = 24 \text{ in.}$$

$$\frac{Q_{1x}}{Q_o} = \frac{8}{\pi} \cos \frac{\pi z}{l} \sin \frac{\pi g}{l} \sin \frac{\pi d}{l} \sin \frac{\pi x}{l} = 0.5426$$

From Chart 22 and 23 with $\gamma = 0.0206$

$$\sum \frac{F_m}{P} \cdot \frac{\bar{\eta}_{im}}{s} = 0.0203 \qquad \text{for loading case c}$$

and
$$= 0.030 \qquad \text{for additional loading case } h_1$$

Then
$$\Delta M_R = 34.15 \text{ k-in/rib} \quad \text{for loading c+}h_1 \text{ and four lanes loaded.}$$

Since the L.L. moment in the ribs, loading c_1 was worse then loading c, therefore
$$\Delta M_R = 29.50 \text{ k.in/rib for loading } c_1+h_1 \text{ was used.}$$

II. Further Effect of Flexibility of Floor Beam Alone

The floor beam alone had further flexibility and deflected locally between truss support points. This additional flexibility corresponded to the span between truss supports, and thus also produced an additional moment for the positive moment regions of floor system. In this case two lanes loaded with a truck on each Fig. 7.8 governed the design. Employing the above formula gave ΔM_R = 8.22 k-in/rib for loading case $c+h_1$ with γ= 0.0037. Again loading c_1 + h_1 gave ΔM_R = 6.85 k-in/rib and this was used due to loading c_1 produced higher L.L. moment in ribs.

III. Moment Relief in Floor Beams

Due to floor beam flexibility, there was a reduction in the moment by the rigid system. This bending moment relief in the floor beam moment was computed by:

$$\Delta M_F = Q_o \; (\frac{1}{\pi})^2 \; \frac{Q_{1x}}{Q_o} \left[\frac{F_o}{P} - \sum \frac{F_m}{P} \overline{\nu}_{om} \right]$$

where l = 57 ft.   Impact = 0.275

$$Q_o = \frac{P}{2g} = \frac{16 \times 1.275}{26} = 0.785 \text{ k/in.}$$

$$\frac{Q_{1x}}{Q_o} = 0.3745 \text{ for three lanes loaded.}$$

Then ΔM_F = 193 k-ft.   for loading case A

And ΔM_F = 120 k-ft.   for loading case B

Since this was a relief moment loading case B had been adopted.

C. Maximum Stress in Ribs

The maximum longitudinal stresses in the ribs are given in Table 7.1. The flexural stresses are determined by using the section modulus.

In the orthotropic deck stresses were defined as:

System I: Deck plate and ribs acting as top cnord of stiffening truss, and top lateral system.

System II: Deck plate and ribs under local flexure due to wheel loads.

The Normal Unit Stress (N.U.S.) for a rib in tension was 0.6 f_y = 24 ksi and the compression was determined by inelastic overall buckling of the deck N.U.S. = 0.6 f_{cr} = 0.6 x 37.4 = 22.4 ksi.

By investigation, rib 3, Fig. 7.9 was the critical rib for maximum negative rib bending moment. Since the floor beam and floor truss flexibility effects were small at rib 3, they could be neglected. For maximum positive bending moment at middle of rib span, rib 13 was the critical one, the effects of floor beam and floor truss flexibility were included.

Loading combination for ribs were tabulated as follows:

System I_a : DL + LL + T   1.0 N.U.S.

System I_b : DL + LL + T + $\frac{1}{2}$WL + WLL   1.0 N.U.S.

System I_c : DL + WL   1.0 N.U.S.

System II : DL + TLL + I   1.0 N.U.S.

System I_a + II   1.25 N.U.S.

I_b + II   1.40 N.U.S.

Where   DL = Dead Load   WLL = Wind Load on Live Load

LL = Uniform Live Load   TLL = Truck Live Load

T = Temperature   I = Impact

WL = Wind Load

System I_c alone did not govern, and wind stresses were low at rib 13,

hence stress combination for system I_b was given at rib 3 only.

D. Bending Moment and Stress in Floor Truss

Table 7.2 shows the bending moment and stress in the floor truss. The combined stresses in the floor beam and the top chord of the floor truss by dividing the force M/d by the top cnord area are shown in Table 7. 3 and Fig. 7.10.

E. Critical Buckling Stress for Rib Plates

I. Local Buckling of Rib Plate

In calculating the local buckling of a rib plate, two systems of stresses were considered. System I produced uniform compressive stresses while System II gave bending compressive stresses in the ribs in the negative bending moment area near the floor beams.

Investigation snowed that under the truck load, the $\frac{1}{4}$ in. thick ribs buckled at a lower stress than the 3/8 in. thick deck plate with 12 in. span and partially fixed ends. Fig. 7.11.

System I

It was assumed that the rib was fixed at the deck plate and simply supported at the bottom. From Table II-1 of AISC manual k value was 5.40. The ideal buckling stress, f_i for the rib was

$$ f_i = k \frac{\pi^2 E}{12 (1 - \nu^2)} = (\frac{t}{h})^2 = 53.3 \text{ ksi} > f_p $$

where $f_p = 0.75 f_y = 30$ ksi

$\nu = 0.3$

$E = 29.6 \text{ a } 10^3$ ksi

$h/t = 13/\frac{1}{4} = 52$

Since the ideal buckling stress, f_i exceeded the proportional limit, f_p, the buckling stress became inelastic. The critical buckling stress, f_{cr}, was smaller than the ideal buckling stress, f_i. The actual critical stress was defined by:

$$f_{cr}/ f_y = 1/(1+ 0.1875 \left(\frac{f_y}{f_i} \right)^2) = 0.904$$

and $$f_{cr} = 36.2 \text{ ksi}$$

where $$f_y/f_i = 40/53.3 = 0.75$$

System II

Since the loading condition had been changed from A to C Fig. 7.12 with the same edge condition k value was 9.89. With the same formula as in System I, $f_i = 97.6$ ksi and $f_y/f_i = 40/97.6 = 0.41$

Then $$f_{cr}/f_y = 1/ (1+0.1875 (f_y/f_i)^2) = 0.968$$

$$f_{cr} = 38.7 \text{ ksi}$$

Of the total stress for the critical case, System II contributed 0.725 of an unit while 0.275 came from System I.

Then, System I + II combined has a critical stress of:

$$f_{cr} = 0.275 \times 36.2 + 0.725 \times 38.7 = 38.06 \text{ ksi}$$

The critical buckling stress was taken as 38 ksi.

II. Overall Buckling of the Deck

The floor beams of steel bridge decks of usual dimensions are sufficiently rigid to act as transverse stiffeners of the deck. Buckling of the individual longitudinal ribs of the deck is impossible, because of the elastic restraint provided by the deck plate and the adjoining ribs.

The ideal buckling stress for the deck was obtained by employing

Euler's buckling formula:

$$f_i = \frac{\pi^2 E}{(\frac{s}{r})^2} = \frac{291500}{(\frac{s}{r})^2} = 117 \text{ ksi}$$

$I_R = 238 \text{ in}^4 =$ the moment of inertia of a rib with effective

width of deck.

The area of a rib and the deck with effective width $A = 16.42 \text{ in}^2$

$$r = \sqrt{\frac{I}{A}} = 3.81 \text{ in.}$$

$$s = 190 \text{ in.}$$

And $s/r = 49.8 \text{ in.}$

Since $f_i = 117 \text{ ksi} > f_p = 30 \text{ ksi}$, the buckling stress became inelastic. The critical buckling stress, f_{cr}, was smaller than the ideal buckling stress, f_i, as mentioned before. The value of f_{cr} was obtained by:

$$f_{cr}/f_y = 1 - 0.1875 \, f_y/f_i = 0.936$$

And $f_{cr} = 37.4 \text{ ksi}$

This stress governed over the rib plate buckling. As mentioned previously, this critical buckling stress was adopted to define the allowable compressive stress in the orthotropic deck system.

7.4 Stiffening Truss Design

7.4.1 General

The main purpose of the stiffening truss is to prevent large distortions of the bridge when the live load extends over only part of its length. The stiffening trusses are subject to little or no stress when the bridge carries no live load. It can also be said that the function of the stiffening trusses is to distribute local live-loading among the suspender ropes, and eliminating uneven roadway-gradients such as would

occur if the cable were the sole restraining influence. In comparison
with that of the loaded cable, however, the stiffening effect of long
span trusses, 3,000 ft. or over, is very small, and deflections are
slightly affected by its presence.

In general, the cable take something more than 95% of primary live
loads, therefore, the stiffening trusses are hardly of any load-carrying
members. Chord-stresses are thus to all intents and purposes directly
related to the moment of inertia of the truss. It would be seen that the
optimum truss-depth is therefore the minimum consistent with effective
control of deflection, and aerodynamic stability.

In establishing the truss-depth, different factors should be con-
sidered. Contributing to this decision were studies of panel-length,
suspender-spacing, and overall-sizes and weights for shipment and erection.

7.4.2 Dimensions and Section Properties

A. Dimensions

The stiffening truss is of the Warren Type, with a vertical member
at alternate panel-points. The panel-length is 7 ft. 11 in. at top and
15 ft. 10 in. at bottom with slight variations near the end panels. The
slope of the diagonals is approximately $50°$. Fig. 7.4 The trusses are
two-hinged, but for structural and aesthetic reasons, the physical dis-
continuity at the towers has been largely concealed by the extension of the
upper chords as far as the ends of the trusses. The trusses, 57 ft. apart,
hang in the planes of the cables, and lateral X-bracing is provided be-
tween the lower chords. The spacing of suspenders is 31 ft. 8 in., lo-
cated at alternate vertical members.

The top chord of the stiffening truss is made up of two horizontal plates 3/8 in. thick and two vertical plates, $\frac{1}{2}$ in. thick while the bottom chord consists of four plates varied from $\frac{1}{2}$ in. to 1 in. thick. Both of these chords are in box form. The diagonals are I section built up with $\frac{1}{2}$ in. to 5/8 in. thick flange plates and 5/16 in. to 3/8 in. thick web plate. The vertical members also form an I-section built up with 2 - 7 in. x 3/8 in. flange plates and 1 - $17\frac{1}{4}$ in. x 5/16 in. in web plate for intermediate verticals, while 2 - 8 in. x 5/8 in. flange plates and 1 - $16\frac{3}{4}$ in. x 5/16 in. web plate are used for suspenders and truss bearings. Finally the bottom lateral system is made up of 2 - 10 in. x 7/16 in. plates and 1 -(10-5/8 in) x 5/16 in. plates, with some increase in thickness at the end panels.

B. Section Properties

The vertical moment of inertia of the stiffening trusses was calculated for the control $\frac{3}{4}$ span and then taken as constant for the full span. The moment of inertia of center span and side span was 5560 in^2 x ft^2 per truss and 5140 in^2 x ft^2 per truss respectively. The lateral moment of inertia of combined top chords and orthotropic deck plate and ribs was 158,000 in^2 x ft^2 constant for all spans. The Young's Modulus was 29.6 x 10^6 psi and the coefficient of expansion ϵ was 65 x 10^{-7} ft/linear ft/$^{\circ}$F.

7.4.3 Stiffening Truss Analysis

For the computation of cable pull, stiffening truss moments, shears, slopes, live load and temperature deflections, the simplified and explicit deflection theory developed by Ling-Hi Tsien[7] was used. It showed a great advance in design by eliminating the inconvenient successive approximation approach. The method enables a direct computation of live load horizontal cable pull to be made from any loading condition. The

accuracy of this method had been compared with the full classical deflection theory, and the maximum difference was found to be 1.5%. A Fortran computer program was written for the Ling-Hi Tsien method enabling preliminary designs to be carried out very rapidly for the stiffening trusses at each of the proposed sites.

Many researchers have shown that the "elastic theory" is not accurate enough for the exact design of a suspension bridge. The "deflection theory" is more accurate but is very tedious and involves many cut-and-try processes. The "trigonometric series" method developed by S. Timoshenko has distinct advantages over the original deflection theory method in several respects; but the expressions are not completely explicit, and the computations are lengthy and involved. Moreover, the location and magnitude of maximum bending moments and shears in a stiffening truss for various loading conditions cannot be determined directly without trial and error.

The important features in Ling Hi Tsien simple method are that:

1. When the live load moves on the bridge, the horizontal tension in the cable varies very closely according to certain circular functions irrespective of both the ratio between the dead load and live load, and degree of stiffness of the truss; and

2. The equations of moments and shears can be reduced to explicit and simple forms in hyperbolic functions which are suitable for the direct determination of maxima by mathematics, with acceptable approximations.

In using this method, the calculated result is probably more accurate than that obtained by the cut-and-try method at the first few trials. The formulas are so clear and explicit that the saving in labour and mistakes can be avoided. Because of its simplicity and accuracy, the method can be used for preliminary design purposes as well as for the final analysis of a suspension bridge.

The design dead load was 5765 lbs/linear horizontal ft. and was assumed to be uniformly distributed throughout the span. The horizontal component of cable pull due to dead load was:

$$H_w = wl^2/8f = 5520 \text{ kips}$$

The following are the design constants for Ling-Hi Tsien's definitions:

$$r = l_1/l = 513.83/1400 = 0.367$$

$$\alpha_1 = 17°30' \; ; \; \sec \alpha_1 = 1.0485$$

$$f_1 = f(w_1/w)(l_1/l)^2 = 17.24 \text{ ft.}$$

$$n_1 = f_1/l_1 = 0.03355$$

$$n = f/l = 0.0914$$

$$n_1/n = 0.367$$

$$q = \frac{p}{w} = \frac{1.0}{2.882} = 0.347$$

$$Q = 8f/pl^2 \times H = 5.224 \times 10^{-4} \times H \qquad \text{For main span}$$

$$Q_1 = 8 f_1/pl_1^2 \times H = 5.224 \times 10^{-4} \times H \qquad \text{For side span}$$

$$EI = 16.465 \times 10^7 \text{ k-ft}^2$$

$$EI_1 = 15.217 \times 10^7 \text{ k-ft}^2$$

$$B = 1 + \frac{9.6 \; EI}{H_w l^2} = 1.150$$

$$B_1 = 1 + \frac{9.6 \ EI_1}{H_w \ l_1^2} = 2.030$$

The factor N_s to reflect the effect of the side spans

$$N_s = \frac{2r}{sec^2 \alpha_1 \ (1-2.35 \ n^2)} \cdot \frac{n_1^2}{n^2} \cdot \frac{q+1.2B}{q+1.2B_1} = 0.0570$$

Due to cable stretch value of L_s :

$$L_s = \sum l(sec^3 \alpha + 8n^2) = 3,435.6 \ ft.$$

Due to temperature change, value of L_t :

$$L_t = \sum l(sec^2 \alpha + \frac{16}{3} n^2) = 3313.5 \ ft.$$

And
$$S = \frac{r^2}{sec^2 \alpha_1 \ (1-2.35 \ n^2)} \cdot \frac{n_1}{n} \cdot \frac{B}{B_1} = 0.02598$$

The factor N_c to reflect cable stretch

$$N_c = \frac{0.187}{n^2} \cdot \frac{H_w}{E_c A_o} \cdot \frac{L_s}{l} \ (\frac{q}{1.2} + B) = 0.2052$$

The factor N_t and T in relation to temperature change for $50^o F$ rise

$$N_t = \frac{0.187 \ \epsilon \Delta t \ L_t}{n^2 \ l} = 0.01722$$

$$T = \frac{B}{q} N_t = 0.0556$$

for $\qquad -75^o F$

$$N_t = 0.02583$$

$$T = 0.0834$$

$$D_{normal \ T} = 1 + N_s + N_c = 1.2622$$

$$D_{+t} = 1 + N_s + N_c + N_t = 1.2794$$

$$D_{-t} = 1 + N_s + N_c - N_t = 1.2364$$

A. Central Span

I. The maximum positive moment in main span

Case I. Fig. 7.13

Case Condition : Maximum temperature rise + load from one end + no load

on side spans

Try with $\qquad x_{+m} = 0.22 \, l = 308$ ft.

And $\qquad k_{+m} = 0.383 \, l = 536.2$ ft.

The horizontal component of cable pull due to live load.

$$H_f = \frac{p \, l^2}{8f \, D_{+t}} \left(\sin^2 \frac{k\pi}{2l} - T \right) = 396 \text{ kips.}$$

$$c = c_f = \sqrt{\frac{H_w + H_f}{EI}} = 0.005920$$

Then $\qquad$ +Maximum $M = \dfrac{p \, l^2}{c^2 \, l^2} (1-Q) \tanh (c x_{+m}) \tanh \dfrac{c x_{+m}}{2} = 15{,}535^{\text{k-ft}}$

II. The maximum positive moment at center of main span

Case III. Fig. 7.13

Case Condition : Maximum temperature + load symmetrical about center line

of main span + no load on side spans.

Try $\qquad k_{+c} = 0.34 \, l = 476$ ft.

$$H_{III} = \frac{p \, l^2}{8f \, D_{+t}} \left(\cos \frac{k\pi}{l} - T \right) = 637.6 \text{ kips.}$$

$$c = \sqrt{\frac{H_w + H_f}{EI}} = 0.006043$$

Then $\quad$ +Maximum $M = \dfrac{p\,l^2}{c^2 l^2}\left[(1-q)\left(1-\dfrac{1}{\cosh\frac{cl}{2}}\right)-\dfrac{\cosh(ck)-1}{\cosh\frac{cl}{2}}\right]$

$\qquad\qquad\qquad = 11{,}500$ k-ft.

III. The maximum negative moment in main span

Case II. Fig. 7.13

Case Condition : Minimum temperature + side spans loaded + center span

$\qquad\qquad$ unsymmetrically load from end

Try $\qquad x_{-m} = 0.21\,l = 294.0$ ft.

And $\qquad k_{-m} = 0.382\,l = 530.6$ ft.

$\qquad H_{II} = \dfrac{p\,l^2}{8f\,D_{-t}}\left(\cos^2\dfrac{k\pi}{2l}+2S+T\right) = 1{,}264$ kips.

$\qquad c = \sqrt{\dfrac{H_w+H_f}{EI}} = 0.006349$

Then $\quad$ − Maximum $M = -\dfrac{p\,l^2}{c^2 l^2}\,Q\,\tanh(c\,x_{-m})\,\tanh\dfrac{cx_{-m}}{2} = -11{,}434$ k-ft.

IV. The maximum negative moment at center of main span.

Case IV. Fig. 7.13

Case Condition : Minimum temperature + side spans loaded + center span

$\qquad\qquad$ symmetrically loaded from ends.

Try $\qquad k_{-c} = 0.337\,l = 480.2$ ft.

$\qquad H_{IV} = \dfrac{p\,l^2}{8f\,D_{-t}}\left(1-\cos\dfrac{k\pi}{l}+2S+T\right) = 999.1$ kips

$\qquad c = \sqrt{\dfrac{H_w+H_f}{EI}} = 0.006221$

Then $\quad$ -Max. $M = -\dfrac{p l^2}{c^2 l^2} \left[Q \left(1 - \dfrac{1}{\cosh \frac{cl}{2}} \right) - \dfrac{\cosh (c\ k) - 1}{\cosh \frac{cl}{2}} \right]$

$$= -7,536 \text{ k-ft.}$$

V. Maximum positive shear at ends

Case I Fig. 7.13

Case Condition: Same as previous Case I

Try $\qquad k_{+v} = 0.257\,l = 359.8$ ft.

$$H_I = \frac{p\,l^2}{8f\ D_{-t}} = (\sin^2 \frac{k\pi}{2l} - T) = 148 \text{ kips}$$

$$c = \sqrt{\frac{H_w + H_f}{EI}} = 0.005791$$

Then $\qquad$ + Max. $V = \dfrac{p l}{c l} \left[(1 - Q) \tanh \dfrac{cl}{2} - \dfrac{\cosh c\ (l-k) -1}{\sinh (c l)} \right]$

$$= 138 \text{ kips}$$

VI. Maximum positive shear at center of main span:

Case I and same condition as above, but

Try $\qquad k_{+v} = 0.5\,l = 700$ ft.

$$H_I = \frac{p l^2}{8f\ D_{+t}} = (\sin^2 \frac{k\pi}{2l} - T) = 665 \text{ kips}$$

$$c = \sqrt{\frac{H_w + H_f}{EI}} = 0.006055$$

Then $\qquad$ +Max. $V = \dfrac{p l}{2\ c l} \tanh \dfrac{cl}{4} = 80.2$ kips.

VII. Negative shear

Case II. Fig. 7.13

Case Condition : Same as previous Case II.

Try $\qquad k_{-v} = 0.265\, l = 371$ ft.

$$H_{II} = \frac{p\,l^2}{8f\,D_{-t}} \left(\cos^2 \frac{k\pi}{2l} + 2S + T\right) = 1504.5 \text{ kips.}$$

$$c = \sqrt{\frac{H_w + H_f}{EI}} = 0.006484$$

Then $\qquad$ -Max. $V = -\dfrac{p\,l}{c\,l}\left[Q \tanh \dfrac{c\,l}{2} - \dfrac{\cosh c\,(l-k) - 1}{\sinh c\,l}\right] = -106.8$ kips

VIII. Maximum negative shear at center of span

Case II. Fig. 7.13

Case Condition : Same as previous Case II.

Try $\qquad k_{-v} = 0.5\, l = 700$ ft.

$$H_{II} = \frac{p\,l^2}{8f\,D_{-t}} \left(\cos^2 \frac{k\pi}{2l} + 2S + T\right) = 954 \text{ kips}$$

$$c = \sqrt{\frac{H_w + H_f}{EI}} = 0.006215$$

Then $\qquad$ -Max. $V = \dfrac{p\,l}{2c\,l} \tanh \dfrac{c\,l}{4} = -78.5$ kips

B. Side Span

1. Maximum positive moment in side span

Case V. Fig. 7.13

Case Condition : Maximum temperature + one side span fully loaded + no

loading on other spans.

$$H_V = \frac{p\,l^2}{8f\,D_{+t}} (S - T) = -44 \text{ kips.}$$

$$c_1 = \sqrt{\frac{H_w + H_f}{EI}} = 0.005918$$

Then $\qquad$ +Max. $M = \dfrac{p\,l_1^2}{c_1^2 l_1^2} (1-Q) \tanh \dfrac{c_1 l_1}{2} \tanh \dfrac{c_1 l_1}{4} = 17{,}040$ k.ft.

II. Maximum negative moment in side span

Case VI. Fig. 7.13

Case Condition: Minimum temperature + L.L. on main span + L.L. on other
side span

$$H_{VI} = \frac{p l^2}{8f \, D_{-t}} (1+S+T) = 1,717 \text{ kips.}$$

$$c_1 = \sqrt{\frac{H_w + H_f}{EI}} = 0.006828$$

Then $-\text{Max. } M = \frac{p \, l_1^2}{c_1^2 \, l_1^2} \, Q \tanh \frac{c_1 \, l_1}{2} \tanh \frac{c_1 \, l_1}{4} = -12,776 \text{ k-ft.}$

Shear force in Side Span

III. Positive shear at side span

Case VII. Fig. 7.13

Case Condition : Maximum temperature + partly loaded from tower + no L.L.
on the portions.

Try $k = 0.5 \, l_1 = 256.92 \text{ ft.}$

$$H_{VII} = \frac{p l^2}{8f \, D_{+t}} (S \cos^2 \frac{k \, \pi}{2 \, l_1} - T) = -64 \text{ kips}$$

$$c_1 = \sqrt{\frac{H_w + H_f}{EI}} = 0.005908$$

Then $+V = \frac{p \, l_1}{2c_1 \, l_1} \tanh \frac{c_1 \, l_1}{4} = 54.2 \text{ kips}$

IV. Maximum shear force at end

Case V. Fig. 7.13

Case Condition : Same as previous Case V

$$H_V = \frac{p \, l^2}{8f \, D_{+t}} (S-T) = -44.3 \text{ kips.}$$

$$c_1 = \sqrt{\frac{H_w + H_f}{EI}} = 0.005918$$

Then
$$+\text{Max. } V = \frac{p \, l_1}{c_1 \, l_1} (1-Q) \tanh \frac{c_1 l_1}{2} = 157.1 \text{ kips.}$$

V. Maximum negative shear at side spans

Case VIII. Fig. 7.13

Case Condition : Maximum temperature + L.L. on main span and one side

span + partial load on other side span.

at
$$x = k = 0$$

$$H_{VIII} = \frac{p l^2}{8f \, D_{-t}} (1+S+S \sin^2 \frac{k\pi}{2l_1} +T) = 1,718 \text{ kips}$$

$$c_1 = \sqrt{\frac{H_w + H_f}{EI}} = 0.00682$$

Then
$$-\text{Max. } V = -\frac{p \, l_1}{c_1 \, l_1} Q \tanh \frac{c_1 l_1}{2} = -124 \text{ kips.}$$

Summary of moments and shears for the bridge is shown in Fig. 7.14

C. Deflection

I. Maximum deflection at center of main span

Case III. Fig. 7.13

Case Condition : Same as previous Case III

$$H_{III} = \frac{p l^2}{8f \, D_{+t}} (1-T) = 1,405 \text{ kips.}$$

$$c = \sqrt{\frac{H_w + H_f}{EI}} = 0.006485$$

$$Q = H \frac{8f}{p \, l^2} = 0.733$$

Then maximum deflection at center of main span, approximate

method: $\eta_c = \dfrac{5}{384} \cdot \dfrac{p\,l^4}{EI}\left[\dfrac{1-Q}{1+\dfrac{c^2 l^2}{9.7}}\right] = 8.54$ ft.

By more exact method the deflection = 8.49 at center of span.

II. Maximum deflection at center of side span

Case V Fig. 7.13

Case Condition : Same as previous Case V

$$H_V = \dfrac{p\,l^2}{8f\,D_{+t}}\,(S-T) = -45 \text{ kips.}$$

$$c_1 = \sqrt{\dfrac{H_W + H_f}{EI}} = 0.006$$

$$Q = H\,\dfrac{8f}{p\,l^2} = -0.0235$$

Then maximum deflection at center of side span

$$\eta_c = \dfrac{p\,l_1^4(1-Q)}{c_1^4\,l_1^4\,EI_1}\left[\dfrac{c_1^2\,l_1^2}{8} - 1 + \dfrac{1}{\cosh\dfrac{c_1 l_1}{2}}\right] = 3.10 \text{ ft.}$$

D. Grade Change

I. Maximum change in grade for side span at tower

Case V. Fig. 7.13

Case Condition : Same as previous Case V.

$$\theta_A = \dfrac{p\,l_1^3}{24\,EI_1}\,\dfrac{(1-Q)}{\left(1 + \dfrac{c_1^2\,l_1^2}{10.5}\right)} = 0.01995 = 1.995\% \text{ say } 2\%$$

Then   Maximum total grade = 4% + 2% = 6%

II. Maximum change in grade for main span at tower

Case II. Fig. 7.13

Case Condition : Same as previous Case II

for $\qquad$ $k = 0.5$ $\qquad l = 700$ ft.

And $\qquad$ $H = \dfrac{p\,l^2}{8f\ D_{-t}}\ (\cos^2 \dfrac{k\pi}{2l} + 2S + T) = 984$ kips

And $\qquad$ $c = \sqrt{\dfrac{H_w + H_f}{EI}} = 0.00629$

$\qquad\qquad$ $Q = H\ \dfrac{8f}{p\,l^2} = 0.514$

$\qquad\qquad$ $\theta_A = \dfrac{p\,l^3}{24\ EI}\ \dfrac{(Q - f\,(k)\,)}{(1 + \dfrac{c^2 l^2}{10.5})} = 0.0161 = 1.61\%$

Where $\qquad$ $f\,(k) = \dfrac{\dfrac{cl}{4} - \tanh \dfrac{cl}{4}\ \dfrac{1}{\cosh \dfrac{cl}{2}}}{cl - 2 \tanh \dfrac{cl}{2}} = 0.32$

Therefore $\qquad$ Grade change $= 1.61\%$, less than on side span

And $\qquad$ Maximum total grade $= 4\% + 1.61\% = 5.61\%$

7.5 Main Cable Design And Suspender Ropes Design

The maximum tension in the cables of a suspension bridge occurs when all the spans are loaded, with the temperature at its lowest point. Throughout the cable, for any given loading, the horizontal component of the tension is constant, the tension itself varying with the angle of slope. In the present case, the heaviest loading of the cables occurs when the three spans are covered with the uniform loading of 500 lb/linear ft. per lane, with the temperature at the selected minimum of -20°F. For the computation of cable pull, again the simplified deflection theory method developed by Ling-Hi Tsien was used.

$$\tan \alpha_1 = \frac{162}{513.83} = 0.3153$$

$$\tan \theta_1 = \tan \alpha_1 + \frac{4 \, f_1}{l_1} = 0.4494$$

$$\theta_1 = 24°12'$$

$$H_w = \frac{wl^2}{8f} = 5520 \text{ kips.}$$
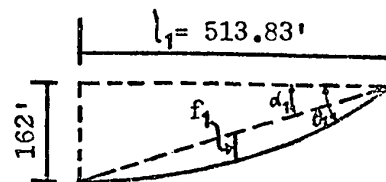
Maximum tension in the cable due to D.L.

$$T_w = H_w \sec \theta_1 = 6050 \text{ kips}$$

To find the tension in the cable due to live load, the main span and the side spans are fully loaded at normal temperature of 55°F

$$H = \frac{pl^2}{8f \, D_{-t}} (1+2S+T) = 1593 \text{ kips.}$$

$$T = H \sec \theta_1 = 1,748 \text{ kips}$$

Total $\qquad T + T_w = 1,748 + 6,050 = 7,798$ kips

Factor of safety base on Minimum Ultimate Strength of Strands

$$= \frac{300 \times 61}{7798} = 2.35$$

The working-unit stress adopted for the cables was 90,000 psi with ultimate strength of 150 tons per strand and minimum $E = 24 \times 10^6$ psi.

Helical strands were used for the cables and not the parallel wire strands recently developed in the U.S. The parallel wire strands are economical for long spans that would previously have required cables to be spun in place. There should be little difference in cost between helical strands and parallel wire strands for shorter spans, the reduction in efficiency of some 4% in the helical strands probably being offset by their greater ease of handling and reeling compared to parallel wire strands.

The natural grouping of parallel strands lying compactly in contact is hexagonal, and that optimum shape demands that the number of strands shall be one of tne series 1, 7, 19, 37, 61, 91, 127 etc. In order to avoid undue stiffness and weignt of strand on the one hand, and too cumbersome an anchorage-assembly on the other, the number in this case was selected as 61, the corresponding strand-diameter being approximately 1-9/16 in. The total cross-sectional area of the cable was 86.7 sq. in. Fig. 7.15.

Wire wrapping has been proved to be a satisfactory method of protecting cables provided that care is taken to protect the galvanizing of the strand wires throughout the manufacturing, prestressing and erection process and provided that the cables are regularly inspected and well maintained. In the final assembly, the hexagonal form is rounded out by six oil-impregnated cedar-wood fillers, the whole being tightly bound together by a continuous serving of No. 9 S.W.G. soft annealed galvanized wire. The finished diameter of the cable is approximately 14-3/8 in.

In the design of suspender ropes, the governing suspender-load was arrived at by consideration of two adjacent 31 ft. 8 in. panels of the bridge deck. The trusses were assumed discontinuous at the ends of each panel and therefore capable only of bridging the space between one suspender and the next. The trucks were then placed on each lane to deliver the worst possible reaction at the middle pair of the six suspenders involved in the hypothetical case.

The type of suspender selected consisted of a wire rope Fig. 7.16, the ends of wnich are attached to lugs on the trusses while the bright

passes over a cable band on the main cable Fig. 11-15. The load is thus
shared by two part of rope. The sockets are of standard open type, each
having a pair of lugs. The lugs straddle of the truss and which like
the latter are bored to receive a $3\frac{3}{4}$ in. pin which in turn is secured by
a $\frac{1}{2}$ in. cotter pin.

7.6 Specification for Cable Strands

A very complete specification was drawn up covering the manufacture
and fabrication of the cables. The clauses pertaining to the cable strands
may be summarized as follows:

"The wire for cable strands and suspender ropes were galvanized cold-
drawn bridge wire manufactured in accordance with the best current practice,
and were the product of a manufacturer of established reputation for this
type of wire.

All steel for cable and suspender wire was made specifically for
this project and was so handled, marked and isolated as to prevent any
possibility of its becoming mixed with other lots or kinds of steel.

The maximum permissible percentage of certain elements in the steel
were specified as follows: carbon 0.85, phosphorus 0.04, sulphur 0.04.

The galvanized wire was sufficiently ductile to be capable of being
coiled around a mandrel of a diameter three times that of the wire without
showing sign of fracture.

The individual wires of each and every main cable strand were con-
tinuous and unspliced for the full length of the strand.

The total metallic area of the wires in each main cable strand, not

including filler wires or galvanizing, was 1.422 sq. in. The individual wires of the strand could not be larger than No. 6 S.W.G. or 0.192 in. norminal diameter measured before galvanizing.

In each strand the outer layer of wires was laid opposite hand to the inner layer to minimize any tendency of the strand to twist.

Strands in respect to their outer wires were to be of right- or left-hand lay according to their positions in the cable, so as to avoid excessive bearing pressure in the saddles due to point-contact between wires of successive layers of strands.

Tensile strength tests were made from specimens cut from both ends of each single wire length or coil of wire.

The minimum ultimate strength of the strand was not less than 300,000 pounds. The modulus of elasticity of the strand after prestressing was not less than 25×10^6 psi of ungalvanized area up to 50% of the ultimate strength."

7.7 Design of Bottom Lateral System

The bottom lateral system of a suspension bridge is controlled by either one of horizontal wind pressure, live load torsion, or aerodynamic effect. The design procedures are shown as follows:

7.7.1 Wind on Bottom Lateral System

To work out the exact distribution of wind load between the top and bottom system is a tedious task. The orthotropic deck acting with the top chord is more rigid than the bottom chord and therefore is capable of taking more load. For simplicity, consider wind acting on lower half

of the stiffening truss to be taken by bottom lateral system, and further-more, restitution from wind on bottom chord is ignored. Then:

The projected area per 15 ft. 10 in. panel = 36.1 sq. ft.

The Height Factor at Elevation of Deck C_h = 1.4

The Fullness Factor k C_{nx} = 1.6

The Shielding Factor k_x = 1.0

In Halifax, maximum wind gust speed for 30 year return period is 88 mph. Then the basic wind pressure q=21 psf. and the wind pressure at the Elevation of Deck = $kC_{nx}qC_h$ = 47 psf. This is equal to a wind gust speed of 105 mph. The force due to wind load at each bottom panel point is shown in Fig. 7.17.

7.7.2 Live Load Torsion on Bottom Lateral System

The live load torsion is produced by any loading which is not sym-metrical about the center line of bridge. The worst case will be two lanes loaded with 500 lb/ft/lane. The simple beam reactions to the truss will be R_1 = 0.71 k/ft. R_2 = 0.29 k/ft. This loading can be replaced by a symmetrical and a skew symmetrical pair of loading. Fig. 7.18. The symmetrical loads produce pure bending while the skew symmetrical loads produce torsion. Only torsion due to live load is of interest in the bottom lateral design. The skew symmetrical loading (iii) of 0.21 k/ft. acts on combined truss and cable, the division of the load between truss and cable depending upon the load system and the torsional stiffness of the box section. With full depth floor trusses every 15 ft. 10 in. Fig. 7.4, acting as intermediate diaphragms, virtually, all the twisting load will be taken by torsional action of the box system of trusses and top and bottom laterals. Due to the participation of these diaphragms, warp-

ing can be ignored and pure tosional shear flow assumed, so that the torsional moment M_t produces horizontal and vertical shearing forces on the box V_h, V_v where:

$$V_h = \frac{M_t}{2d}$$

$$V_v = \frac{M_t}{2b}$$

$$M_t = V_h d + V_v b = Vb$$

And here   d = depth of stiffening truss = 10 ft.

           b = width of bridge c. to c. of truss = 57 ft.

There are three cases, in which the truss shear V depending on the loading system can be defined.

Case A

Load on one side of the bridge only. Fig. 7. 19. This loading will produce downward load on near truss and upward on the far truss, and the torsional deflected shape will not have an intermediate node i.e. n=1. From suspension bridge theory, the truss shear V is in terms of bending rigidity EI and not in terms of torsional rigidity. Thus an equivalent bending rigidity EI_T must be calculated reflecting the torsional rigidity before the usual shear analysis can be applied. This has been done by trial and error to choose an EI_T value such that the bending deflection under type (iii) loading using EI_T is the same as the torsional deformation calculated from the V values. This technique would only be accurate if the deflected shape for bending and torsion were of the same form, and to be precise a new calculation of EI_T would be required for each loading case. However, study reveals that with the very large values

of EI_T , the critical load lengths are long, and the deflected shapes for
bending and torsion under these long load lengths are of similar form.
The EI_T analysis was carried out for a load covering the full span, and
also for a load covering half the span from tower to center line, and the
same value of EI_T resulted from both cases. This value of EI_T=10,000 x
10^6 k-ft^2 (compared the actual EI of 164.65 x 10^6 k-ft^2) was thus assumed
to be satisfactory for all case A loads, as the critical lengths for maxi-
mum V all were in the range of half to full span load lengths. The Ling-
Hi Tsien method was used to calculate the V value, but it was found that
Elastic Theory gave V value within 10% for a bridge with this very high
EI_T value. Thus superposition method could be applied with sufficient
accuracy.

For general case of loading for maximum positive shear at section
x is shown in Fig. 7.20. If k_1 = x and define the value of k_2 (or m_2)
to give maximum shear at each point. By the following equation, the
value of m_2 can be obtained.

$$\frac{\pi}{clD} \frac{\sinh c\left(\frac{l}{2} - k_1\right)}{\cosh c\, k_1} \sinh \frac{cl}{2} = \frac{\sinh cm_2}{\sin \frac{m_2 \pi}{l}}$$

By trial and error for

$$k_1 = 0,\ \tfrac{1}{32},\ \tfrac{1}{16},\ \tfrac{1}{8},\ \tfrac{1}{4},\ 3\tfrac{1}{8}\text{ and }\tfrac{1}{2}$$

all give m_2 = 0 except m_2 = 0.222 for k_1 = 0

to obtain maximum end shear.

And the shear

$$V_x = \frac{p_s l}{cl}\left[- Q\,\frac{\sinh c\left(\frac{l}{2} - k_1\right)}{\cosh \frac{cl}{2}} + \frac{\left(\cosh c\left(l - k_1\right) - \cosh c\, m_2\right)}{\sinh cl}\right].$$

$$\left. \cosh c \; k_1 \right]$$

Case B

Load on both sides, diagonally symmetrical Fig. 7.21, this loading will produce equal up and down loads on any truss, and the torsional deflected shape will have an intermediate node i.e. n = 2.

For this case the equivalent EI_T would be higher than Case A, and Elastic Theory would be even more accurate and could be applied. For this loading by Elastic Theory, there would be no change in cable tension, thus H = 0. The shear equation is:

$$V = V' - H \tan \phi$$

Where $\quad V' =$ simple span shear

$\phi =$ the inclination of the cable at the section considered.

From Fig. 7.22, simple truss shear for anti-symmetrical loading, the general case

$$R = \frac{p_s k}{l} \; (l - k - 2n) \qquad \text{where} \quad p_s = 0.21 \text{ kip/ft.}$$

for Maximum +ve shear

$$V = \frac{p_s}{l} \left(\frac{l}{2} - n \right)^2 \qquad \text{where } m = 0$$

for Maximum -ve shear

$$V = - \frac{p_s}{l} \left(\frac{l}{2} - m \right)^2 \qquad \text{where } n = 0$$

Case C

Load on both sides, but not symmetrically. This would require an analysis of the type carried out for Case A, but would become very complex and is unlikely to be the governing load case for any point.

7.7.3 Design of Bottom Laterals

The wind load and live load torsion is shown in Fig. 7.17, where all members were designed as a double acting system i.e. tension and compression.

Force in each diagonal member was :

$$F = \frac{V}{2} \left(\frac{42.6}{28.5} \right)$$

And the allowable stresses in bottom laterals were:

Full wind only	1.0 NUS
Live load torsion only (no temperature effect)	1.1 NUS
Live load torsion+$\frac{1}{2}$ wind + wind on L.L.	1.25 NUS

It should be notice that wind on L.L. would not affect the bottom laterals design. Most of the bottom laterals were governed by L.L. torsion except some panels at main span due to aerodynamic effects. The average area of bottom lateral was 12.22 sq. in. while area of 12.38 sq. in. for aerodynamic study was 1% less. This was insignificant and the design was satisfied.

There were four types of bottom laterals depending on the critical loading in the panel.

Type A. Fig. 7.23

An I section composed of two 8$\frac{1}{2}$ in. by 3/8 in. flanges and a 10$\frac{3}{4}$ in. by 5/16 in. web.

The section area

$$A_G = 9.73 \text{ sq. in.}$$

The radius of gyration r = 1.98

$$\frac{kl}{r} = 129$$

Capacity in compression = 84.6 kips

Capacity in tension = 197 kips

This type was used for all side span except at end panels 0 to 12

and 52 to 64

Type B   Fig. 7.23

    Same as Type A but composed of two 10 in. by 7/16 in. flanges and a 10-5/8 in. by 5/16 in. web.

$$A_G = 12.07 \text{ sq. in.}$$

$$r = 2.46$$

$$\frac{kl}{r} = 104$$

Capacity in compression = 162 kips

Capacity in tension = 227 kips

    This type was used for center span at panel 12 to 88 and for side span at panel 0 to 12 and 52 to 64.

Type C   Fig. 7.23

    Same as Type A but composed of two 10 in. by $\frac{1}{2}$ in. flanges and a $10\frac{1}{2}$ in. by 5/16 in. web.

$$A_G = 13.28 \text{ sq. in.}$$

$$r = 2.5$$

$$\frac{kl}{r} = 102$$

Capacity in compression = 185 kips

Capacity in tension = 247 kips.

    This type was used for center span at panel 4 to 12.

Type D   Fig. 7.23

    Same as Type A but composed of two 10 in. by 9/16 in. flanges and a 10-3/8 in. by 5/16 in. web.

$$A_G = 14.48 \text{ sq. in.}$$

$$r = 2.54$$

$$\frac{kl}{r} = 101$$

Capacity in compression = 203 kips

Capacity in tension = 266 kips

This type was used for center span at panel 0 to 4.

7.8 Main Tower Design

7.8.1 General Description of the Towers

The two main towers, of fixed base type, are shown in Fig. 7.24. Each tower is 290 ft. high with a pair of slender columns carrying the main cable-saddles and thus providing primary support for the suspension-system. The tower is braced to resist transverse loads, and is restrained longitudinally at the top by the cables themselves. The saddles are attached positively to the towers. The two columns of each tower are built up cruciform shapes, consisting of a constant 8 ft. x 4 ft. core section flanked by two tapering wings, giving overall dimensions of 8 ft. by 10 ft. at the top and 8 ft. by 13 ft. 6 in. at the base. The sections are stiffened by T-shaped load bearing stiffeners.

The importance of the appearance of the towers was realized from the outset, and every effort was made by the engineers to render these dominating structures pleasing to the eyes. To this end the form and arrangement of the tower-bracing were carefully considered, the X-type being selected and possessing those satisfactory aesthetic qualities which normally derive from a "functional" design. The tower diagonals are 2 ft. x 4 ft. welded sealed boxes also internally stiffened.

An inspection-ladder is provided in each chamber of the tower columns. These ladders are continuous for the full length of the chambers, and

manholes give access from one chamber to another at various levels. Entrance to the interior of the columns is effected by doors at roadway-level and at the base of the tower. Other access is located at the top of the columns. There are also fenced walkways along the top-struts. Electric lighting is installed in all the chambers, the controlling switches being situated near the principal points of entrance.

7.8.2 Main Tower Design

The design was carried out for the Dartmouth Tower. Loading to the Halifax Tower was the same but the movement was less, therefore, Dartmouth Tower governed the design, and both towers were built identically. Under any condition of bridge-loading, the cables assume a position of equilibrium so that the horizontal component of tension is constant throughout the system. Since, however, the reaction-pressure of the cable on the main saddles is sufficiently great to preclude cable slip at those points, and as in any case it would be undesirable to permit such sliding to occur, any balancing-forces are accommodated by longitudinal displacements of the tower tops.

The conditions of loading which govern the design of the towers are apparent from inspection. Thus, the heaviest cable-reaction will occur when all three suspended spans are fully loaded at the minimum temperature. The greatest saddle-movement, however, will take place when the central and far-side spans are loaded at maximum temperature. The latter case, together with wind-loading, was found to be controlled.

Under a particular live load and temperature condition, the top of the towers move a fixed distance which can be calculated from the changes

in the length of the deflected cable and the cable pull. Under such
deflection, there will be longitudinal bending stress in the tower legs
due to eccentricity of the cable reaction and other vertical loads, and
due to any unbalanced horizontal cable pull P at the top of the tower.
The total movement at any point will be the sum of the deflection due to
a free standing tower under the eccentric moments, and the deflection due
to the unbalanced horizontal cable pull P.

The first step in design was the assumption of a suitably tapered
"trial" column, capable of withstanding the loading from the cable with
the saddle in its deflected position. The second step was the assumption
of an elastic curve for the column when subjected to a particular loading
and simultaneously deflected by the appropriate amount. With this assump-
tion, the moments in and deflections at the various sections were figured.
The top deflection was differed, one way or the other, from the original
amount, owing to the moments caused by the eccentricity of the vertical
loads. That original amount is entirely independent of the dimensions of
the column for all practical purposes. Accordingly, the next step was
the evaluation of the induced horizontal load necessary to maintain the
status. The elastic curve due to this induced load was then superimposed
on that due to the vertical loading-condition, and the resulting composite
curve gave the required actual saddle-deflection but did not necessarily
agree throughout its length with the assumed curve. New assumptions for
the curve were then tried until such agreement occurred. The stresses
over the various sections were then inspected, and suitable alternations
in size and disposition of metal were made. The procedure was then repeated
to determine the new elastic curve. Similar computations were performed

for all important loading conditions including those involving longitu-
dinal wind-loads, which set up a cable-pull in addition to the above
induced load.

As the method requires a successive approximation approach to find
the elastic curve for the tower for each loading case, it is ideally suited
to solve by computer, and a Fortran program was written and used for the
study phase and the final design. The maximum value for the tower move-
ment was 1.44 ft. and the maximum value of the unbalanced horizontal cable
pull P at top of the tower was 7.64 kips. A design assumption for the
truss analysis is that the horizontal component of the cable pull is the
same throughout the length of the cable. The small value of P, compared
to the total horizontal cable pull of 6,970 kips for this loading, illus-
trated that the effect of the tower bending rigidity on the cable pull can
be ignored and the assumption is thus valid.

The tabulation given below, Table 7.4 summarizes the cable reactions,
suspended trusses reaction, tower moment, and induced cable pulls for the
principal conditions of loading, applied to the column finally adopted.

The use of an orthotropic deck instead of a standard deck for the
suspended structure affected economies in the tower design by reducing
the dead load cable reaction, and by giving a better distribution of lateral
wind load to the towers. Under the action of lateral wind, the trusses
and cables deflect transversely with a portion of wind load from the
suspended structure transferring to the cables, and hence to the tops of
the towers. The higher lateral stiffness of the orthotropic deck compared
to the standard deck reduces this transfer. Thus a greater proportion of
the total wind load on the suspended structure is applied to the towers

at the stiffening truss level, which reduces the axial load in the tower legs due to wind, the wind load in the tower diagonal bracing above the roadway and the transverse bending in the tower legs resulting from the omission of diagonal bracing near deck level.

7.9 Tower Base Plates and Saddles

The tower base-plates are built up entirely of heavy plates of steel. In plan they are shaped to conform with the outline of the tower legs, their overall dimension, being 15 ft. and 9 ft. $7\frac{1}{2}$ in. The bottom slab which provides bearing surface is 3 in. thick, while the top slab which acts as disphragm is a perforated plate $\frac{1}{2}$ in. thick. A series of transverse and longitudinal vertical stiffeners were made up of 1 in. plates. Semi-circular drain-holes, 4 in. in diameter, are cut at the bases of the webs in order to prevent accumulation of water inside the member.

The tower leg is welded directly to the base plate, and the plate is anchored to the pier by thirty-four 3 in. bolts 14 ft. 3 in. long. After the concrete piers were carefully dressed to be flat and level, heavy canvas approximately 1/8 in. thick and saturated with the specified prime paint was then laid over the bearing area and the base of the tower erected in place thereon.

The cable-saddles for the towers are also all-welded. The bearing surface for the strands is a billet of medium steel 1 ft. 9 in. wide, 9-13/16 in. deep, and 10 ft. long. Its top surface is at the level of the centre-line of the cable, and is curved to a radius of 12 ft. 8-9/64 in. The billet is machined out to receive the lower half of the cable, and the bottom, and sides of the cut are grooved to seat the individual strands. The billet is supported from a base-plate by two main longitudinal webs

1-7/8 in. thick. The base plate is 1-3/4 in. thick and of the same plan as the top of the tower column. In order to gain lateral stability, six transverse 1 -$\frac{3}{4}$ rib plates are also provided. Continuous $\frac{1}{2}$ in. fillet welds are employed for all connection joints. The main saddle, tighted with 16 high strength 1-1/8 in. in diameter bolts, has a $\frac{3}{4}$ in. thick bent plate with two wedges to obviate the possibility of the upper strands of the cable being displaced from any cause. Each saddle is secured to the tower by 52-1 in. high strength bolts.

7.10 Cable Bent Design

The cable bent serves the dual purposes of supporting the cables and the suspended-span bearings at the end of the side-span, and of providing bearing for the expension end of the approach-spans. Support for the cables is provided at this location with a purpose to deflect them towards the anchorage at a slope approximately to the maximum inclination already established near the tower-saddle.

The cable bents has a height of 131 ft. on the Dartmouth side and 86 ft. on the Halifax side from the pedestal-concrete to the cable intersection. Below the level of the approach-span bearings, the two columns are connected by lateral X - bracing, similar to the main tower, and the legs of the cable bent are vertical and 57 ft. apart, center to center.

A load-bearing, cross-strut is provided. It supports the vertical pin which receives the wind-reaction of the suspended span. The strut has substantical connection to the columns, designed to resist lateral forces from the cable-saddles.

The lower chords of the stiffening-trusses are each pin-connected to a

pair of bronze plates which can slide horizontally inside the column of the cable-bent. The ends of the truss are thus free to move to accommodate both vertical and horizontal rotations of the span, though they are restrained against vertical movements.

Each of the cable bent column is a constant dimension 3 ft. by 5 ft. box. All sections are welded from 7/16 and $\frac{1}{2}$ in. thick plate, and the plates are stiffened internally by T-shaped load bearing stiffeners. The inside face of the column below the strut is stiffened by two 9 x 4 x $\frac{1}{2}$ angles, 2 ft. apart to which are bolted the 2 ft. by 1 ft. 6 in. box diagonals. The sectional area of the column varies from 82 sq. in. at the top to 121 sq. in. at the base. Horizontal diaphragms are located at approximately 7 ft. intervals throughout the length of the column.

The cable-bent saddles, like the main saddles, are of all welded construction and are rigidly attached to the supporting columns, subjected to much smaller loads. However, they are smaller than the tower-saddles, the overall size of the 1-$\frac{1}{4}$ in. base-plate being 3 ft. by 5 ft. with two 1 in. longitudinal webs and four 1 in. transverse ribs. In order to prevent slipping of the cables and consequent forward-movement of the bent, the saddles are equipped with heavy curved covers which are bolted down with fourteen 1-$\frac{1}{4}$ in. high tensile bolts.

The cable-bent fixed at the base and subjected simultaneously to known loadings and known saddle-movements, is susceptible to the same analytical process of design as the tower. Saddle-movements, being influenced by the back stay-length alone, are small; the range of movements being 6-1/16 in. on Dartmouth cable-bent and 3-3/16 in. on Halifax

side from normal conditions. Loading conditions are more complicated, owing to the presence of the Elastomeric Expansion Bearings of the approach-girders, and to the horizontal shear-force developed by these under the influence of expansion-movements. The materials and permissible stresses were similar to those for the tower.

7.11 Cable Bands and Cable Anchorages Steel

7.11.1 Cable Bands

The cable band, from which the suspender rope hangs, consists of a pair of symmetrical steel castings, one placed against either side of the cable and the two bolted together onto the cable sufficiently tighted to overcome their tendency to slide under the influence of the suspender-pull. The inner surface of each casting is shaped to fit the profile of the outer strands of the cable, the flutings being left rough-cast in order to develop as much friction as possible. The inside dimensions of the castings were permitted to vary by only $\pm$ 1/32 in. from the specified figure, and after some experimentation, this tolerance was closely adhered to. The hexagonal exterior of the castings is modified by the presence of machined bosses for the holding-bolts, and by the provision of a saddle-grove made to various angles with the casting in accordance with the cable-slope. These were cast to the nearest multiple of three degrees, the consequent slight diviations from verticality in some cases being negligible in their effect upon the ropes. At each end of the groove a small keeper-casting, secured by two tap-bolts, is provided to hold the suspender in place after erection. The ends of the bands are counterbored to a depth of $\frac{1}{2}$ in. to furnish a housing for the wrapping. Fig. 11.14.

The castings are bolted together with $1\frac{1}{2}$ in. bolts of high-tensile steel, tightened to a specified tension of 36,000 lb. each. The bands

on the flatter parts of the cables are fastened with four bolts each, but six bolts are required where the cable is steeper and the tendency to slip is consequently greater. The number of bolts was computed on the conservative assumption that there would be available a frictional resistance amounting to 30% of the aggregate of the bolt-tensions. There are 146 cable-bands. Of this total, 86 are the 4 bolt type, while the remainder, are the 6 bolt type.

7.11.2 Cable Anchorage Steel

The main feature of the anchorage steel is a group of seven circular steel slab "buttons", symmetrically arranged normal to the direction of the cable, whereby the load from the cable is concentrated into seven parts, each of which is then delivered into the concrete anchorage-mass by three heavy anchor-bars. Fig. 11.10 and Fig. 11.11.

The buttons, burned from a 6-in. slab of steel, are 3 ft. 6 in. in diameter, that size being determined by the clearance required between strand-sockets for field-assembly. The front face of each is plane, but the rear, or shoreward, face is machined to a spherical radius of 30 ft., the central thickness being $5\frac{3}{4}$ in., and that at the edge 5-1/8 in. Each button is perforated by three 6-in. holes for the admission of the main anchors; and attachment of the strand-sockets is effected by bolts passing through a further set of nine (or, in the case of the central button, seven) 3-3/8 in. holes. The buttons are so arranged on the main anchors that their rear face all lie on the surface of a sphere, the center of which is 30 ft. away and on the center line of cable. That same point is made for the theoretical origin of the splaying-out of the strands from their compact hexagonal formation in the cable proper, with the result that

the splayed strands are radial to the spherical surface.

The 21 primary anchors, embedded into the pier during its construction, are A-235 steel with the total length ranging from 29 ft. 6 in. to 42 ft. 6 in. They are, except for the length of about 5 ft. which was not embedded until after assembly of the cable, machined into a series of tapered lengths in order to secure positive bond by wedge-action. The lower ends of the anchors are spread to engage an adequate mass of concrete, and the upper ends, which are upset and finished to screw-threads $5\frac{3}{4}$ in. in diameter, converge to the larger holes in the buttons.

Connection of the strands to the buttons is effected by bolts 3 ft. 3 in. long. Each bolt is screwed into the strand socket, and its other end is secured by a nut which bears on the spherical rear surface of the button. The threads on the ends of the bolt being of opposite hand, and the bolt shaft being of hexagonal section, the bolt could be used for adjusting the position of the socket during cable-assembly.

The splay of the strands is controlled by a heavy collar, part of which fits tightly to the profile of the compacted cable, and the remainder of which is shaped to load the strands into their radial positions without abrupt changes in alignment. Each of the four splay-collars consists of two steel castings 2 ft. $7\frac{3}{4}$ in. long, bolted together onto the cable with 2 in. high-tensile-steel bolts. The splay-collars are located in open chambers inside the anchor-piers, so that they, together with the splayed strands and socket-assembly, are always accessible for inspection.

The entrance of moisture into the chambers is prevented by water-tight connection of the tubular flashing to a cast-iron collar on the

cable and to an "eyelet-casting" built into the front wall of the concrete anchorage.

7.12 Approach Span Design

The approach spans have an $8\frac{2}{3}$ in. thick reinforced concrete deck, supported by transverse steel floor beams, and in turn these beams are held by two steel box girders. The cross beams are 2 ft. $4\frac{3}{4}$ in. deep of built up plate girders except the diaphragm beams which are 3 ft. 2 in. deep. The spacings of these beams are 7 ft. 6 in. and 7 ft. $9\frac{3}{4}$ in. for the 150 ft. spans and 125 ft. span respectively. The floor beam spans are 30 ft. with an 11 ft. 6 in. cantilever outside the box girders. The top and bottom flanges are 5/8 in. thick plate while the web is 5/16 in. thick. In addition, the webs were stiffened by $4\frac{1}{2}$ x 5/16 plates on alternative sides. In order to achieve satisfactory bond stress, double lines of Nelson studs were provided at top flange spaced at 1 ft. 6 in. Haunches made up of 5/16 in. thick and $10\frac{1}{2}$ in. x 5/8 in. plates, were used at each diaphragm beam. Fig. 7.25.

The size of the steel box girders is 8 ft. x 5 ft. for the 150 ft. spans and 8 ft. x 4 ft. for the 125 ft. spans. The thickness of top and bottom flanges vary from 3/8 in. to $1\frac{1}{2}$ in. plate while the webs are 3/8 in. thick plates overall. The webs were stiffened by 3 x 2 x 5/16 angles and 4 x 3 x 3/8 angles for the longitudinal and vertical directions respectively. Five lines of shear connectors placed in a staggered pattern were also provided at the top flange of each girder.

With such an arrangement, the approach structure is composed of two principal load-carrying elements:

(1) The steel girders transfer the loads along the bridge

longitudinal axis.

(2) The concrete slab distributes the loads in the longitudinal direction to the floorbeams and in turn these loads are transferred to the steel girders.

The function of these connectors is to transfer horizontal shear from the slab to the girders and thus to force the concrete and the steel parts to act as an unit. Since the slab is connected to the steel girder, it cannot deform independently; it acts as a cover plate of the girders and at the compressive zone of top flange it assists the girders to carry the load in the longitudinal direction.

The $8\frac{1}{2}$ in. thick concrete deck was reinforced with 5/8 in. and $\frac{3}{4}$ in. deformed bars at top and bottom respectively. Then, the concrete deck was waterproofed by the application of a rubberized mastic asphalt. Finally, the concrete slab was covered by $1\frac{1}{2}$ in. dense graded asphalt concrete. This made the approach decks a total thickness of 10 in.

To facilitate inspection below the deck of the approach span, 6 movable platforms were suspended at the outside edge of box girders. Along the center line of the deck, a full length of catwalk was provided for the approach span on both sides.

Since the approach span lengths are much shorter than the suspension span, an increased uniformly distributed live load of 800 lbs/lin.ft./lane was used or one standard H20-S16 truck per lane per span. The combination of stresses was DL + LL + I at Normal Unit Stress; and DL + LL + I + 1/3 WL + WLL at 1.25 N.U.S.

7.13 Materials of the Superstructure

Generally, all the structural steel was adopted in accordance with the standard CSA or ASTM specification. The various steels and their application are listed below.

Main Span

1. CSA - G40.8 Grade B Normalised

   Deck plate, longitudinal ribs, floorbeam webs.

2. CSA - G40.8 Grade B

a. Stiffening truss top chords, bottom chords, diagonals, verticals.

b. Floorbeam bottom flanges

c. Floor truss top and bottom chords.

d. Bottom laterals.

e. Legs, diagonals and struts for main towers and cable bents.

3. CSA - G40.8 Grade A

   Floor truss diagonals.

4. High Strength Low Alloy Steel

   Stiffening truss bottom chords where 46 ksi. yield point steel apply locally where maximum moment occurs.

5. ASTM - A36

a. Buttons and anchor plates in cable anchorages.

b. Ribs and base plates for main tower saddles and cable bent saddles.

c. Ladders for main towers and cable bents.

d. Galvanized roadway fence.

6. ASTM - A440

   Anchor bolts for main towers and cable bents.

7. ASTM - A284 Grade C

   Machined seats and covers for main tower saddles and cable bent saddles.

8. ASTM - A235 Class R Annealed

Cable anchorage bars, strand sockets, strand adjustment bolts, suspender sockets.

9. ASTM - A27 Grade 65-35

Cable band castings and splay castings.

10. ASTM - A354 Grade BB

Cable band bolts, splay casting bolts, cable saddle bolts.

11. ASTM - A325

High strength bolts for connections and splices.

12. CSA - G40.2

Galvanized ladder rungs on suspenders.

Approach Spans

1. CSA - G40.12 killed, fine-grained Normalised

Box girder flanges wherever tension can develop and where G40.12 material is called at the maximum moment points.

2. CSA - G40.8 Grade B Normalised

Box girder flanges wherever tension can develop and where G40.8 material is called at the maximum moment points.

3. CSA - G40.12 killed, fine-grained

Box girder flanges where no tension can develop.

4. CSA - G40.8 Grade B

Floorbeams and all box girder material not covered in the three preceeding headings.

5. ASTM - A36

a. Fascia beam and traveller track.

b. Roadway fence, catwalk, inspection travellers.

6. ASTM - A325

High strength bolts for all splices and connections.

7.14   Special Epoxy Asphalt Wearing Surface

The 2,420 ft. long steel deck of this suspension brdige was paved with the Concresive epoxy surfacing mixture. It was only the third deck in the world and the first in snow country to use an epoxy asphalt wearing course. This kind of mixture was provided by the Adhesive Engineering Company of San Carlos, California, U.S.A. world-wide agents for the unique material developed by Shell Oil Company.

Although the Concresive mix is about 10 times more expensive than traditional hot-mix, it is far superior under bridge traffic loadings and reduce maintenance and repair costs. One of its outstanding characteristics is that its thermal elasticity closely approximates that of steel. Both materials will therefore tend to elongate and contract together with temperature changes. Therefore the problem of pavement damage will be reduced. Additional advantages are as follows:

1.   Very durable and good fatigue properties.

2.   Excellent anti-skid properites.

3.   Very good waterproof protection.

4.   Good bond to steel deck.

The above characteristics are essential in a location subject to wide range of ambient temperatures; especially when a corosion preventive material is required due to the use of salts.

The Concresive epoxy asphalt is a highly specialized product that differs from conventional hot-mix asphalt.

1.   Epoxy Asphalt Bond Coats consists of two components: component A,

an epoxy resin, and component B, asphalts mixed with epoxy resin hardeners.

Component A is a liquid diepoxy resin obtained entirely from the condensation of bisphenol A and epichlorohydrin. No diluents, flexibilizers, or plasticizers should be present. It also contains no inorganic fillers, pigments, or other contaminants or insolubles.

Components B is a homogeneous composition of a petroleum-derived asphalt and epoxy resin hardeners. It contains no insolubles such as inorganic fillers or pigments, and no contaminants which would adversely effect automatic metering, mixing, or dispensing.

The mixture of the two yields the following properites:

Ultimate tensile strength at $77^{\circ}F$	175 psi to 350 psi
Elongation at break at $77^{\circ}F$	175% minimum
Swelling ratio at $77^{\circ}F$	3.5 maximum
Leaching at $77^{\circ}F$	35% maximum
Thermoset property at $600^{\circ}F$	shall not melt
Water absorption (demineralized water immersion for 7 days at $77^{\circ}F$)	0.3% maximum

Deflection under load (264 psi) at temperature $-15^{\circ}C$ to $-25^{\circ}C$

2. Epoxy Asphalt Concrete consists of epoxy asphalt binder and aggregate

   a. Epoxy asphalt binder consists of the same materials that are specified for epoxy asphalt bond coats as shown above.

   b. Aggregate consists of mixture of coarse and fine aggregate and a filler material, if required. Aggregate should conform to the applicable requirements for 3/8 in. maximum

aggregate, and the fine aggregate should pass through a no. 200 sieve.

The most crucial parameter in the batching of the mix is the time control and precise temperature. This requirement is further complicated by the fact that the chemical reaction between the epoxy resin and its hardening agent is one which gives off heat. Too hot a mix could mean premature setting of the entire mix, but too cool a mix would mean placement and compaction would be unsatisfactory. Air voids in the mix are kept to 1%.

Before the Epoxy Asphalt Bond Coats is applied, the steel surface should be cleaned to white metal by sandblasting and then priming with one coat of inorganic zinc paint.

TABLE 7.1

MAXIMUM LONGITUDINAL STRESS IN RIBS

Location on Rib	Loading Combination	Rib Stresses in ksi						Allowable Stress ksi	
		Mid Point Side Spans		Mid Point Centre Span		Panel 40 Central Span			
		Top	Bottom	Top	Bottom	Top	Bottom	Ten.+	Comp.-
Rib 13 Mid Span between Fl. Beams	System Ia	- 7.14	+ 5.37	- 4.87	+ 3.24	- 6.53	+ 4.83	+24.0	-22.4
	System II	- 5.49	+17.06	- 5.49	+17.06	- 5.49	+17.06	+24.0	-22.4
	System Ia+II	-12.63	+22.43	-10.36	+20.30	-12.01	+21.80	+30.0	-28.0
Rib 3 at Floor Beam	System Ia	+ 5.37	- 7.14	+ 3.24	- 4.87	+ 4.83	- 6.52	+24.0	-22.4
	System Ib	+ 6.03	- 8.24	+11.61	-11.84	+10.71	-11.62	+24.0	-22.4
	System II	+ 6.05	-18.80	+ 6.05	-18.80	+ 6.05	-18.80	+24.0	-22.4
	" Ia+II	+11.42	-25.94	+ 9.29	-23.67	+10.88	-25.32	+30.0	-28.0
	" Ib+II	+12.08	-27.04	+17.66	-30.64	+16.76	-30.42	+33.6	-31.4

(Refer to Fig. 7.9 p.107)

Table 7.2   BENDING MOMENT AND STRESS IN FLOOR TRUSS

Location	Loading Cases	Moment k.ft.	Stress in ksi		
			Top	Mid	Bottom
Floor Truss	D.L. Erection Stage	258	-	-2.63	+ 2.49
Entire Section of Floor Beam (Truss with Deck)	D.L. Superimposed L.L. Rigid System L.L. Effect of Flexibility	162 1428 -120	-1.66	-1.66	+12.16
	Total	1470	-1.66	-1.66	+12.16
Total Maximum Stress			-1.66	-4.29	+14.65

TABLE 7.3   THE COMBINED STRESSES IN FLOOR BEAM AND TOP CHORD OF FLOOR TRUSS

(Refer to Fig. 7.10 p.107)

Loading Case	Midspan ksi				Support ksi			
	①	②	③	④	①	②	③	④
a. Erection D.L. Axial,57 ft. Floor Truss	-	-	-2.45	-2.45	-	-	-2.45	-2.45
b. Erection D.L. Bending,14 ft. continuous Floor Beam	-	-	-3.01	+5.28	-	-	+6.02	-10.56
c. Superimposed D.L. Axial,57 ft. Floor Truss	-0.21	-0.21	-0.21	-0.21	-0.21	-0.21	-0.21	-0.21
d. Superimposed D.L. Bending,14 ft. Continuous Floor Beam	-0.08	+0.11	+0.11	+0.17	+0.15	-0.21	-0.21	-0.33
e. TLL + I Axial,57 ft. Rigid Fl. Truss	-1.72	-1.72	-1.72	-1.72	-1.72	-1.72	-1.72	-1.72
f. TLL + I Axial,57 ft. Fl. Truss Flex.	+0.16	+0.16	+0.16	+0.16	+0.16	+0.16	+0.16	+0.16
g. TLL + I Bending, 14 ft. Cont. Fl. Bm.	-1.34	+1.90	+1.90	+2.95	+1.97	-2.80	-2.80	-4.35
$\sum$ STRESSES	-3.19	+0.24	-5.22	+4.18	+0.35	-4.78	-1.21	-19.46

TABLE 7.4 TOWER LOADING AND DEFLECTIONS

Loading Combination	Allowable Factor x Basic Unit Stress	Cable Reaction (Saddle Included) kips	Suspended Trusses Reaction kips	Tower Move- ment @ feet	Horizontal Force @@ Required For Equilibrium kips
DL + LL	1.00	5787	4	+1.181	+5.804
DL+LL+T(HOT)	1.10	5702	20	+1.440	+7.639
DL+LL+T(HOT)+WL$_{L/2}$	1.25	5702	20	+1.440	+7.639
DL+LL+T(HOT)+0.71 (WL$_{L/2}$+WLL+WL$_{T/2}$)	1.25	5702	20	+1.440	+6.751
DL+T(COLD)+WL$_T$	1.25	4624	65	-0.405	+3.772

@ Tower Movement "+" Towards Main-Span, "-" Towards Cable-Bent.

@@ Horizontal Force Required For Equilibrium "+" in same direction as Tower Movement.

Where:

DL = Dead Load

LL = Live Load

WL$_T$ = Lateral Wind Perpendicular to Bridge ₵

WL$_L$ = Longitudinal Wind Parallel to Bridge ₵

WL$_L$ (Stiffening Truss) = ½WL$_T$ (Stiffening Truss)

WLL = Wind on Live Load

T = Temperature: T(HOT) = 105 °F, Normal 55 °F, T(COLD) = -20 °F

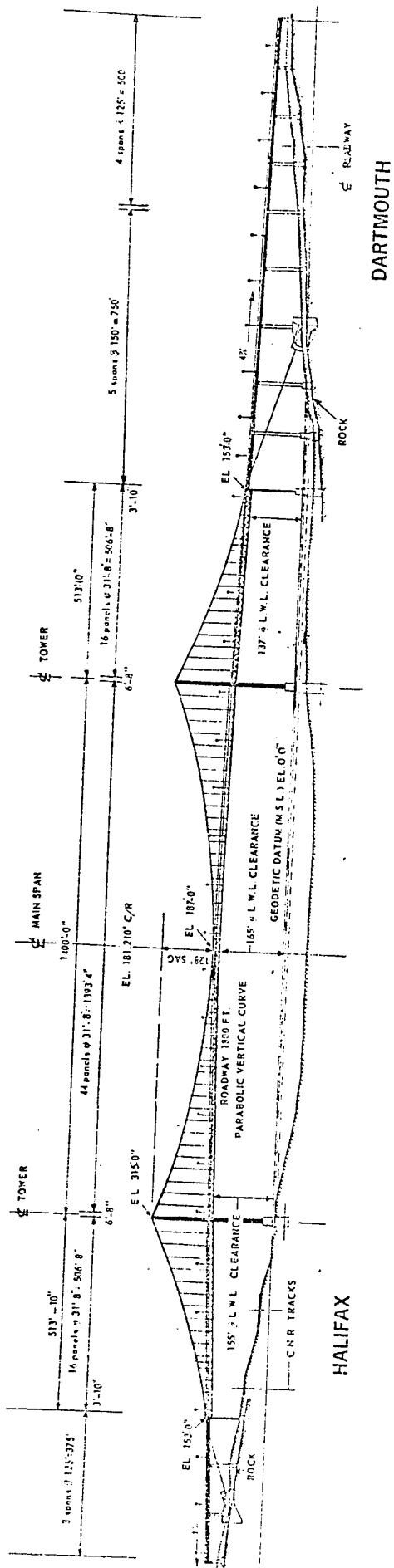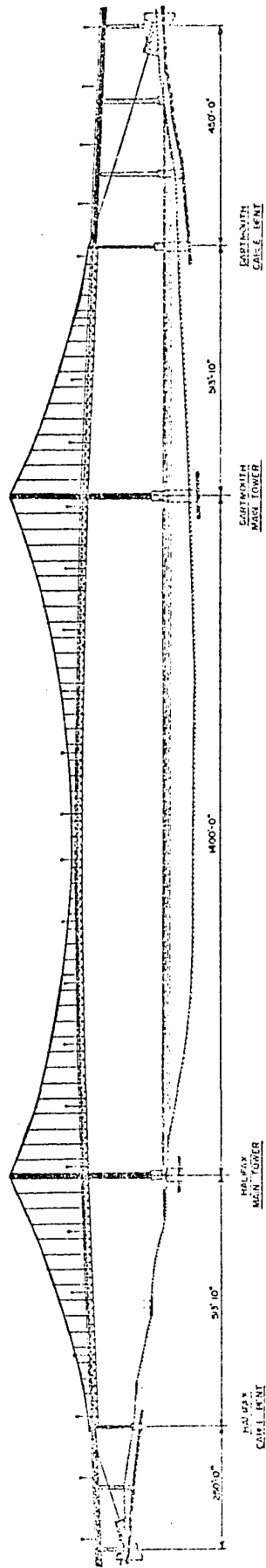FIG. 7.1 THE PANORAMIC VIEW OF THE A. MURRAY MACKAY BRIDGE

FIG. 7.2 ELEVATION OF THE BRIDGE

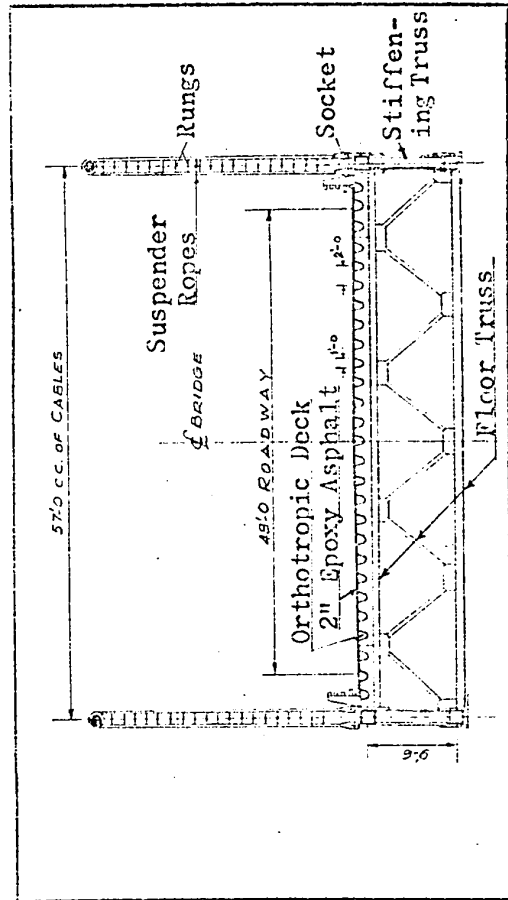FIG. 7.3 CROSS SECTION OF THE BRIDGE

ELEVATION

0' 5' 10'

A. THE STIFFENING TRUSS

PLAN A-A

0' 5' 10'
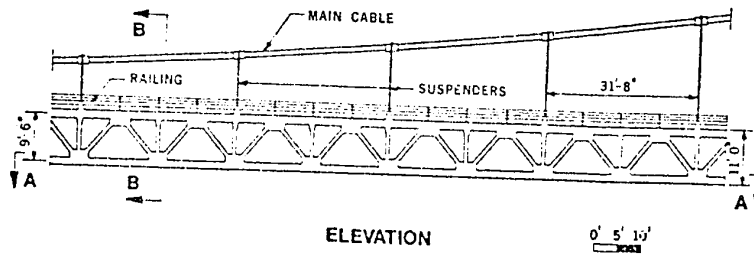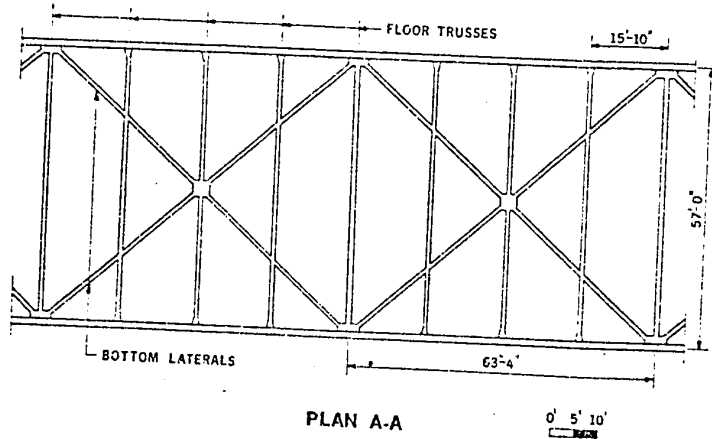
B. THE BOTTOM LATERAL

SECTION B-B

0' 5' 10'
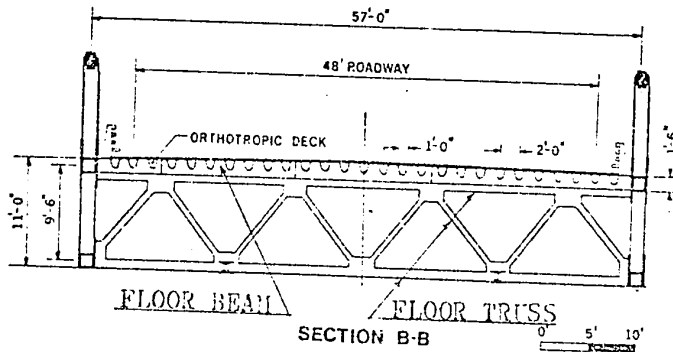
C. FLOOR BEAM AND FLOOR TRUSS

FIG. 7.4 DETAILS OF THE SUPERSTRUCTURE
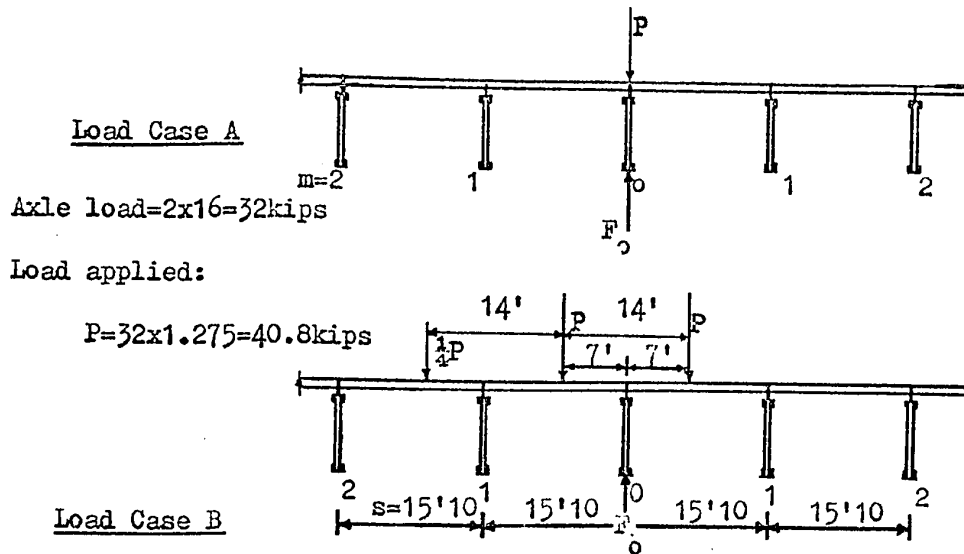
FIG. 7.5 MAXIMUM LOAD, F_o, ON A FLOOR BEAM DUE TO ONE H20-S16 TRUCK
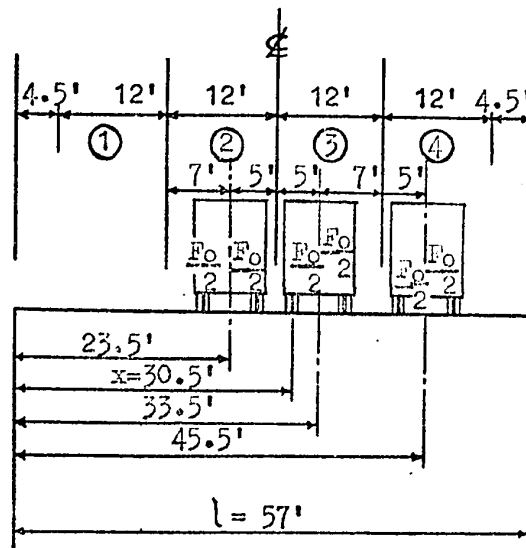
FIG. 7.6 LOADING USED IN THE COMPUTATION OF THE MAXIMUM L.L.

MOMENT IN FLOOR BEAM
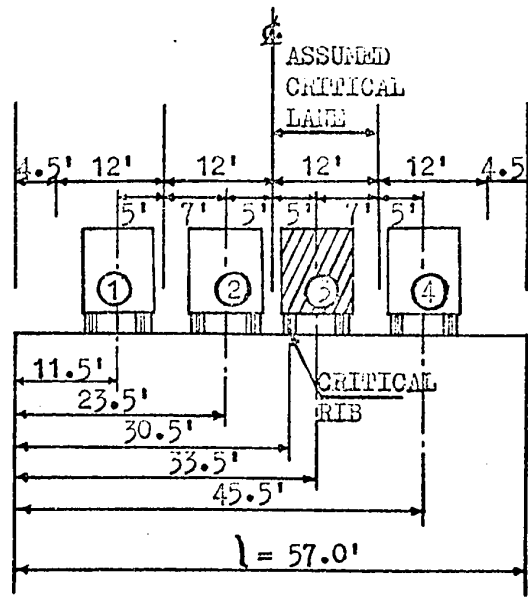
FIG. 7.7 LOADING USED IN THE COMPUTATION OF THE BENDING MOMENT

INCREMENT DUE TO FLOOR BEAM FLEXIBILITY
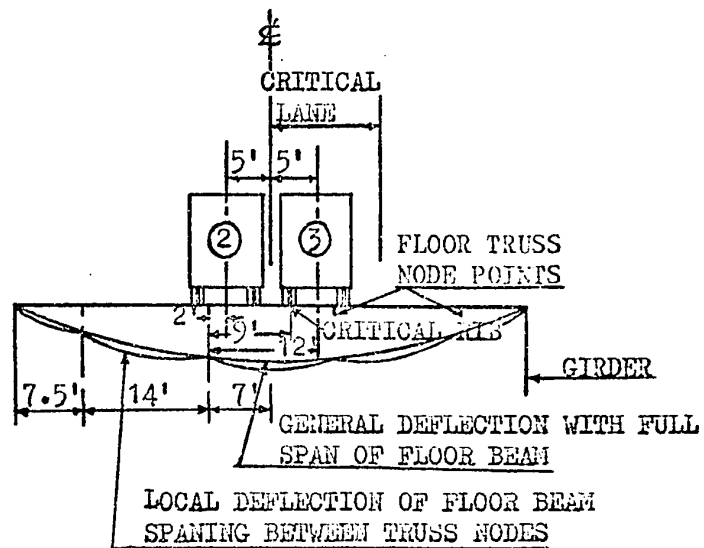
FIG. 7.8 LOADING USED IN THE COMPUTATION OF FURTHER EFFECT OF

FLEXIBILITY OF FLOOR BEAM ALONE

FIG.7.9. RIB MARKINGS FOR MAXIMUM NEGATIVE AND POSITIVE MOMENTS
(Refer to TABLE 7.1 p. 98)
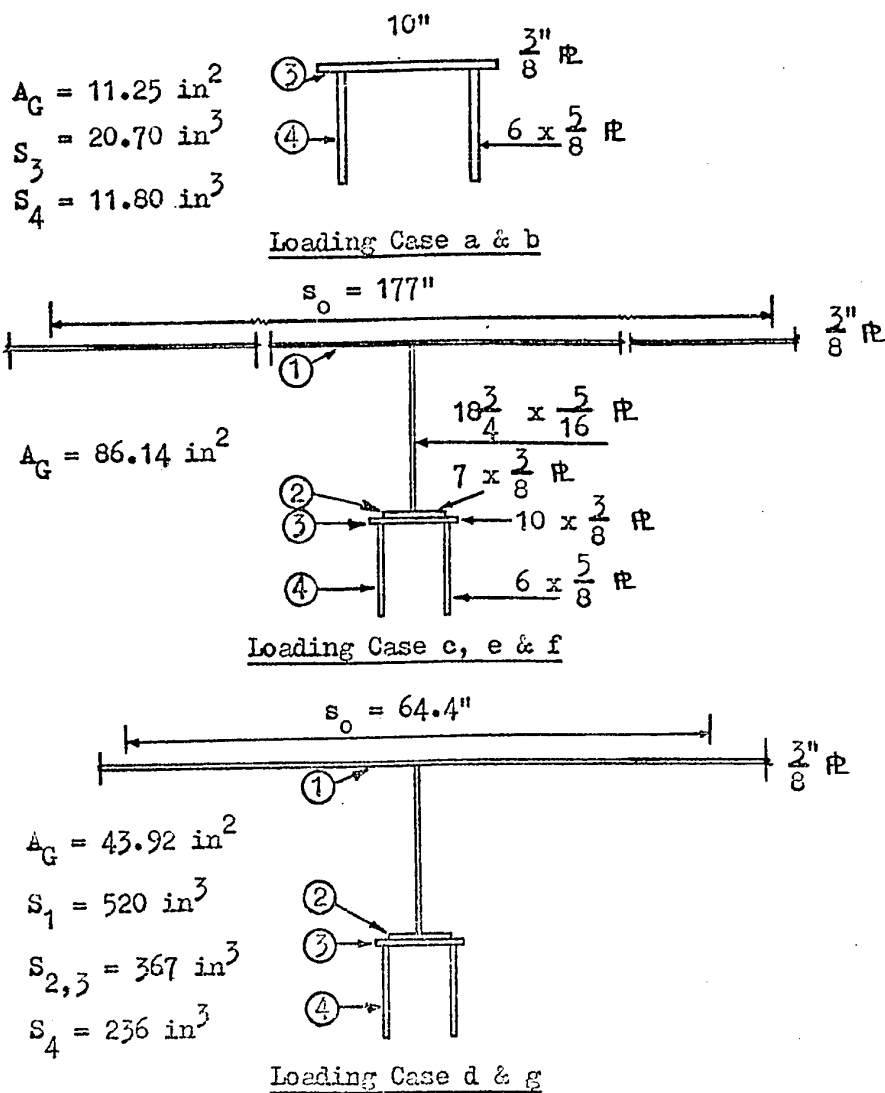
FIG. 7.10 FLOOR BEAM AND TOP CHORD OF FLOOR TRUSS

(This FIG. in accordance with TABLE 7.3)

EDGE CONDITION OF CLOSED RIBS
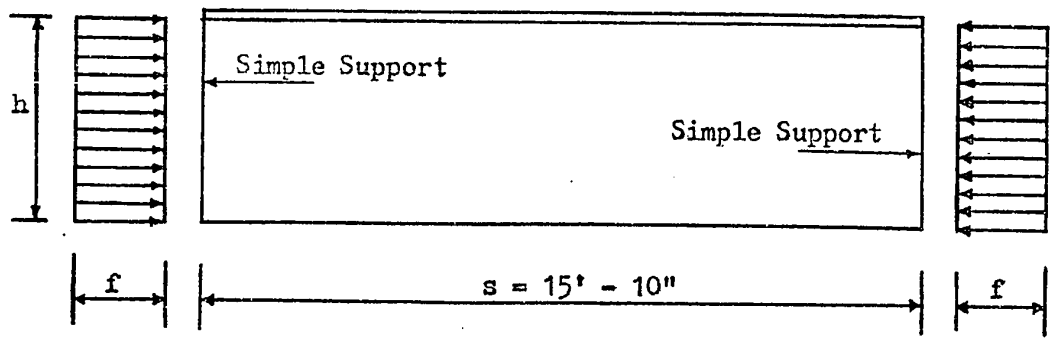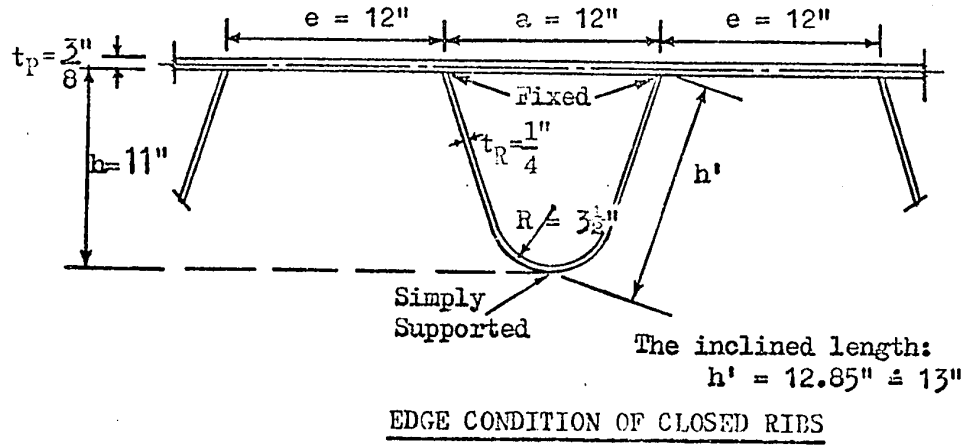
LOADING A

FIG. 7.11 ASSUMED EDGE CONDITION OF RIBS FOR LOADING A
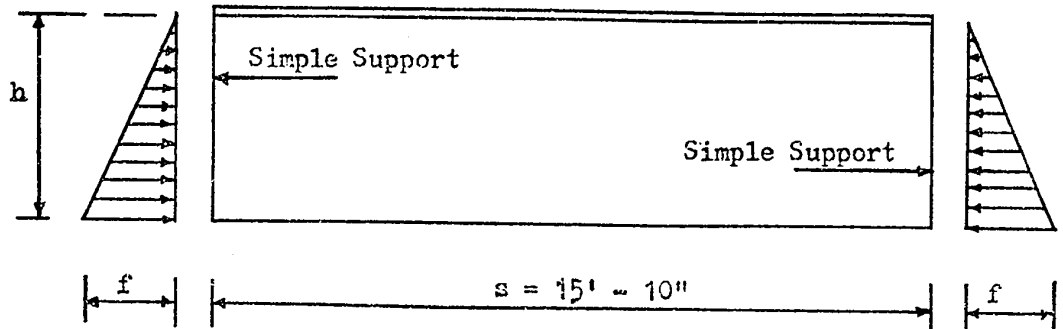
FIG. 7.12 LOADING C CONDITION OF RIBS

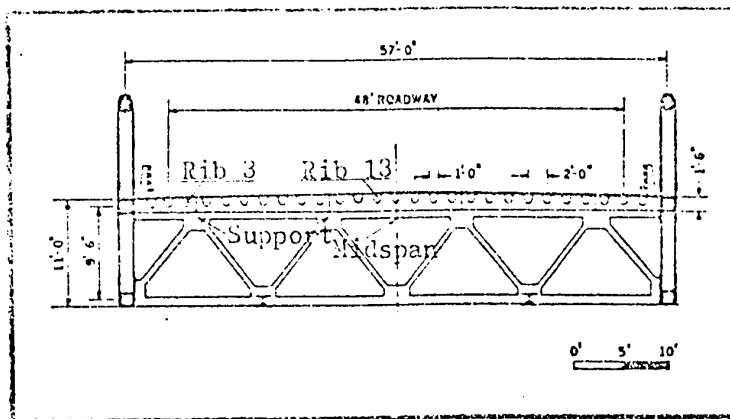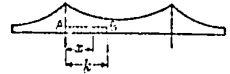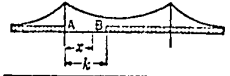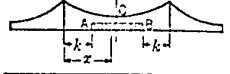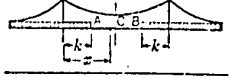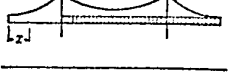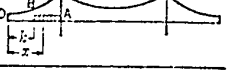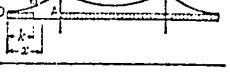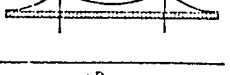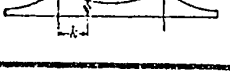| Case	Loading condition	Temperature	Equation
I		Highest	$H_I = \frac{p\,l^2}{8\,f\,D_{+t}}\left(\sin^2\frac{k\,\pi}{2\,l} - T\right)$
II		Lowest	$H_{II} = \frac{p\,l^2}{8\,f\,D_{-t}}\left(\cos^2\frac{k\,\pi}{2\,l} + 2\,S + T\right)$
III		Highest	$H_{III} = \frac{p\,l^2}{8\,f\,D_{+t}}\left(\cos\frac{k\,\pi}{l} - T\right)$
IV		Lowest	$H_{IV} = \frac{p\,l^2}{8\,f\,D_{-t}}\left(1 - \cos\frac{k\,\pi}{l} + 2\,S + T\right)$
V		Highest	$H_V = \frac{p\,l^2}{8\,f\,D_{+t}}(S - T)$
VI		Lowest	$H_{VI} = \frac{p\,l^2}{8\,f\,D_{-t}}(1 + S + T)$
VII		Highest	$H_{VII} = \frac{p\,l^2}{8\,f\,D_{+t}}\left(S\cos^2\frac{k\,\pi}{2\,l_1} - T\right)$
VIII		Lowest	$H_{VIII} = \frac{p\,l^2}{8\,f\,D_{-t}}\left(1 + S + S\sin^2\frac{k\,\pi}{2\,l_1} + T\right)$
IX		Lowest	$H = \frac{p\,l^2}{8\,f\,D_{-t}}(1 + 2\,S + T)$
X		Highest or lowest	$H = \frac{P\,l\,x}{16\,f\,D_{x\,t}}\left(\sin\frac{k\,\pi}{l} \mp T\right)$

FIG. 7.13 VARIOUS LOADING CONDITIONS FOR STIFFENING TRUSS DESIGN
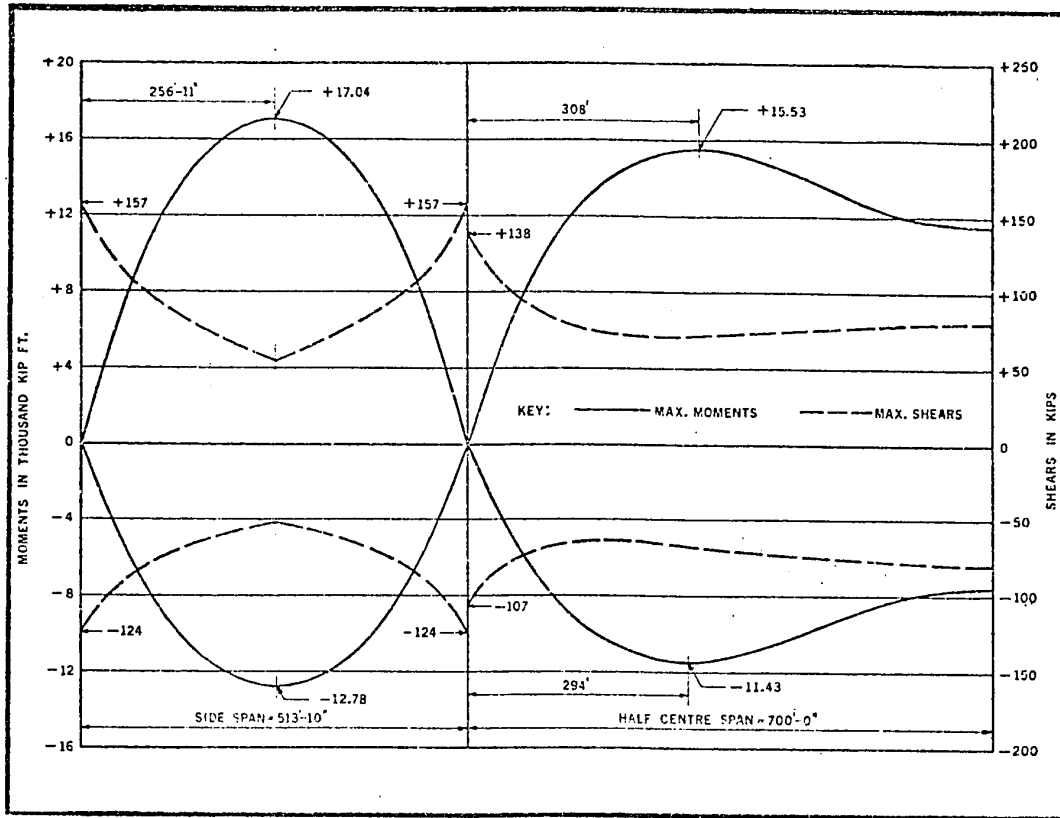
FIG. 7.14 MAXIMUM STIFFENING TRUSS MOMENTS AND SHEARS

NOMINAL GALV. STRAND DIA. = 1.571"
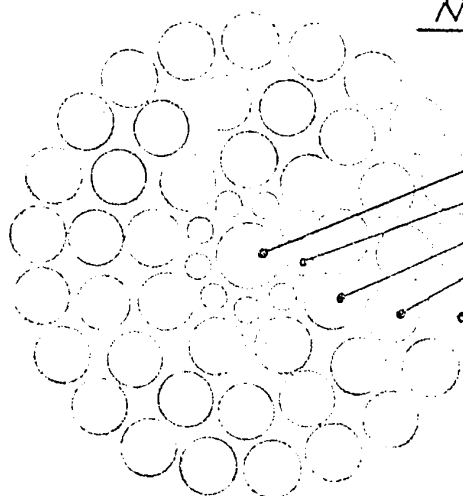
NO. WIRE	WIRE DIAMETER	
	GALV'D	BRIGHT
1 CORE	.218	.215
9 INNER	.108	.1055
9 INNER	.196	.193
15 INNER	.196	.193
21 OUTER	.196	.193

DETAILS OF 1 9/16" ⌀ CABLE STRAND

Nominal Diameter 14 11/32" Outside Wrapping

Nominal Diameter 14 1/16" Inside Wrapping.

5 3/4"

1 9/16"

Cedar Wood Fillers.

These Strands "X" marked for Suspender Location

Wrapping Wire #9 Gauge soft steel annealed and galvanized

Five Guide Strands.
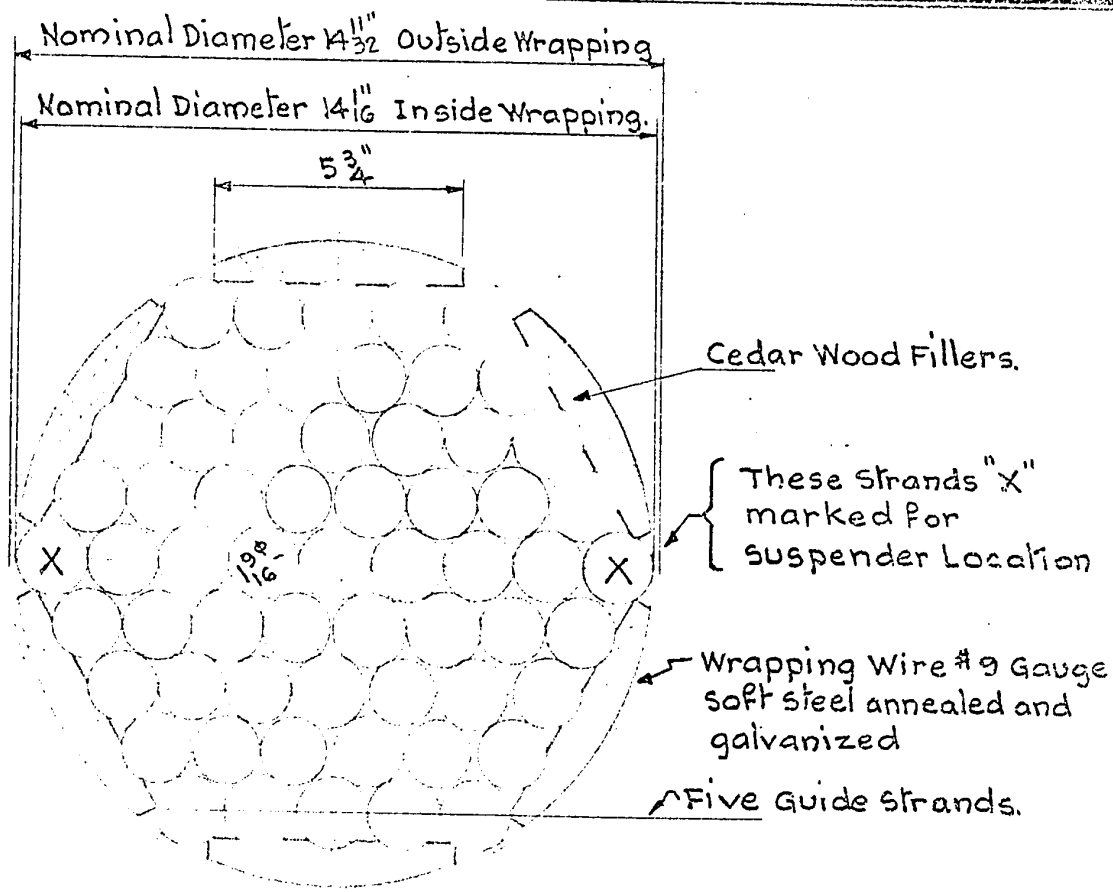
CROSS SECTION OF CABLE

Scale 3" = 1 Foot

FIG. 7.15 CROSS SECTION OF CABLE AND CABLE STRAND

STRAND

I.W.R.C.

DESIGN DIAMETER OF ROPE – 2.123"
STRAND – WIRE DIAMETERS

NO. WIRE	GALV'D	BRIGHT
1 CORE	.106	.1035
6 INNER	.104	.1015
6 FILLER	.044	.0415
12 INNER	.100	.0975
18 OUTER	.100	.0975

I.W.R.C.
6 OUTER STRANDS

NO. WIRE	GALV'D	BRIGHT
1 CORE	.096	.0935
6 OUTER	.087	.0845

1 CORE STRAND

NO. WIRE	GALV'D	BRIGHT
1 CORE	.106	.1035
6 OUTER	.096	.0935
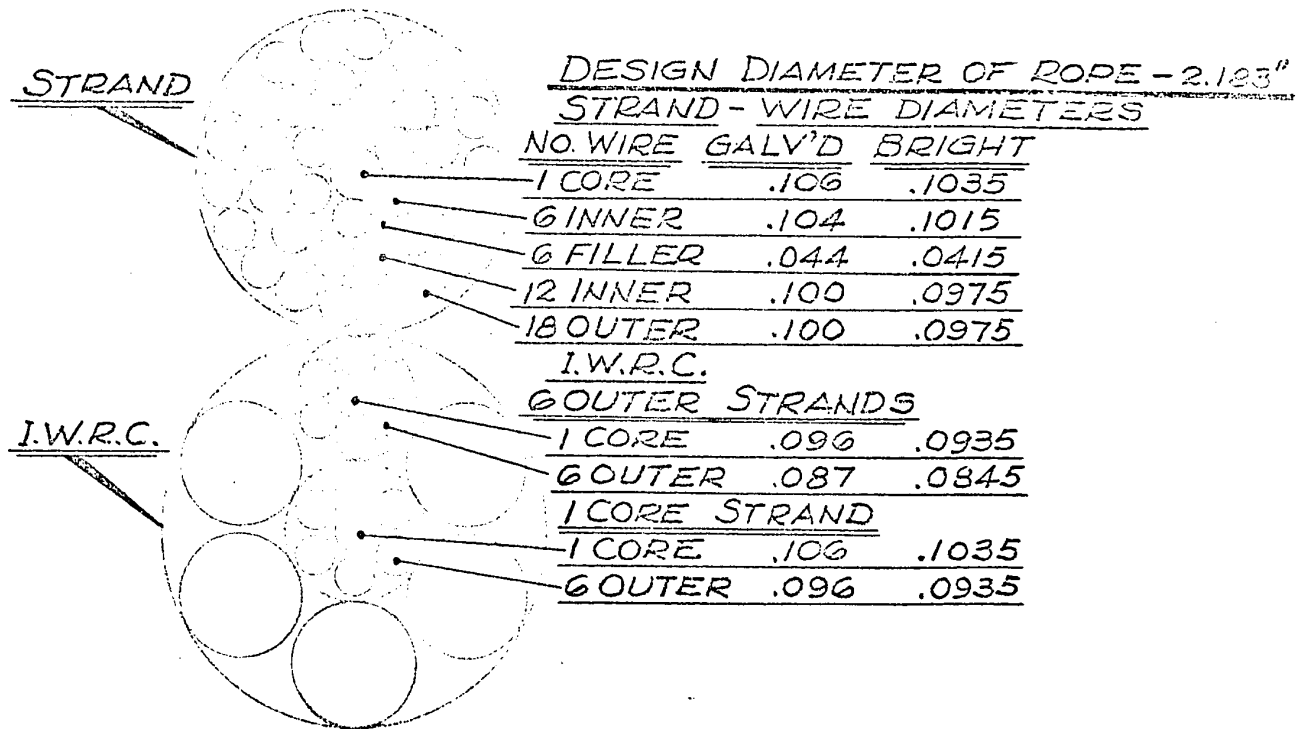
DETAIL OF SUSPENDER STRAND & I.W.R.C.

2⅛" Dia.
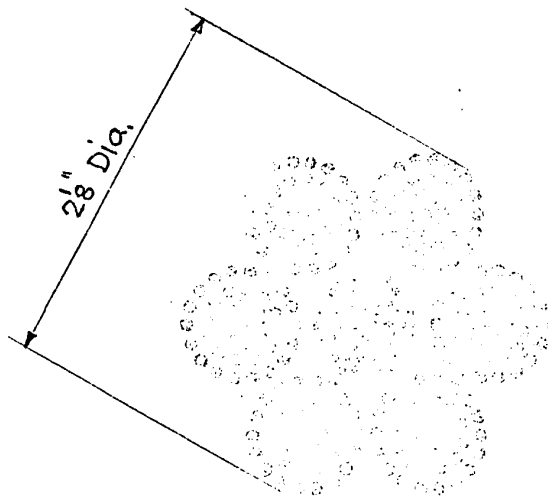
Note:

I.W.R.C.= Independent
Wire-Rope
Centre

CROSS SECTION OF SUSPENDER ROPE
(6 strands with 7 x 7 I.W.R.C.)

FIG. 7.16   CROSS SECTION OF SUSPENDER ROPE AND SUSPENDER STRAND

FIG. 7-17 LOADING AT PANEL FOR BOTTOM LATERAL DESIGN

V_W	V_T	F_W	F_T	Design Load +F@ NUS	Type	Ten. Cap.	Comp. Cap.
37.4	210.0	27.9	156.8	142.5	B	227	162
37.4	196.0	27.9	146.2	133.0	B	227	162
37.4	180.0	27.9	134.3	122.1	B	227	162
37.4	165.0	27.9	123.2	112.0	B	227	162
37.4	150.0	27.9	112.6	101.8	B	227	162
37.4	135.0	27.9	100.7	91.7	B	227	162
44.2	134.0	33.0	100.0	93.3	B	227	162
51.0	138.0	38.1	103.0	97.7	B	227	162
57.8	142.0	43.2	106.0	102.0	B	227	162
64.6	146.0	48.3	109.0	106.5	B	227	162
71.4	150.0	53.4	112.0	111.0	B	227	162
78.2	155.0	58.4	115.6	115.8	B	227	162
85.0	160.0	63.5	119.3	121.0	B	227	162
91.8	165.0	68.5	123.2	126.1	B	227	162
98.6	170.0	73.6	126.8	130.8	B	227	162
105.4	176.0	78.7	131.2	136.3	B	227	162
112.2	183.0	83.8	136.5	142.8	B	227	162
119.0	190.0	88.9	141.8	149.0	B	227	162
125.8	198.0	94.0	147.8	155.8	B	227	162
132.6	207.0	99.1	154.5	163.2	C	247	185
139.4	218.0	104.2	162.6	171.8	C	247	185
146.2	230.0	109.2	171.7	181.0	D	266	203
51.0	139.0	38.1	103.7	98.3	B	227	162
44.2	121.0	33.0	90.2	85.4	B	227	162
37.4	105.0	27.9	78.3	73.8	B	227	162
30.6	91.0	22.9	67.9	63.5	A	197	84
23.8	77.0	17.8	57.4	53.0	A	197	84
17.0	66.0	12.7	49.2	44.7	A	197	84
13.6	59.0	10.0	44.0	40.0	A	197	84
13.6	77.0	10.0	57.5	52.2	A	197	84

Shear in Panel V_W = Wind Load; V_T = Torsion.

Force in Lateral $F = \dfrac{V}{2} \times \left(\dfrac{42.6}{28.5} \right)$

F_W = Wind; F_T = Torsion

Deck Load

Truss Loading
(i)
Anti-Symmetric
Loading

0.71 k/ft.   0.29 k/ft.

(ii)
Symmetric -
Loading

0.5 k/ft.   0.5 k/ft.

p_s=0.21 k/ft.

(iii)
Skew Symmetric
Loading

$p_s^!$=0.21 k/ft.

Truss Loading (i) = (ii) + (iii)
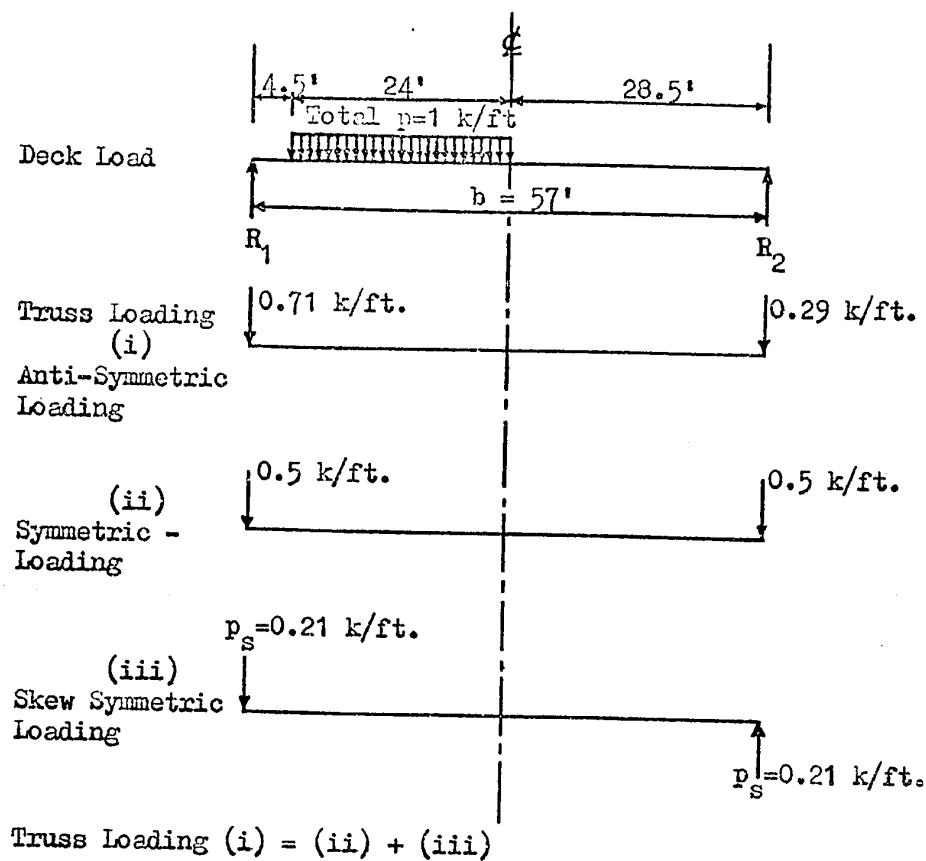
FIG. 7.18 BREAKDOWN OF ANTI - SYMMETRIC LOADING INTO A PAIR OF
SYMMETRIC AND SKEW SYMMETRIC LOADING
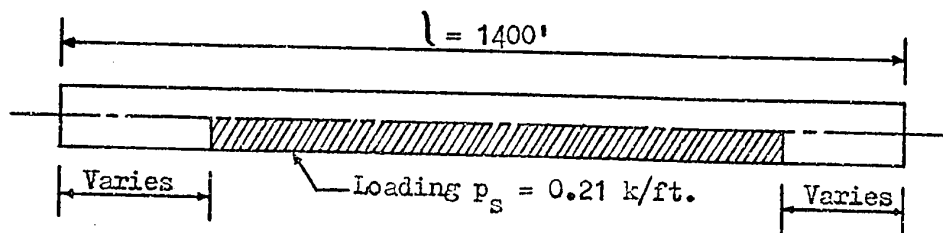
FIG. 7.19 ANTI - SYMMETRIC LOAD LENGTH ON THE SPAN
(CASE A LOADING)
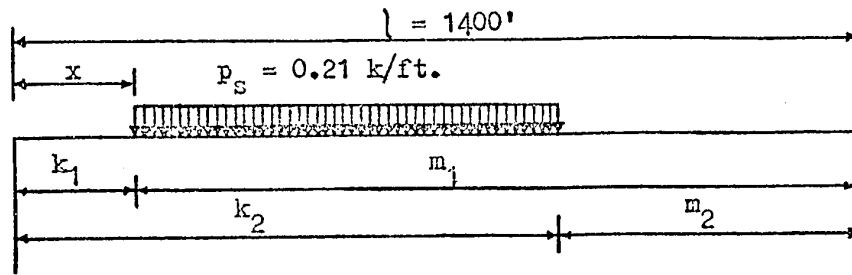
FIG. 7.20 GENERAL CASE OF ANTI - SYMMETRIC LOADING TO FIND

MAXIMUM POSITIVE SHEAR   (CASE A LOADING)
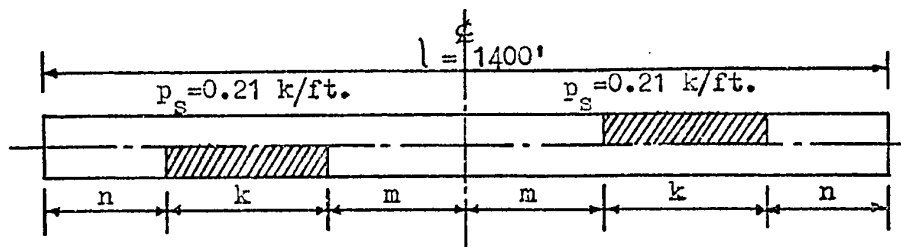
PLAN
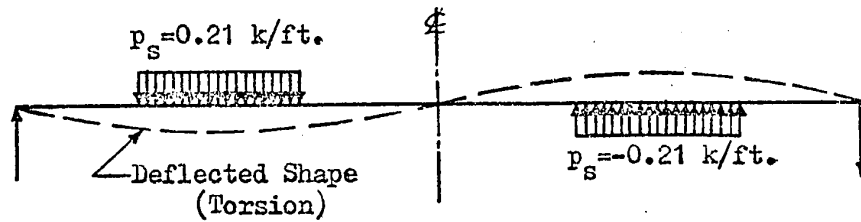
ELEVATION

FIG. 7.21 DIAGONALLY SYMMETRIC LOADING CASE

(CASE B LOADING)
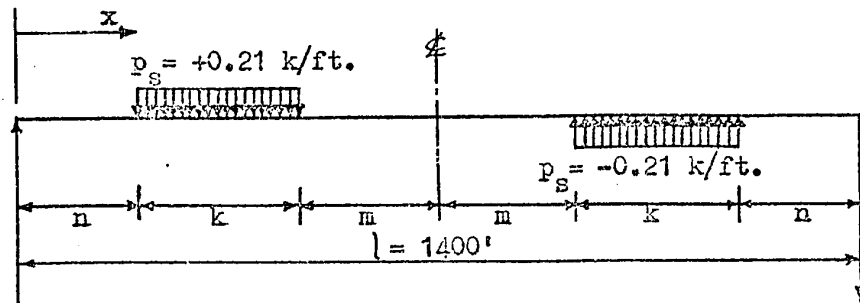
FIG. 7.22 SIMPLE TRUSS SHEAR FOR ANTI - SYMMETRIC LOADING

(CASE B LOADING)
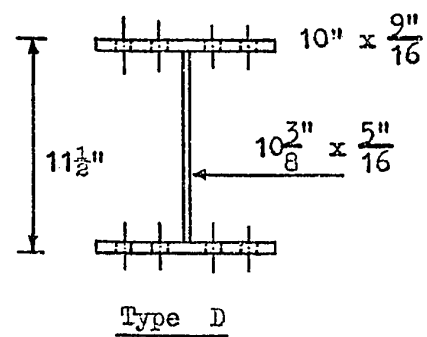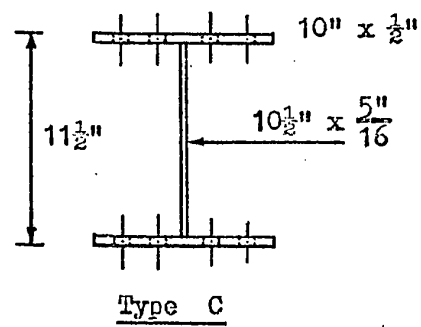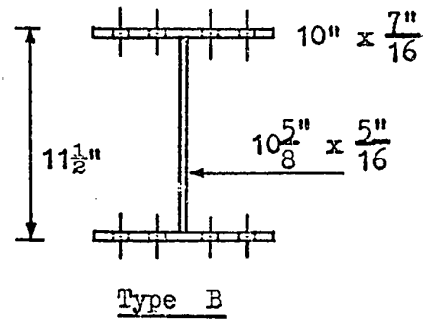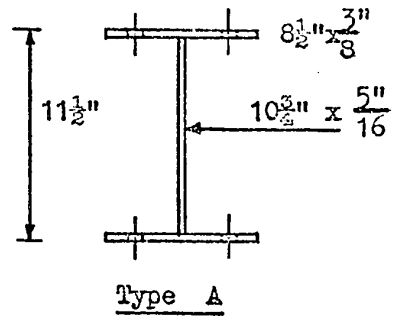
FIG. 7.23 SECTIONS OF BOTTOM LATERAL
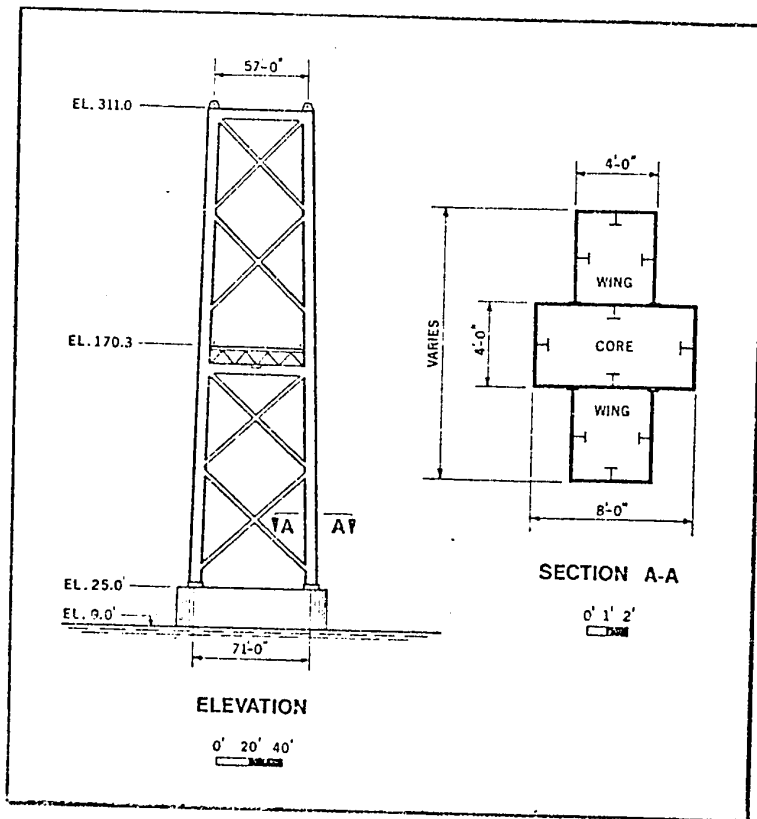
FIG. 7.24. ELEVATION OF MAIN TOWERS AND TYPICAL COLUMN CROSS SECTION
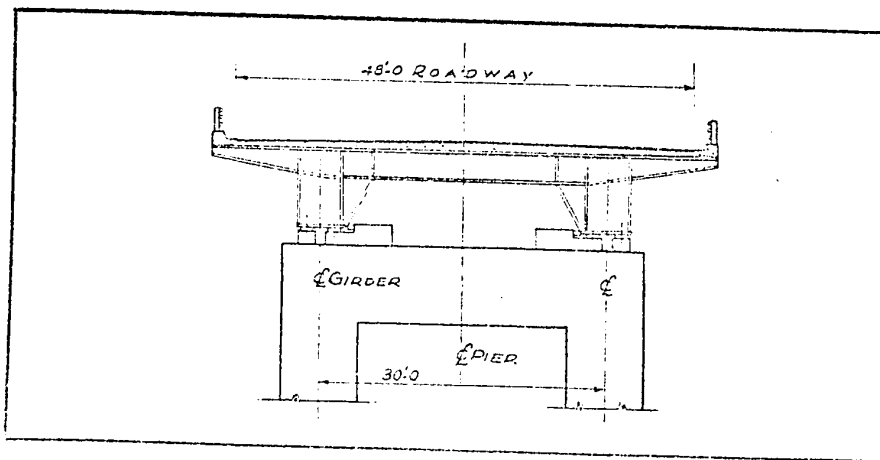
FIG. 7.25 TYPICAL CROSS SECTION OF THE APPROACH SPAN

CHAPTER 8

AERODYNAMIC STABILITY AND WIND TUNNEL TEST

8.1 Introduction

Since the disaster of the Tacoma Narrows Bridge, the problem of aerodynamic stability and critical wind velocity has been worrying all suspension bridge designers. A series of investigations made in connection with the Tacoma Narrows Bridge and several other bridges, showed that numerous bridges are not aerodynamically stable for all wind conditions. However, a soundly constructed suspension bridge will stand severe oscillations for a considerable time without any serious trouble.

For a new bridge there is no reason to allow any severe oscillation, since all movements will be unpleasant and give a feeling of insecurity to the motorist. However, if a bridge can stand under very heavy storms and only exhibit small unharmful oscillations, this should be sufficient for all public use of a bridge.

It is important to find easy and quick methods which can give critical wind velocities and oscillation amplitudes with sufficient accuracy. This is of importance in the early stages of planning and design of the bigger suspension bridges. Through this quick preliminary investigation of the aerodynamic stability, it is readily seen how and where the structure may be improved, and thus making it possible to produce better and safer bridges without any great increase in cost.

Following the failure of the Tacoma Narrows Bridges, a number of empirical stiffness indices were established, based on experience, to

guide design. A significant development was the formulation of aerodynamic theories and experimental wind tunnel procedures for studying the dynamic or aeroelastic behaviour of suspension bridges under wind action. Great progress was made principally in the United States, United Kingdom, Norway, Japan and Canada.

In modern bridges design, a preliminary investigation is carried out by testing a model in a wind tunnel. The previous test results demonstrate that there is a correlation between the behavior of bridge and model. Trouble has never been reported with a bridge which gave good model test results. Usually, the sections model of fairly short length of the bridge deck is tested under wind action and predicts the aerodynamic characteristics of the whole bridge. However, a model of the complete bridge will give more accurate results.

The aerodynamic effect and natural modes of vibration of a bridge, are determined completely by its mass, mass distribution, and elastic properties. Usually, for the modern suspension bridge, a high natural frequency of vibration is favourable. This can be obtained by increasing the truss stiffness or by providing two lateral systems in the planes of top and bottom chords of the stiffening truss. It is possible to design a suspension bridge with a high degree of security to stand against aerodynamic forces. This involves the calculation of natural modes of motion of the proposed structure, the performances of dynamic section model test to determine the factors of behaviour, and the application of these factors to the prototype by suitable analysis.

8.2 Method of Approach to Aerodynamic Stability Analysis

The 1952 report of the Advisory Board on the Investigation of Suspension Bridge[8] was used as a guide in the analysis of the aerodynamic characteristics. The truss vertical stiffness was initially selected to give a value for Ammann's Bending Stiffness Index equal to the recommended minimum of 600. The Stiffness Index is a function of the span lengths, dead weight, cable sag and truss moment of inertia, and gives an empirical indication of probable aerodynamic stability based on a statistical study of the behaviour of existing bridges. The validity of the stiffness index approach has not been confirmed by wind tunnel tests and rational analysis. However, it is an useful guide for medium and short span truss stiffened bridges.

Although there is no compact mathematical theory to explain all aspects of aerodynamic behaviour of suspension bridges, wind tunnel tests indicate that the flutter theory, first developed for suspension bridges by F. Bleich[9], is the best mathematical approach for truss stiffened sections. The flutter theory applies to an infinitely thin plate supported so it can move both vertically and torsionally. Under wind action of increasing velocity, the natural vertical frequency of oscillation increase and the natural torsional frequency reduces until they coincide at a common frequency. This compling occurs at the flutter velocity, when the motion becomes violent. The accuracy of the pure flutter theory depends on how closely the bridge deck and top chords resemble a flat plate.

The finite depth of the chords and deck, and any other obstruction near the leading edge, will produce a vortex action which causes the coupled oscillations to occur at a critical velocity v_c below the flutter velocity v_F. The modifying effect of the vortex action on the calculated flutter velocity is normally found by testing sectional models in a wind

tunnel. Selberg carried out a number of wind tunnel tests on three sim-
plified deck section models, each with various depth to width ratio and
with angles of attack from 0° to $\pm 10^\circ$, to establish k values. The cri-
tical velocity, in terms of flutter velocity, is shown in the equation
$v_c = kv_F$ [10,11,12]. With these k value graphs Selberg considers that medium
and short span bridges can be investigated for aerodynamic stability with-
out model test.

Similar model tests have been carried out for purely vertical oscil-
lations, which are rarely dangerous to the structure but may be objection-
able for traffic. Selberg's methods were used for the calculation of the
final natural vertical and torsional frequencies. In the calculation of
natural frequencies, Steinman's method is not clear for handling unequal
top and bottom lateral system and Bleich's method assumes both top and
bottom lateral systems are equal. However, the method proposed by Sel-
berg gives the most accurate result. With his recommendation, the combined
orthoplate top system and bottom laterals can be adequately handled.

The calculated critical velocities had to be compared with a design
wind velocity for the site of the bridge. Using Selberg's method, the
structure should have a minimum factor of safety of 1.38 with regard to
aerodynamic stability subjected to a horizontal wind pressure.

8.3 Bending and Torsional Stiffness Indices

8.3.1 Ammann's Bending Stiffness Index

An index value of 600 minimum was proposed by Ammann's in 1956. The
choice of original section based on the stiffness index was proved satis-
factory.

$$S_1 = \left[1 - 0.6 \frac{l_1}{l}\right]\left[\frac{8.2 \, w}{f} + \frac{0.14 \, I}{l^4}\right] = 598 \doteq 600$$

8.3.2 Ammann's Torsional Stiffness Index

In 1964 Ammann derived a formula to check the torsional index during the design of Verrazano Narrows Bridge. The minimum stiffness index is S = 450 for the resistance to torsional oscillations.

$$S = \left[\frac{B}{A} + 1\right]\frac{\pi^2}{4} \cdot \frac{w}{f}$$

Where

$$A = \frac{b^2}{2} \cdot \frac{H_w}{E}$$

$$B = \frac{A_v U_v \, A_h \, U_h \, 2bd}{\frac{b}{d} A_v U_v + \frac{d}{b} A_h U_h}$$

and

w = dead weight plf of bridge = 5615 plf.

f = sag = 128 ft.

H_w = dead load pull per cable

b = c to c of cable distance

d = c to c of top and bottom distance of a truss

A_d = section area of stiffening truss diagonal = 10.65 in.^{2}

$A_v = \Sigma A_d U_v$ in one panel

A_D = section area of bottom lateral diagonal = 8.87 in.^{2}

$A_h = \Sigma A_D U_h$ in one panel

$U_h = \sin^2 \phi_n \, \cos \phi_h = 0.66913^2 \times 0.74314$

$U_v = \sin^2 \phi_v \, \cos \phi_v = 0.78405^2 \times 0.62069$

Case 1   Assume top laterals are the same as bottom laterals

Then $A = 2.05$

$B = 8.75$

$A_h U_h = 0.041$

$A_v U_v = 0.282$

and $S = 570$

Case 2   By applying Selberg's method, consider the effect of an orthotropic

deck.   The actual plate web top lateral system A_h add to bottom

lateral A_h for the total.

Then $A_h U_h = 0.0772$

$A_v U_v = 0.0282$

$A = 2.05$

$B = 15.85$

and $S = 944$

This value is more reasonable for the effect of the orthotropic deck.

8.3.3   Steinman's Stiffness Criteria

Steinman introduced the stiffness criteria based on 100 mph design

wind speed in 1945.   The stiffness factor:

$$K = \frac{\pi^2 n^2 H}{l^2} + \frac{\pi^4 n^4 EI}{l^4} \qquad \text{for one cable and truss}$$

For the case of first anti-symmetric mode $n = 2$

then $K = K_W + K_T = 4.93\,\frac{W}{l} + \frac{0.0467}{(\frac{1}{100})^4} = 108.5 + 67.5 = 176$

the breadth factor

$$B = \frac{b^2}{w} = 1.155$$

$$\frac{K}{B} = 152.5$$

$$R = \frac{K_T}{K} = 0.384$$

and

$$R\sqrt{\frac{K}{B}} = 4.74$$

8.3.4 Compare the Stiffness Data on Existing Bridge

The stiffness data of A. Murray MacKay Bridge with other existing bridge is shown in Table 8.1. It includes all 11 modern bridges which have movements recorded, and most of these modern bridges are over 1,200 ft. span.

8.3.5 Conclusion on stiffness indices

Before the oscillations on the Peace River, Beauharnois and Liard River Bridges were reported vertical stiffness indices appeared satisfactory for separating the stable from the unstable sections. Based on Steinman's or Ammann's values all bridges with indices below a certain figure showed oscillations, and all above had none reported. Thus vertical stiffness appeared to be a prime factor in stability, although wind tunnel test and flutter theory calculation had not found it to be so.

The vertical index of Ammann's S_1 differs from Steinman's K/B in that it includes a side span term but no width term. The Ammann's index appears to be a better agreement with Selberg's method as the index does not reduce with the increasing width as the K/B index does. Thus the A. Murray MacKay Bridge $S_1 = 598$ is close to the recommended 600, and is well in

excess of the Angus Macdonald Bridges' value of 482 and the Lion Gate

Bridge's value of 386. However, the K/B value is lower than the said

bridges due to the increased width and low weight. The torsional index

S = 944 is well in excess of the recommended 450 minimum.

The most accurate of Steinman's indices is the $R\sqrt{\frac{K}{B}}$. The A.M.M.

Bridge has a value of 4.74, close to the recommended 5.0. On the Stein-

man's graph, it is on the borderline of the torsional oscillation curve,

but its torsional stability is assured by the double lateral systems.

8.4 Natural Frequencies of Oscillation in Anti-Symmetric Mode

The natural vibrations of a suspension bridge can be classified as

anti-symmetric modes and symmetric modes. Each mode may consist of

vertical oscillations or torsional oscillations.

The anti-symmetric mode has an even number of loops, one of the node

points is at mid-span. The waves of the mode are balanced vertically

above the normal position which makes it possible for the main span to

vibrate, while the side spans are still. Different methods have been

used to calculate the natural frequencies and the final results have

proved satisfactory.

8.4.1 Vertical Oscillation for First Anti-Symmetric Mode by Steinman's Method[13]

For the anti-symmetric mode, all even values of n, the difference

in horizontal cable pull is zero (i.e. $\Delta H = 0$). Then the coefficient of

rigidity (or spring constant) should be:

$$K = \frac{\pi^2 n^2}{l^2} H + \frac{\pi^4 n^4}{l^4} EI = 350 \text{ lb}/ft^2 \qquad \text{for } n = 2$$

The natural frequency of vertical oscillation N_v should be:

$$N_v = \frac{60}{2\pi} \sqrt{\frac{K}{m}} = 13.54 \text{ cycles/min.}$$

where $\quad m = \frac{w}{g}$

and $\qquad g = 32.2 \text{ ft/sec}^2$

This natural frequency of vertical oscillation is high, compared to the existing long span suspension bridges of Verrazano Narrows bridge, George Washington Bridge, Golden Gate Bridge, Mackinac Bridge and the original Tacoma Bridge, with frequencies between 6.0 and 8.0. The above calculation is based on no central tie between cable and truss and no side span participation.

8.4.2 Torsional Oscillation for First Anti-Symmetric Mode by Steinman's Method

In order to comply with the formula, the top and bottom lateral system were assumed to be equal. Then the equivalent area of truss diagonal per panel $A_v = 8.14 \text{ in}^2$ and the equivalent area of top and bottom lateral diagonals $A_h = 11.8 \text{ in}^2$. The coefficient of rigidity should be:

$$K = \frac{\pi^2 w}{2f} + \left(\frac{1-k}{1+k}\right)^2 \cdot \frac{16\pi^4 EI}{l^4} + \left(\frac{4k}{1+k}\right) \frac{\pi^2 4\, EA_v}{l^4}$$

$$= 1,155 \text{ lb/ft}^2 \qquad \text{for } n = 2$$

where $\qquad k = \frac{A_h}{A_v} \cdot \frac{d^2}{b^2} = 0.0446$

and $\qquad d = $ bridge depth $= 10 \text{ ft.}$

$\qquad\qquad b = $ bridge width $= 57 \text{ ft.}$

The coefficient of torsional rigidity

$$K_t = (b/2)^2 \, K = 938,149 \text{ lb.}$$

The polar radius of gyration

$$r^2 = \frac{\Sigma(mr^2)}{\Sigma\, m} = 462 \text{ ft.}^2 \quad (\text{or } r = 21.5 \text{ ft.})$$

and $\qquad$ $b/2r = 1.325$ $\qquad$ (with the usual range of 1.3 to 1.5)

The natural frequency of torsional oscillation should be

$$N_t = \frac{30}{\pi} \sqrt{\frac{K_t}{mr^2}} = 32.5 \text{ cycles/min.} \qquad \text{for n=2}$$

Both the vertical and torsional frequencies have high values which is desirable for stability. Since the N_t/N_v ratio is $2\frac{1}{2}$ times, the 1952 Report of the Advisory Board recommends the flutter theory to predict critical wind velocities.

8.4.3 Critical Velocity by Flutter Theory for First Anti-Symmetric Mode

To obtain the critical velocity, F. Bleich's Flutter Theory has been widely used, but in this case the vertical frequencies were calculated by using Steinman's method instead of the more complicated Ritz's method given by Bleich.

Then $\qquad$ ω = flutter frequency or circular frequency

and $\qquad$ $N_t/N_v = 2.4$

The natural frequency of vertical oscillation or vertical circular frequency

$$\omega_1 = 2\pi N_v = 1.42 \text{ rad/sec}$$

The natural frequency of torsional oscillation or torsional circular frequency

$$\omega_2 = 2\pi N_t = 3.40 \text{ rad/sec}$$

The flutter frequency

$$\omega = \frac{\omega_1}{\sqrt{2}} = 2.59 \text{ rad/sec}$$

The critical flutter frequency

$$N_c = \frac{\omega}{2\pi} = 24.7 \text{ cycles/min.}$$

The critical wind velocity

$$V_c = \frac{\omega b}{2k_c} = 306 \text{ ft/sec} = 209 \text{ mph}$$

This critical wind velocity is the same by Bleich's approximate method given in other articles. Therefore, the approximate method was used for all further studies.

8.4.4 Natural Frequencies of Oscillation in First Anti-Symmetric Mode By Selberg's Method

In employing this method assume no side span action and ignore the effect of central tie. The vertical frequency would be the same as for Steinman's method.

$$N_v = 13.54 \text{ cycles/min.}$$

The torsional frequency, by considering orthotropic deck as top lateral would be

$$\frac{L_{s2}}{L_s} \cdot \frac{1}{\lambda_2} \sum_n \frac{1}{n^2\left(\omega_T^2 - \dfrac{S(h_r - h_v)}{\mu}\right) - \alpha_{T2}\, n^4 - \beta_{T2}\, n^2\right)} = 1$$

After some computation, the torsional frequency can be obtained, $\omega_T = 4.88$ rad/sec and the natural frequency of torsional oscillation should be

$$N_T = \frac{\omega_T}{2\pi} = 46.6 \text{ cycles/min.}$$

and

$$\frac{\omega_V}{\omega_T} = 0.29$$

The flutter velocity for the first anti-symmetric mode (n=2) for the coupled oscillation should be

$$v_F = 0.44\,\omega_T\, b \sqrt{\left(1 - \left(\frac{\omega_V}{\omega_T}\right)^2\right)\frac{IY}{\mu}} = 459 \text{ ft/sec} = 313 \text{ mph}$$

With the pure torsional oscillations the flutter velocity should be

$$v_T = 0.44\,\omega_T\, b \sqrt{\frac{IY}{\mu}} = 480 \text{ ft/sec} = 327 \text{ mph}$$

8.5 Natural Frequencies of Oscillation in Symmetric Modes

The symmetric mode has an odd number of loops. The waves of this mode are symmetrical about the center line of the main span. The calculation shows that the symmetric mode for n = 1 is the worst case and governs the design.

8.5.1 Vertical Oscillation in Symmetric Mode by Steinman's Method

For symmetric modes, the difference of horizontal cable pull does equal to zero ($\Delta H \neq 0$) and the cable stretch term in the spring constant K must be considered. The general formula of K should be

$$\sum{}^{'}\left(\frac{1}{n^2} \cdot \frac{C\frac{f}{l}}{K - K_n}\right) = 1$$

where $\sum{}^{'}$ denoted the summation of odd values on n in all span

$$K_n = \frac{\pi^2 n^2}{l^2} H + \frac{\pi^4 n^4}{l^4} EI \qquad \text{for each span}$$

$$C = \frac{512 \, f \, E_c \, A_c}{\pi^2 \, l^2 \, L_s}$$

And

$$L_s = \sum \int_0^l \frac{ds^3}{dx^2} \doteq \sum (l + \frac{8f^2}{l}) \sec^3 \gamma$$

In A. Murray MacKay Bridge, the known constants are

Section Area of 2 cables	A_c	$= 2 \times 86.7 \text{ in}^2$
Elastic Modulus	E_c	$= 24 \times 10^6 \text{ psi}$
Total Length of Cable	L_s	$= 3435.6 \text{ ft.}$
Length of Main Span	l	$= 1,400 \text{ ft.}$
Length of Side Span	l_1	$= 513.83 \text{ ft.}$
Bending Rigidity of Main Span	EI	$= 329.3 \times 10^9 \text{ lb/ft}^2$

for 2 trusses

Bending Rigidity of Side Span	EI_1	$= 304.3 \times 10^9 \text{ lb/ft}^2$

for 2 trusses

Sag of cable at Main Span	f	$= 128 \text{ ft.}$
Sag of cable at Side Span	f_1	$= 17.24 \text{ ft.}$
Horizontal Cable Pull	H	$= 10,748 \times 10^3 \text{ lbs.}$

for 2 cables

Then $\qquad C = 2 \times 2050 \text{ lb/ft}^2$

for $\qquad n = 1$ at main span

$\qquad K_n = 62.5 \text{ lb/ft}^2$

and $\qquad n_1 = 1$ at side span

$\qquad K_n = 827 \text{ lb/ft}^2$

By trial and error from the general formula

$\qquad K = 307.5 \text{ lb/ft}^2 \qquad$ for n=1 dominant in main span

and $\qquad$ K = 1232 lb/ft^2 $\qquad$ for n_1 = 1 dominant in side span

The natural frequencies for these K values

For main span $\qquad$ n = 1 $\qquad\qquad\qquad$ For side span $\qquad$ n_1 = 1

$$N = \frac{30}{\pi} \cdot \sqrt{\frac{Kg}{w}} = 12.69 \text{ cyc/min.} \qquad N = \frac{30}{\pi} \cdot \sqrt{\frac{Kg}{w}} = 25.4 \text{ cyc/min.}$$

The K values for superimposed modes (n=3, n=1,3, n_1=1) have been checked. A 2% lower value than K = 307.5 for n = 1 dominant in main span was found, and thus the n = 3 component was ignored.

8.5.2 Torsional Oscillation in Symmetric Mode by Steinman's Method

The first symmetric mode (for n = 1, and n_1 = 1) is the worst case. For the safety factor, ignore the second symmetric (n=3) effect and the effect of torsional stiffness of the tower. The general formula of spring constant is the same as for vertical oscillation except the K_n value which should be obtained from

$$K_n = \frac{\pi^2 n^2}{l^2} H + \left(\frac{1-k}{1+k} \right)^2 \frac{\pi^4 n^4}{l^4} EI + \left(\frac{4k}{1+k} \right) \frac{\pi^2 n^2}{l^2} EA_v$$

Assuming the top lateral is the same as bottom lateral instead of deck plate, and k = 0.0446

For main span $\qquad$ n = 1

Then $\qquad$ K_n = 268 lb/ft^2

For side span $\qquad$ n_1 = 1

Then $\qquad$ K_n = 2,295 lb/ft^2

for n = 1 dominant, by trial and error

$\qquad$ K = 591 lb/ft^2 $\qquad$ in the general formula

Then the natural frequency of torsional oscillation should be

$$N_t = \frac{b}{2r} \cdot \frac{30}{\pi} \cdot \sqrt{\frac{Kg}{w}} = 23.3 \text{ cycles/min.}$$

Compare the anti-symmetric mode and symmetric in Steinman's method. The latter governs the design, giving lower frequency and making it more critical.

8.5.3 Critical Velocity by Flutter Theory in First Symmetric Mode

Employing Bleich's Approximate Method, the critical wind velocity, based on the calculation of Steinman's method should be

$$N_v = 12.69 \text{ cycles/min.} \qquad \therefore \omega_1 = 1.328 \text{ rad/sec}$$

$$N_t = 23.2 \text{ cycles/min} \qquad \therefore \omega_2 = 2.44 \text{ rad/sec}$$

$$\mu = 0.07$$

and

$$\omega_2/\omega_1 = 1.835$$

From Bleich's table

$$k_c = 0.280$$

$$\omega/\omega_1 = 1.492$$

$$\therefore \omega = 1.98 \text{ rad/sec}$$

The critical wind velocity

$$v_c = \omega b/2k_c = 202 \text{ ft/sec} = 138 \text{ mph}$$

For symmetric mode the critical wind velocity, of 138 mph minimum is much less than the critical wind velocity in the anti-symmetric mode.

8.5.4 Natural Frequency of Oscillation in Symmetric Mode by Selberg's Method

The natural frequency in vertical oscillation for $n=1$ and $n_1=1$ should be

$$\frac{L_{s2}}{L_s} \cdot \frac{1}{\lambda} \cdot \frac{1}{(\omega^2 - \alpha_2 - \beta_2)} + \frac{L_{s1}}{L_s} \cdot \frac{2}{\lambda_1} \cdot \frac{1}{(\omega^2 - \alpha_1 - \beta_1)} = 1$$

where
$$\alpha_m = \frac{\pi^4 \, EI_m}{m_m l_m^4}$$

$$\beta_m = \frac{\pi^2 \, \overline{H}_{wm}}{m_m l_m}$$

and
$$\frac{1}{\lambda} = \frac{512 \, f_m^2 \, E_c A_c}{\pi^2 \, l_m^3 \, m_m \, L_{sm}}$$

For main span $\alpha_2 = 0.0478$ For side span $\alpha_1 = 2.44$

$$\beta_2 = 0.31 \qquad\qquad\qquad \beta_1 = 2.42$$

$$\frac{L_{s2}}{L_s} \cdot \frac{1}{\lambda} = 2.15 \qquad\qquad \frac{L_{s1}}{L_s} \cdot \frac{2}{\lambda} = 1.58$$

Then by several trials

$$\omega_v = 1.335 \text{ rad/sec} \qquad \text{for } n=1 \text{ dominant}$$

The natural frequency in vertical oscillation should be

$$N_v = \frac{\omega_v}{2\pi} = 12.75 \text{ cycles/min.}$$

This value agree with the value of $N_v = 12.69$ cycles/min. by Steinman's method.

For the case of natural frequency in torsional oscillation, Selberg gives other formulas.

The distance from the upper lateral system to the rotation center at the cross-section of the bridge should be

$$e = \frac{A_2}{A_1 + A_2} \, d \left(1 - 2 \, \frac{b}{d} \frac{\xi}{\theta_h} \right) + \frac{1}{\theta_u} \, \xi b = -2.16 \text{ ft.}$$

(minus means 2.16 ft. above the deck)

Where $\quad A_1 = A_u + (1/6) b\, t_u = 100.7 \text{ in}^2 = 0.70 \text{ ft}^2$

$\quad A_2 = A_l = 61 \text{ in}^2 = 0.423 \text{ ft}^2 \text{ (for main span)}$

and $\quad A_2 = 55 \text{ in}^2 = 0.382 \text{ ft}^2 \text{ (for side span)}$

$\quad \theta_u = b\, t_u = 1.78 \text{ ft}^2$

$\quad \theta_l = \dfrac{E}{G} 2A_D \sin^2 \phi_h \cos \phi_h = 0.1062 \text{ ft}^2$

$\quad \dfrac{1}{\theta_h} = \tfrac{1}{2} \left(\dfrac{1}{\theta_u} + \dfrac{1}{\theta_l} \right) = 4.986$

and $\quad \theta_h = 0.2005 \text{ ft}^2$

$\quad \theta_v = \dfrac{E}{G} A_d \sin^2 \phi_v \cos \phi_v = 0.0731 \text{ ft}^2$

$\quad A_D = 8.87 \text{ in}^2$

$\quad A_d = 10.65 \text{ in}^2$

$\quad \dfrac{E}{G} = \dfrac{29.6 \times 10^6}{11.4 \times 10^6} = \dfrac{1}{0.385}$

$\quad \xi = \dfrac{b d \theta_v \theta_h}{b^2 \theta_v + d^2 \theta_h} = 0.0325 \text{ ft}^2$

The center of gravity (c.g.) is 8.8 ft. above the bottom of truss.
The distance between the center of rotation and the c.g. is 3.86 ft.
The torsional modulus

$$I_D = 2\, db\, \xi = 37 \text{ ft}^4$$

The warping factor

$$C_W = 2\, \frac{A_1 A_2}{A_1 + A_2} b^2 d^2 \left(\tfrac{1}{2} - \frac{d\xi}{b\theta_v} \right)^2$$

The factor

$$\alpha_T = \frac{\pi^4 \Sigma C_W E}{l^4 M}$$

and
$$\beta_T = \frac{\pi^2 (\overline{H}_w \frac{b^2}{2} + G I_D)}{l^2 \mathcal{M}}$$

For main span $C_{w2} = 30,500$ for side span $C_{w1} = 28,500$

$\alpha_{T2} = 0.041$ $\alpha_{T1} = 2.11$

$\beta_{T2} = 4.33$ $\beta_{T1} = 32.5$

The hanger force $S = 2,416$ lb/ft/cable

The distance from c.g. of suspended section to center line of suspender pins should be

$$h_r - h_w = 2.87 \text{ ft.}$$

and $\mathcal{M} = \Sigma mr^2 = 80,500$

Then the natural frequency in torsional oscillation should be

$$\frac{L_{s2}}{L_s} \cdot \frac{1}{\lambda_{T2}} \cdot \frac{1}{(\omega_T^2 - \frac{S(h_r - h_w)}{\mathcal{M}} - \alpha_{T2} - \beta_{T2})} + \frac{L_{s1}}{L_s} \cdot$$

$$\frac{2}{\lambda_{T1}} \cdot \frac{1}{(\omega_T^2 - \frac{S(h_r - h_w)}{\mathcal{M}} - \alpha_{T1} - \beta_{T1})} = 1$$

by several trials

$$\omega_T = 2.81 \text{ rad/sec.}$$

Then $N_T = \frac{\omega_T}{2\pi} = 26.85$ cycles/min.

This value agrees with $N_T = 23.3$ cycles/min. by Steinman's method. Thus using orthotropic deck instead of top laterals increases the N_T by 15% and shows that Steinman's method is not so accurate as Selberg's method for unequal top and bottom laterals.

8.6 Comparison of Bleich's Flutter Theory with Rocard, Selberg and Frandsen Theories

Recently, Rocard, Selberg and Frandsen have brought out much simplified methods of calculating critical flutter velocity, which have checked accurately with model studies. These methods are shown in Frandsen's paper.[14]

The critical velocity v_c obtained by Bleich, Rocard, Selberg and Frandsen for n=1, and n_1=1, revealed a good agreement within a 3% difference. The v_c value was based on the low value of ω_2 and excluded the effect of an orthotropic deck.

8.7 Critical Velocity Due to Coupled Oscillation and Vertical Oscillation by Selberg's Method

8.7.1 Coupled Oscillations

The coupled vertical-torsional oscillation with mode n=1, n_1=1, the critical velocity $v_c = k\,v_F$, k values could be obtained from graphs in Selberg's paper depending on various ω_T/ω_V ratio. The angle of attack are $\alpha = 0°$, $\pm 5°$ and $\pm 10°$ to horizontal surface.

From Fig. 8.1 $d/b_1 = 0.0256$

The preliminary design with

$$A_2 = A_l = 61 \text{ in}^2 = 0.423 \text{ ft}^2$$

and $\qquad A_1 = A_u + (1/6)bt_u = 72.3 \text{ in}^2 = 0.502 \text{ ft}^2$

where $\qquad A_1 = A_u$ (upper chord area of stiffening truss) + $(1/6)bt_u$

$\qquad A_2 = A_l$ (lower chord area of stiffening truss)

$\qquad b$ = width of bridge = 57 ft.

$$t_u = \text{thickness of deck plate} = 3/8 \text{ in.}$$

then $\omega_T = 2.81$

$\omega_V = 1.335$

$\omega_T/\omega_V = 2.1$

and $\qquad v_F = 0.44\,\omega_T\,b\sqrt{(1 - (\dfrac{\omega_V}{\omega_T})^2)\,\dfrac{\sqrt{v}}{\mu}} = 165 \text{ mph}$

This value is higher than before, which includes the orthotropic deck action. It is the most accurate calculated value and used throughout the design.

The result of critical velocities $(v_c = k\,v_F)$ on various attack angles is shown in table 8.2.

TABLE 8.2 CRITICAL VELOCITIES FOR VARIOUS ATTACK ANGLES

Angles of Attack	$\alpha = 0°$		$\alpha = +5°$		$\alpha = -5°$		$\alpha = +10°$		$\alpha = -10°$	
Critical Velocity	k	v_c mph	k	v_c mph	k	v_c mph	k	v_c mph	k	v_c mph
v_1	0.79	130	0.36	59	0.37	61	0.162	27	0.17	28
v_2	0.75	124	0.455	75	0.47	78	0.310	51	0.315	53
v_3	0.60	99	0.50	83	0.51	84	0.365	61	0.37	62

where v_1 = the high wind velocity where an initiated oscillation of

$\phi_1 = \pm\,0.01$ radian (i.e. $0°35'$) will be stable or decrease.

v_2 = the wind velocity where an initiated oscillation of

$\phi_2 = \pm\,0.1$ radian (i.e. $5°44'$) will be stable or decrease.

v_3 = the wind velocity where an initiated oscillation of

$\phi = \pm 0.2$ radian (i.e. $11°27'$) will be stable or decrease.

To verify the accuracy of results, the following factors should be considered.

A. Factor which would reduce the above critical velocities

	Factor	Rough Estimate of effect
1.	Presence of handrail, lower truss, curbs etc. instead of idealised deck.	-10%
2.	The actual μ value of 0.07 exceeds the value of 0.018 used for the model testing.	-10%
3.	The model k values are based on damping logarithmic decrement $\delta = 0.04$ to 0.05. This probably high for orthotropic deck structure, generally may be down to 0.02	-5%
4.	Effect of lateral wind force neglected in model tests	-5% to -10%

B. Factor which would increase the above critical velocities

1.	v_F value is calculated for no damping effect. The effect of tower bending and torsional stiffness of towers is also ignored	+ 10%
2.	Assume identical vertical and torsional modes by putting D=1 in Bleich's terminology is not correct.	+5% to +10%
3.	Oscillations are not self induced by steady wind.	+5%

From all above factors, the critical velocities against wind may be 10% too high. However, this is compensated by the high figures used for mean design wind. In addition, the final flutter velocity v_F = 180 mph is 10% higher than the preliminary v_F = 165 mph and is completely safe based on the required maximum horizontal design wind velocity (i.e. 104 mph). Therefore, the results of critical velocities in Table 8.2 are quite justified.

8.7.2 Vertical Oscillations

Compared with the coupled and torsional oscillations, the vertical oscillations are of minor interest. They will not be of a catastrophic nature. However, they are frequently observed on bridges, but have never been the main reason for disaster.

The critical velocity in vertical oscillation with the mode n=1 and n_1=1 should be

$$v_c = k_v \omega_v b$$

where $\omega_v b = 1.335 \times 57 = 76$

k_v is given in graph from model tests.

Refer to the graph in Selberg's paper k_v values show complete stability from 0 to 0.25 and from 0.4 to 3.8.

$$v_c = 76 k_v \text{ ft/sec} = 51.8 k_v \text{ mph}$$

Thus the bridge will be completely stable with wind speeds of 0 to 13 mph and from 21 mph to 197 mph.

The amplitude of vibration is

Maximum $a_\mu = a \text{ diagram} \sqrt{\dfrac{\mu}{0.018}} = 1.12$ ft.

where $a_{diagram}$ = 0.01 b for low velocity vibration.

8.7.3 Conclusion on Coupled Oscillation and Vertical Oscillations

A. Coupled Oscillations

1. For attack angle $\alpha = 0^\circ$

This is a horizontal wind where $v_1 > v_2 > v_3$ and thus the section is completely stable up to v_1 = 130 mph. When velocity exceeds 130 mph will immediately become catastrophe, then v_2 and v_3 are not important.

2. For attack angle $\alpha = \pm 5^\circ$

The bridge will undergo small oscillations but of no danger under a steady wind of 59 mph at 5° angle of attack. Comparison with Severn Bridge site wind studies shows a maximum speed of 44 mph at 4° angle of attack. Thus 59 mph at 5° attack can be considered highly improbable and 75 mph for v_2 or 83 mph for v_3 unlikely. Hence the bridge should be stable up to 5° angle of attack.

3. For attack angle $\alpha = \pm 10^\circ$

The bridge will undergo small oscillations but of no danger under a steady wind of 27 mph at 10° angle of attack. No figures are available for likely site wind speeds at this angle, but steady wind for an extended period of several minutes on whole bridge length, must be considered highly improbable. Steady wind of 51 mph at 10° angle of attack may also consider impossible. This is confirmed by wind test at the Forth Bridge site. Thus the bridge is completely safe against dangeous or catastrophic coupled oscillation.

B. Vertical Oscillation

The vertical oscillations with amplitude up to just over one foot

are possible at low wind velocities in range of 13 to 21 mph. This would
not effect the safety of the bridge and it can be overcome by increasing
damping capacity in order to reduce this possibility. Selberg states
that possibility of this low velocity vibration may be over emphasised
as only possible on model if induced at correct amplitude, thus may not
be self induced by wind in practice.

8.8 Studies of Mean Wind Velocity at Site

The National Building Code Supplement No. 1, 1965 shows at Halifax,
maximum wind gust speed of 88 mph on a 30 year return period, at a 30 ft.
height. To set up oscillation a steady wind over the whole structure is
required. The bridge truss is at the height of 130 ft. to 190 ft. for
which the N.B.C. gives a height factor of 1.4 to be applied to the wind
pressure. As the wind pressure is αv^2, the wind velocity factor at this
height would be $\sqrt{1.4} = 1.183$. Then maximum design wind velocity at truss
level of the bridge would be

$$v_{design} = 1.183 \times 88 = 104 \text{ mph}$$

NBC also assumes gust speed increased in proportion to $(height)^{1/10}$,
and this is used in table of pressure for increasing height. Taking average
truss elevation of 170 ft., the gust speed on 30 year return should be

$$v = \frac{(170)^{1/10}}{(30)^{1/10}} \times 88 = 105 \text{ mph}$$

Selberg gives a mean wind velocity for design in Norway v_{mean}
$= 0.77 \, v_{gust}$. Then the mean wind velocity in Halifax bridge on 30
year return should be $v_{mean} = 81$ mph.

Davenport in Canada proposes formula for changing annual velocity

U to velocities for different return period.

$$v = U + (1/a)\log_e r$$

where   r = return period in years

         1/a = a scale factor taken as 8.0

Then for 30 year return period

$$v = U + 27$$

for 100 year return period

$$v = U + 37$$

Thus annual velocity (r=1) increased by 27 mph to get 30 year value (r=30) and 37 mph to get 100 year (r=100) value. The difference from r=30 to r=100 is 10mph. Then the mean wind velocity on 100 year return period should be 91 mph.

Compared with Hirai's Method[15] which gives height formula applied to mean speed, with different factors for different topography, for the gust speed = 88 mph at 30 ft. on 30 year return, then mean speed

$$v_{30 \text{ ft.}} = 0.77 \times 88 = 68 \text{ mph}$$

at 170 ft. the mean wind velocity for 30 year return should be

$$v_{170 \text{ ft}} = 68 \left(\frac{170}{30}\right)^p = 84 \text{ mph}$$

where   p = 1/8 for open water

Then the mean wind velocity on 100 year return should be 94 mph. Therefore the assumed design mean wind velocity of 104 mph was high and would balance possible 10% error in the critical velocity. (referred to section 8.7.1)

8.9 Bottom Lateral Revision and Affect on Aerodynamic Stability

In order to take care of live load torsional stresses, the bottom laterals had to be increased in size to $12\frac{1}{2}$ in. by 10 in. average in main span, after the preliminary stduies were completed. The I section was made up of 2-10 in. by 7/16 in. flanges and 1 - 11-5/8 in. by 5/16 in. web, and the area was 12.38 in.^{2} The distance from the upper lateral system to the rotation center at the cross-section of the bridge, by Selberg's method, should be

$$e = -1.61 \text{ ft (i.e. 1.61 ft. above deck)}$$

where

$$A_1 = 100.7 \text{ in}^2 = 0.7 \text{ ft.}^2$$

$$A_2 = 61 \text{ in}^2 = 0.423 \text{ ft}^2$$

$$\theta_u = 1.78 \text{ ft}^2$$

$$\theta_l = 0.148 \text{ ft}^2$$

$$1/\theta_h = 3.66$$

$$\theta_h = .273 \text{ ft}^2$$

$$\theta_v = 0.0731 \text{ ft}^2$$

$$\xi = 0.043 \text{ ft}^2$$

The center of gravity (c.g.) is 8.7 ft. above the bottom of truss. The distance between the center of rotation and the c.g. is 3.41 ft. The torsion modulus

$$I_D = 49 \text{ ft}^4$$

The warping factor C_w

For main span $C_{w2} = 26,900$ For side span $C_{w1} = 25,200$

and the factor $\alpha_{T2} = 0.0362$ $\alpha_{T1} = 1.866$

$$\beta_{T2} = 5.55 \qquad\qquad \beta_{T1} = 41.6$$

The hanger force

$$S = 2,416 \text{ lb/ft/cable}$$

The distance from c.g. of suspended section to $\cancel{c}$ of suspender pins should be

$$h_r - h_w = 2.97 \text{ ft.}$$

Then the natural frequency in torsional oscillation by several trials

$$\omega_T = 3.03 \text{ rad/sec}$$

Then

$$N_T = \omega_T/2\pi = 29.0 \text{ cycles/min.}$$

And

$$\omega_V/\omega_T = 0.44$$

The flutter velocity $v_F = 264 \text{ ft/sec} = 180 \text{ mph}$

By increasing the bottom lateral area the critical velocity against the wind rose from 165 mph to 180 mph. This is about 10% higher than the preliminary critical velocity.

8.10 Bridge Model Under Wind Tunnel Test

8.10.1 Introduction

The effect of wind load is an important factor in the suspension bridge, both when the structure is completed and during erection phases. Most of the wind tunnel tests to date have been based on the steady wind blowing from various directions against the completed bridge. The information of the partially-built situation and the contractor's potential problems with winds during field assembly is little known.

A series of models tests were carried out by Dr. A.G. Davenport in the Univeristy of Western Ontario during the year of 1969. The behaviour of suspended spans during erection phases and the completed bridge in turbulent flows was of great interest to the researchers. On the other hand

the superstructure contractor was also concerned about erection stresses and wanted to know how strong winds would have to be before lifting schedules were affected. They particularly wanted to know whether steel work on the center span should be installed in complete units or with deck plates left off. Finally the consulting engineers wished to confirm the calculated behavior of the completed structure by model studies. The three parties therefore collaborated for the wind tunnel tests.

The investigation covered four stages of construction and included:[16]

1. A 1/150 scale mechanical model to aid in the determination of the dynamic behaviour during erection.

2. A 1/40 scale section model to investigate the critical velocities for instability during erection phases and the effect of partial removal of the deck plate.

3. A 1/320 scale aeroelastic model of the full bridge in turbulent boundary layer flow representative of the natural wind and in smooth uniform flow.

The study began with the determination of the critical wind speeds at various stages of erection from the section model. Next, the influence of removing the central third, the two other thirds, and then all of the deck plate on these critical wind speeds was considered. From these studies, four erection phases, Fig. 8.2, were selected for study using the full bridge aeroelastic model.

8.10.2 Mechanical Model

A mechanical model of 1/150 scale of the A. Murray Mackay Bridge was set up in order to determine the dynamic properties of the bridge during

the various construction phases. The model represented the entire
suspension bridge from the Dartmouth to Halifax cable anchorages.

The frequencies and the mode of oscillations of the bridge were
determined from the mechanical model for various construction stages
of the bridge.

The lowest natural frequencies of the bridge vary significantly
throughout the deck construction phases. The lowest symmetric and anti-
symmetric frequencies of lateral oscillation are approximately half the
final values. The vertical oscillations are slightly greater than the
final value after 20% erection. It falls to a value slightly below the
final value as construction progresses until bolting of bottom chords and
addition of roadway surfacing takes place. Torsional frequencies through
construction are lower than the final value.

The mechanical model showed a close agreement with the mode shape
and natural frequencies obtained theoretically.

8.10.3 Section Model Tests

A model representing a 160 ft. section of bridge deck was set up
to a geometric scale of 1:40. The section model was mounted on springs
in order to allow the simulation of appropriate drag, vertical, and
torsional frequencies of oscillation.

The purpose of the section model tests was to determine the wind
velocity at the onset of aerodynamic instability of the bridge during
various construction stages. In order to permit an evaluation of diff-
erent bridge deck erection procedures, the influence of deck plate
coverage on the critical velocity v_c was studies. Since aerodynamic

instability was expected to occur in the form of coupled vertical and torsional oscillations, the most critical construction phase was considered to occur when the ratio of vertical to torsional frequency approached unity. This would be more likely to happen only during initial construction Phase 1 (i.e. 4 to 12 number of 31 ft. 8 in. deck section were erected at the center of the main span).

In addition to measurement of mean and dynamic deflection of the model, mean coefficient of lift force, drag force, and torsional moment were measured for the final deck configuration with guard rails for a range of attack angle $-9° \leq \alpha \leq 9°$. All section model tests were carried out in smooth uniform velocity flow.

The dynamic response of the model was irregular and typically very small until a critical wind speed was reached. Increasing the wind speed beyond this critical value resulted in a sharp increase in response amplitudies. The motion became very regular and consisted of coupled vertical torsional oscillations. The frequency of these oscillations was between the uncoupled vertical and torsional frequencies and was found to reduce slightly with further increases of wind velocity. The effective center of rotation was found to be upstream from the bridge center-line.

The influence of removing part of the bridge deck plate was to increase the critical velocity during construction Phase 1. It was seen to increase from about 50 mph full scale with full deck plate to about 150 mph with deck plate only along the central third of the bridge. The influence of increasing mechanical damping for the final bridge with all deck plate in place was to slightly increase the critical wind velocity.

8.10.4 Full Aeroelastic Model

An aeroelastic model of the full bridge was constructed to a geometric scale of 1:320. The main towers of the model were rigid, mounted on splines at their base to give the required longitudinal bending stiffness for a point load applied at the top of the tower. The torsional stiffness of the towers, defined in terms of the opposite acting longitudinally applied forces at the top of tower leg required to produce unit tower leg displacements in opposite directions, was only approximately modelled. The cable bents were cantilevered from the model base and represented the combined stiffness and mass of the full scale cable bent and cable backstages.

The test program consisted of investigating the time-average and dynamic response of the bridge during the four construction phases over a representative range of wind speed and direction. To realize wind condition at the bridge site, two wind exposures were used in the model investigation. One wind exposure, referred to as "smooth exposure", was representative of wind coming over Bedford Basin or Halifax Harbour. The other exposure referred to as "rough exposure" was representative of wind over a relatively rough, built-up terrain quartering wind or winds parallel to the prototype bridge. The full bridge model in the wind tunnel with floor surface roughness used to develop the "smooth" and "rough" wind exposures were tested. Hot wire anemometer measurements were made of both the mean and turbulent flow properties.

The aeroelastic model representing the final bridge Phase 4, was also tested in uniform smooth flow. The response of the aeroelastic model in smooth flow was considerably different from that observed in turbulent boundary layer flow. Dynamic response amplitudes were generally small.

however, mean lift and torsional deflections increased with velocity until the bridge became statically unstable at about 135 mph full scale.

8.10.5   1:320 Scale Section Model

In order to clear the possible cause for the observed difference in aerodynamic stability between section and aeroelastic model in geometric scale, a 1:320 scale section model was constructed to represent approximately a 170 ft. portion of the bridge. This model was mounted on springs and placed between stationary end plates in the wind tunnel. Tests on this model were conducted in uniform smooth flow for an angle of attack $\alpha=0^\circ$ and with one value of mechanical damping.

The response of the 1:320 scale section model was found to be quite similar to that of the corresponding 1:40 scale section model. Response amplitudes were small until a critical velocity was reached. Above this velocity regular coupled vertical-torsional oscillation were observed. From these results it was concluded that the difference in response of the full aeroelastic model and the section model could not be explained by the scale difference.

8.10.6   Conclusions on Model Tests

After the full series of model tests, the following conclusions were reported by Prof. Davenport:

1. The critical velocities for instability during erection phases were indicated by section models to be substantially lower than those for the completed bridge.

2. Turbulence in the airstream had a profound influence on the behaviour during all erection phases.

3. Instability of the coupled torsional-vertical mode were encounted in Phase 1 of the erection but at a wind speed considerably in excess of that indicated by the section model test. In an extended test with the completed bridge coupled torsional-vertical instability was noted at 200 mph. At 210 mph divergent instability occurred in turbulent wind.

4. Measurements on the full aeroelastic model integrated with meteorelogical information indicated that aerodynamic instability with the full deck was improbable during any construction phase.

5. Prediction of behaviour of bridge during the erection phases indicate that maximum vertical deflection may be expected during Phase 2.

6. Predictions of behaviour of the completed bridge appear to be in accordance with normal criteria. Maximum hourly single vertical amplitudes approximately 1/400 of the span may be expected once every 30 years: transverse amplitudes are smaller.

TABLE 8.1   STIFFNESS INDICES ON EXISTING SUSPENSION BRIDGES

No.	Bridge	Year	Type *	Lat. **	Span ft.	STEINMAN'S INDICES			AMMANN'S INDICES		Observations On Movements
						K	K/B	$\sqrt{K/B}$	Bending S_1(1965)	Torsion S(1964)	
1.	Verrazano-Narrows	1965	T	D	4260	238	414	1.12	702	488	n=2 V&T modes a=6 ft. v=70mph
2.	Golden Gate I	1937	T	S	4200	116	151	0.73	336	111	-
3.	Golden Gate II	1958	T	D	4200	116	151	0.73	364	292	-
4.	Mackinac	1958	T	D	3800	81	83	1.65	220	-	-
5.	George Washington I	1931	B	S	3500	244	344	0	654	221	Slight T & Mild V
6.	George Washington II	1962	T	D	3500	319	568	0.75	950	694	-
7.	Forth Bridge	1963	T	D	3282	106	95	1.43	301	-	-
8.	Tacoma Narrows I	1940	PG	S	2800	62	117	0.18	158	61	Catastrophe T over 30mph
9.	Tacoma Narrows II	1950	T	D	2800	112	135	3.70	394	-	-
10.	Transbay	1936	T	S	2310	324	705	10.17	1004	-	-
11.	Bronx Whitestone I	1939	PG	S	2300	141	142	0.42	388	-	n=2 V mode a=15 in.
12.	Bronx Whitestone II	1947	T	S	2300	188	216	2.59	578	-	-
13.	Delaware Memorial	1951	T	D	2150	160	242	3.02	483	-	-
14.	Walt Whitman	1957	T	D	2000	259	267	3.01	760	-	-
15.	Ambassador	1929	T	S	1850	212	375	5.50	800	-	-
16.	Chesapeake Bay	1966	T	D	1600	165	392	8.82	564	-	-
17.	Lion Gate	1939	T	S	1550	119	172	4.72	386	-	n=1, V mode, a=3in. v=50mph
18.	Mid Hudson	1930	T	S	1500	262	655	11.00	880	-	-
19.	Angus Macdonald	1955	T	S	1447	141	204	5.66	482	944	-
20.	A. Murray MacKay	1970	T	D	1400	176	153	4.74	598	-	-
21.	Triborough	1936	T	S	1380	547	570	8.00	1550	-	-
22.	St. Johns	1930	T	S	1207	252	373	7.00	800	-	-
23.	Mount Hope	1928	T	S	1200	201	436	10.00	700	-	-
24.	Ogdensburg	1961	T	S	1150	259	412	13.40	974	-	-
25.	Deer Island	1939	PG	S	1080	69	150	2.40	190	-	n=1 V mode a=12.5 ft. v=72mph
26.	Ile d'Osleans	1935	T	S	1059	229	378	13.20	900	-	-
27.	Peace River	1943	T	S	930	442	1105	24.2	1560	-	n=1 T mode Ø=5° v=40mph
28.	Thousand Islands	1938	PG	S	800	127	219	3.3	350	-	n=1 V Mode a=12 in.
29.	Fykesund	1937	B	S	755	106	294	4.2	230	-	n=2,3,4 V mode a=2.62 ft.
30.	Beauharnois	1948	PG	S	580	517	985	22.5	2400	-	n=1 V mode a=6.5 in.
31.	Liard River	1943	T	S	543	678	1145	27.0	2700	-	Small torsion v=35 mph
	Recommended Stiffness				-	-	300	5.0	600	450	

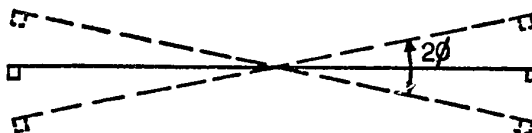- = Recommended Stiffness Value if no model tests

* T=Truss PG = Plate Girder B = Beam   ** D = Double Laterals S=Single Laterals
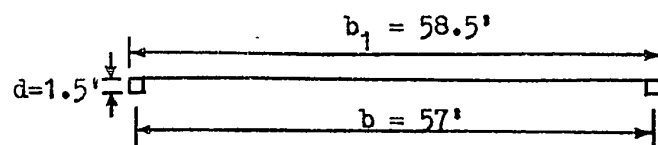
A. IDEALISED DECK AND TOP CHORD

B. ANGLE OF WIND ATTACK α

C. ANGULAR DISPLACEMENT ϕ

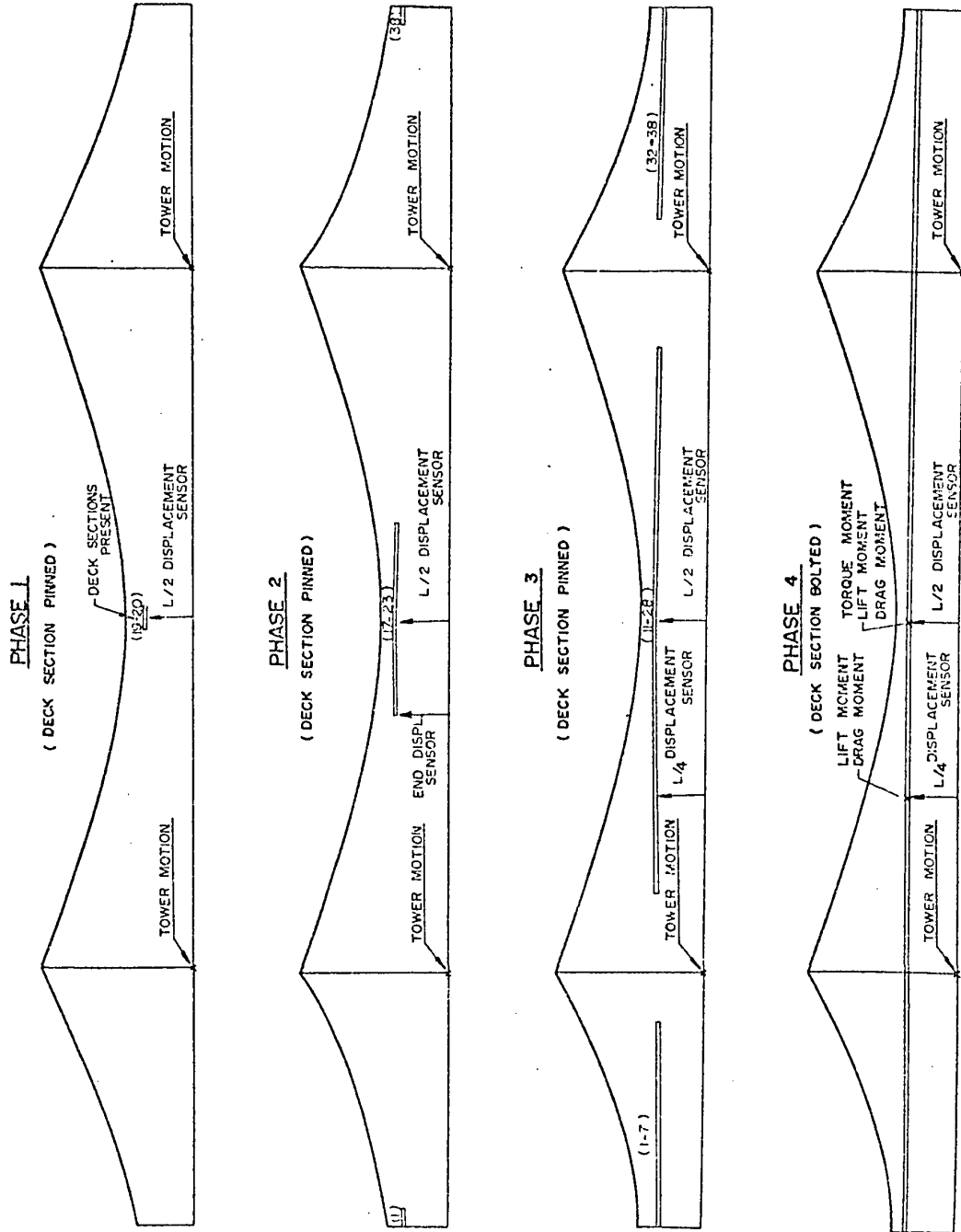FIG. 8.1 DETAILS OF CONFIGURATION TO FIND THE CRITICAL VELOCITIES

FIG. 8.2 CONSTRUCTION PHASES INVESTIGATED

CHAPTER 9

SUBSTRUCTURE DESIGN

9.1 Main Pier Design

The Halifax main pier is located about 60 ft. offshore and that of Dartmouth is about 814 ft. beyond the shore. The rock line elevation is -31.5 ft. at Halifax and -73.1 ft. at Dartmouth. The bed of the Narrows consists of a soft coarse gravels, sand and boulders at an average depth of about 15 ft. Underneath these overburden, the solid quartzite bed rock is found. The rock pressure capacity is 20 ksf for normal loading and 25 ksf with wind load. The stream flow is 1.27 ft/sec based on $\frac{3}{4}$ knot/ hr. and the design wind pressure on tower foundations is 31.5 psf.

Two boreholes were made at each pier, which were carried well into the solid rock formation. After extensive analysis of the bedrock, it was found that adequate pressure was available to construct the piers on both sides. In order to anchor the piers and be sure of sound rock, they were embedded two ft. below the rock line.

The direct load from the superstructure to each main pier is about 13,200 kips. Both piers are rounded at the ends and have a dimension of 24 ft. by 95 ft. at the lower portion and 20 ft. by 91 ft. at the upper as is shown in Fig. 9.1. A total of 34 anchor-bolts, 3 in. diameter and 14 ft. 3 in. long, were embedded into each pier. The bolts were set to a steel template and the entire tower seat was ground to the required level.

Two types of concrete were used. In the upper portion an ultimate strength of 4,000 psi while 3,500 psi were employed in the lower portion. Both ways temperature bars of 5/8 in. diameter at 18 in. were placed at all side surface and 1-1/8 in. dowels, 4 ft. 6 in. long at 18 in. were set between the upper and lower portions.

9.2 Cable Bents and Portal Frame Piers

The Dartmouth cable bent pier is located about 300 ft. offshore. The design conditions are exactly the same as for the main pier. This pier is also rounded at the ends and has a dimension of 18 ft. by 75 ft. at the lower portion and 15 ft. by 72 ft. at the upper portion. The direct load from the superstructure is about 3000 kips.

Two other piers of the approach spans are also partially underwater at the Dartmouth side. Both of these piers are constructed to the same configuration as the main piers.

The approach spans are supported by slender concrete portal frames. All the shafts and horizontal struts of the frames on the Dartmouth side, except the two closest to the abutment which have smaller size, are 8 ft. by 8 ft. The Halifax shafts are much shorter, consequently, the size is only 7 ft. by 6 ft. The footings, vary from 13 ft. square to 16 ft. square, embedded 2 ft. below rock level. One of these frames on each side stands directly on the anchorage. This extra load from the frame is always advantageous to the anchorage and increase its stability.

9.3 Abutments for Approach Spans

The abutments on each side are identical in configuration. They

consist of a L shape seat beam and two rectangular columns in the form of
a portal frame. This is an open filled type abutment and the superstruc-
ture is simply supported on the rubber bearings of the seat beam. The
whole abutment is covered by soil or granular fill. Therefore, no wind
pressure has been considered except that transferred from the superstructure.

The seat beam is 4 ft. deep and 7 ft. wide with a 1 ft. 3 in. back
wall. The columns, 30 ft. apart, are tapered from 6 ft. by 5 ft. at top
to 9 ft. by 5 ft. at the bottom. These columns are rigidly connected to
the combined footing (5 ft. 6 in. deep) also embedded 2 ft. below the
rock level.

9.4 Anchorage Piers

The anchorage pier is of mass concrete sufficiently heavy to resist
the anchorage pull of the main cables. The shape takes advantage of the
lateral support from the surrounding earth. The weight is concentrated
towards the rear in order to minimize undue tow pressures from the over-
turning effect of the cable pull and a heel block extends 20 ft. further
into ground in order to gain more horizontal resistance.

The size of the anchorage pier is 88 ft. by 94 ft. with 63 ft. height
at Dartmouth side and 85 ft. by 94 ft. with 57 ft. height at Halifax. Both
are U shape with the mass of concrete at the heel. The wing blocks are
28 ft. by 39 ft. with 46 ft. height.

Basically, the anchorage consists of a heavy concrete box providing
anchorage for the main cables, together with suitable inspection chambers.
The shafts of the portal frame, from which the approach span is supported,
are carried on the flat roof. The exterior of the anchorage is treated

architecturally. Access to the anchorage is provided by a door at ground level. These chambers are ventilated by concrete grilles set low down in the side walls.

With reference to the stability of the anchorage, sliding due to the horizontal pull of the cables is resisted by the horizontal friction developed between the concrete and the rock foundation; and by positive horizontal bearing on the front pedestal, the battered sides of the main structure and of the heel block. A coefficient of friction of 40% was assumed and the allowable horizontal bearing on the rock is 5 kips/ sq. ft. The resistance to sliding developed over the base area only is just greater than the horizontal component of the cable pulls. However, the total factor of safety is slightly higher than 1.5 with 14,208 kips horizontal cable pulls.
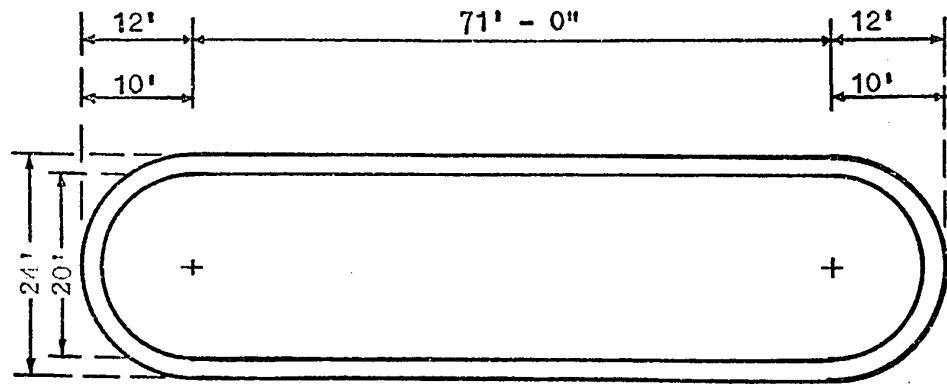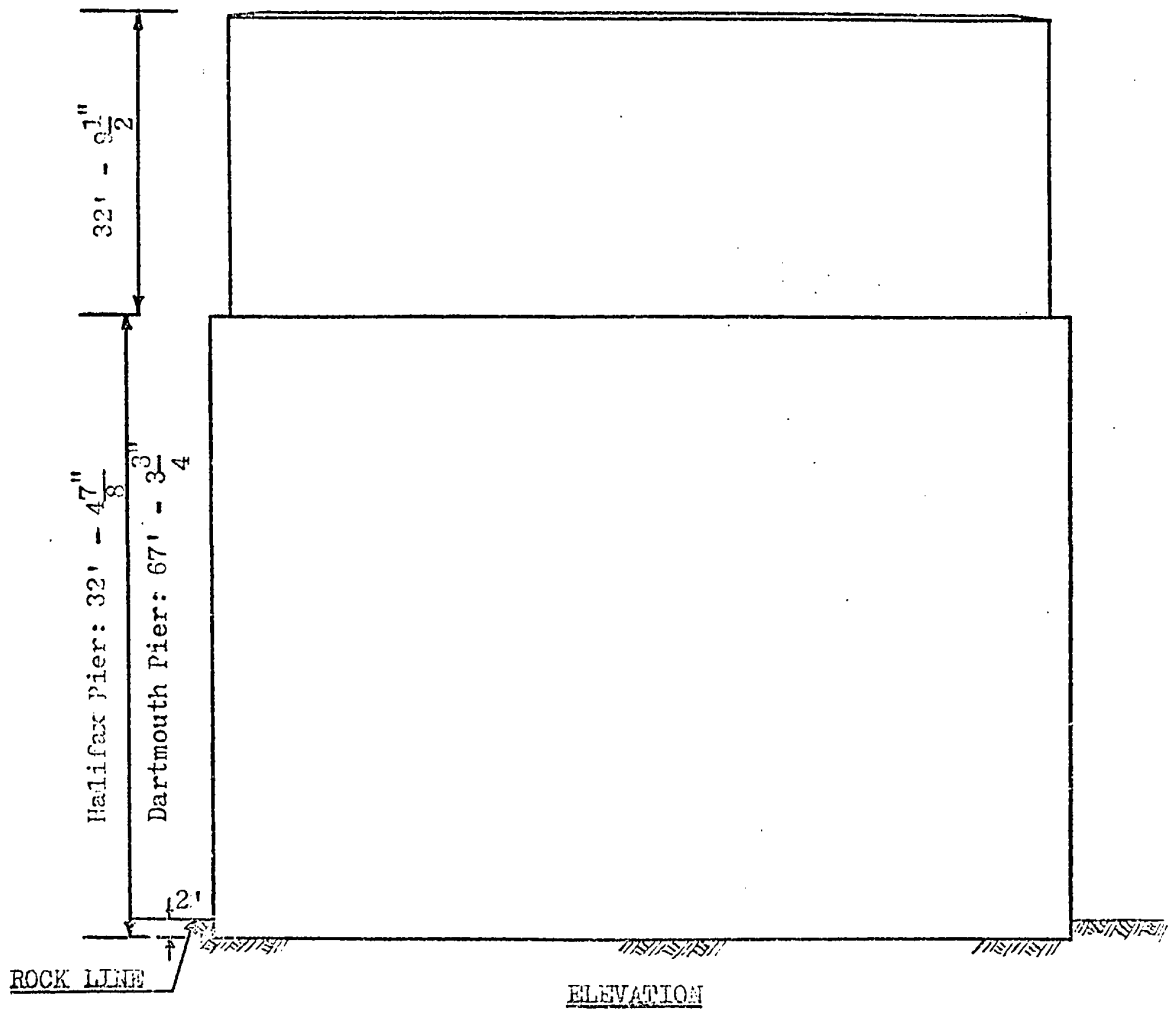
PLAN

ELEVATION

FIG. 9.1 MAIN PIERS

CHAPTER 10

STEEL FABRICATION

10.1 Fabrication of the Orthotropic Deck

The rapid evolution of orthotropic bridge primarily depends on the wide application of welding and prefabricating in the shop. The large number of welded joints affords a good opportunity to sub-assemble the section for automatic welding and modern fabrication methods. Since most of the deck sections are identical, they may be set up in a jig and welded rapidly and efficiently.

The superstructure contract was awarded to Canadian Bridge Division of Hawker Industries Ltd. in August 1967. The orthotropic deck was sublet to Eastern Car Ltd. and all the sections were built in their Trenton plant, Nova Scotia, about 100 miles from the site. The deck panels of the main span were assembled on shore at the site while the side span sections were hoisted in position piece by piece and assembled in mid-air.

The middle deck sections were built to 18 ft. by 31 ft. 8 in.[±] while the two outside deck sections were constructed to 18 ft. 3-5/8 in. by 31 ft. 8 in.[±] These three sections combined to form a 57 ft. wide deck. At the time of fabrication, automatic welding processes were widely adopted, and the submerged arc method was used for rib to deck plate welding. In order to eliminate splicing at each floor beam, the ribs ran the full length of a panel, with webs of the floor beams cutout to fit around the ribs. The closed ribs were bevelled along the edges for the V-groove

welded connection to the deck plate, which called for 90% penetration.
All these welding had 100% magnetic particle inspection for the first
3,000 ft. of longitudinal ribs, and after that, a 3 ft. long inspection
at each end of the fabricated section was required. Each section was
made airtight by the end diaphragms to prevent corrosion of the inside
surface and pressure tested.

All the field splices were connected with A-325 high strength bolts,
this being more rapid and convenient than field welding. On the other
hand, an orthotropic deck truss would have a lower damping capacity than
a truss with a standard floor system, as the frictional damping provided
by stringers sliding on floorbeams as the truss deflects would be lost.
Riveted and bolted structures have higher damping than welded structures,
hence all orthotropic deck field splices to be bolted rather than welded.
It should be noted that the floor beams were welded to the ribs in each
deck section and bolted to the floor trusses at the site.

10.2 Fabrication of Stiffening Truss and Main Tower

10.2.1 Stiffening Truss

In order to achieve the correct load distribution between cables and
truss wherein the latter are unstressed under dead load at normal temper-
ature, it is essential that the field-geometry of the structure shall
conform closely to the theoretical dimensions. The lengths of cables
and suspenders were obtained accurately, and every effort was made to
attain equal precision in the profile of trusses.

The contractor made complete detail drawings of the trusses from the
end of the side-span to the middle of the central span, and each section

was fabricated individually. On account of the constantly changing gradient of the suspended structure, the only repetitive details were those of the vertical member. The engineers required accurate facing of the ends of chord-members at all splices, and the varying angles of these members necessitated extremely precise workmanship.

The trusses were fabricated in sections of approximately 39 ft. 7 in. in overall length, each shipping-piece comprising two vertical members, four diagonals and 31 ft. 8 in. of each chord. The upper chord splices were made immediately underneath the hanger. The truss sections were shop-assembled and levels and dimensions were checked before reaming and bolting took place.

10.2.2 Main Towers

The main towers were sublet to Bridge and Tank Ltd., and all the sections were fabricated in their Hamilton Plant, Ontario.

In view of the importance of precise alignment of the tower-columns to ensure their verticality when erected, great care was taken in the fabrication. At least three sections of each main tower-column, comprising core and both wings, were assembled together in the shop before reaming the holes of the first splice. One additional section was added before reaming each subsequent splice so that no fewer than three sections would be assembled at each stage. In practice the core section would sustain the full bearing, utmost care was taken before reaming the holes. The longitudinal centre line of the tower-column was marked on the first sections assembled and prolonged and checked for straightness as the work proceeded.

The length of the tower-columns as detailed and fabricated was 1 in.
longer than the theoretical, that amount representing the normal compres-
sive strain when in service.

10.3 Fabrication of Cable Strands and Suspender Ropes

The strand of the main cable was built up of a core of 9/9/1 with
two outer layers of 15 and 21 wires respectively. 45 of the total of
55 wires were of 0.193 in diameter, (the core wire was 0.215 in diameter
while the rest 9 wires of first inner layer were 0.1055 in diameter)
before galvanizing. The normal diameter of the galvanized strand was
1.571 in. and the weight was 5.11 lbs. per ft. Fig. 7.15

The fabrication of the strands was done at Wire Rope Industries
plant at Lachine, Quebec. The strands were spun in two operations, the
first of which consisted in laying up the core of 19 wires together with
the intermediate row of 15 wire, all in the same direction. In the second
operation, this assembly of 34 wires became the core onto which, but in
opposite direction, were laid the 21 outer wires. Linseed oil was used
as a lubricant to preserve the galvanizing.

The suspender rope was fabricated in the same manner as main cable.
It was built up of six 43-wire strands laid around an independent-wire-
rope center of seven strands of seven wires each. Six sizes of wire were
involved, the total number of wires being 307. The nominal diameter of
the galvanized rope was 2.183 in. and the weight was 7.84 lbs. per ft.

10.4 Cable Strand and Suspender Rope Prestressing

In the cable of a suspension bridge it is important that the tensile
stress should be as nearly uniform as possible over the whole cross section,

since any departure from such uniformity means that certain of the component wires or strands are receiving more than their share of the load. In the case of a parallel-wire cable, even stress-distribution is assured by the uniformity of the wire material, which is attained by careful manufacture and strict inspection; and by the method of erection, whereby the individual wires are all assembled to a common sag. With a stranded cable as in the present case, two further considerations are involved. It is desirable in the first place, that the component wires of any one strand shall share the strand-load equally; and secondly, that the strands themselves shall posses uniform elastic properties in order to participate equally in the cable-tension.

The first of these requirements depends upon the design and fabrication of the strand, and the degree of its achievement may be demonstrated by tests to destruction. In an ideal strand all the component wires would fail simultaneously, but, owing to the slight additional stress in some of those wires due to their helical shape, the "efficiency" of the strand can never attain to the ideal value of unity.

The second requirement is obtained by pre-stressing the strands before their assembly into the bridge-cable. Although during fabrication the wires are laid into the strand under considerable tension, further consolidation of the assembly is needed in order to obviate the gradual lengthening, of uncertain amount, that ordinarily occurs when a wire rope is first put into service. The process of pre-stressing consists in the subjection of each strand to considerable tension, and maintaining that tension until such time as stretching has ceased or has become negligible, the effect upon the strand being to increase its modulus of elasticity

from a comparatively low figure which varies somewhat for different
strands, to a higher and much more uniform value. While the strand is thus
unrealed it is the practice to reduce the tension to a figure approximately
to the normal dead-load tension, when it is accurately measured and marked
for cutting and socketing.

The pre-stressing process provides an opportunity for inspection of
the strand; and it also demonstrates its capacity to support greater loads
than what is actually required.

The specification regarding pre-stressing and measurement of the
strand is as follows:

"Each strand shall be finished to a length in excess
of the final length of the strand in place, and then
pre-stressed to a tension of at least one-half of the
specified ultimate strength of the strand (i.e. to
150,000 pounds) and held at this tension until stretch-
ing has ceased, but in no case for less than 30 minutes.
The tension shall then be decreased to about 96,000
pounds at which load the strand shall be measured and
the necessary reference points established for use
during erection. The marking tension shall be maintained
while a suitable mark is painted along the strand as a
tell-tale in case of subsequent twisting. Tests for
modulus of elasticity shall be made on long lengths of
all strands during the pre-stressing process. No depart-
ure from the specified pre-stressing procedure will be
permitted without prior written approved by the Engineer."

The pre-stressing was also done at Wire Rope Industries plant at Lachine, Quebec. Sufficient space was not available for the full length of the main cable in this manner, and permission was granted by the engineers to lay each strand out in 900 ft. sections which were in turn unrolled, prestressed, and reeled in again.

All pre-stressing and marking was done at night, commencing some time after sunset to ensure that uniform temperature obtained throughout the strand. The thermometers were laid against the strand, approximately at the quarter points, and the mean of their readings was taken as the temperature of the strand. All the pre-stressing of the cable strands was done in June, 1969.

The pre-stressing procedure of suspender rope was substantially the same as for the strands, the main difference being in the length of pre-stressing period. The specified minimum for this was two hours. The modulus of elasticity initially an uncertain quantity was uniform after pre-stressing, being 18×10^{6} psi.

CHAPTER 11

CONSTRUCTION

11.1 Construction of Substructure

The construction of the substructure was carried out by Robert McAlpine Ltd., Halifax. This 2.7 million dollars bridge substructure contract including piers, abutments and cable anchorages was started in June, 1967.

The construction of cable anchorages began with the heel block, which took the form of an open cell caisson with its outer walls poured directly in contact with undisturbed ground. Placing of the concrete walls and base slab was done before the middle well of the caisson was filled. The two outer wells, which were shaped to accommodate the splayed anchorage steelwork, remained open to receive the steel at a later date. After the mass concrete, at the base of both wings had been placed, the cable anchorage steel was positioned in the outer walls, and incorporated into the pier inside the wedge-shaped concrete mass. The junction of this concrete with earlier pours was reinforced, in common with all other important bonding planes, by heavy dowels. The anchorage remained in its unfinished state, with the cable chambers exposed, until the cable assembly was sufficiently advanced to admit of the placing of concrete behind the anchor buttons, followed by the roof slab and the stairway treads.

During the forming of the anchorages, the main tower piers were being constructed simultaneously. While the caissons were being prepared, the rock at the pier site was excavated, 2 ft. below rock surface, to make

a level landing. At Dartmouth pier, the rock was drilled and blasted from floating equipment, the broken material removed by dipper-dredge, and the bearing-area then cleaned and trimmed by divers.

The main pier work was a fairly straight forward task of cofferdamming with sheet piling and tremie pouring the pier down to bedrock. Fig. 11.1. Three military style landing crafts were used to deliver the pre-mixed concrete out to the mid-channel pour area on the Dartmouth side. Each craft carried four 2-cu-yd. buckets shuttling back and forth from shore-based batching trucks. The tremie placement at a rate of 60 cu. yd. per hr. was hit. It took about 5 days to complete the 5,000 cu. yd.of tremie concrete pouring at the main pier.

For the Dartmouth cable-bent base which was closer to shore, "Belt-crete" conveyors were employed. The pre-mixed concrete was carried across the water to reach the pour site.

The concrete shafts of the portal frame piers were erected at both approach spans during the casting of anchorages and main piers. Fig. 11.2. Since most of the shafts were identical in size, steel shuttering was widely used. Fig. 11.3

The piers cross beams, with the same shuttering, were generally shaped by special self-supporting Delta steel forms that bridged between the completed columns.

The tower pier at Halifax side was erected in dry conditions, where access was available by a construction dike. Fig. 11.4

About 93% of the substructure was completed by the end of August, 1968.

The remaining work such as the completion of the front walls and roofs of the cable anchorages had to be built after the completion of the main span.

11.2 Construction of Main Towers and Cable Bent

After the bearing surfaces of the concrete piers were carefully dressed to be flat and level, heavy canvas sheets approximately 1/8 in. thick and saturated with red lead paint were then laid over the bearing areas and the bases of the towers erected in place thereon. The nuts on the anchor bolts were then tightened down with 50 kips per bolt to pre-load the anchor bolts.

Each cruciform column of the towers was made up of a constant rectangular steel section 8 ft. by 4 ft. and two tapered wings on either side of the 8 ft. length. All sections were welded from plate with internal T shaped stiffeners. The wing sections consisted of only three plate in a U shape with continuous narrow flanges welded to the free edges to facilitate bolted assembly in the field.

After the base and 2 sections of the tower were in position, a creeper consisting of a structural framework built to embrace the two tower columns, and on which was erected a steel stiff-leg derrick. The derrick had a capacity of 40 tons at a radius of 50 ft. enabling loads to be picked up from scows moored alongside the pier.

The entire creeper-assembly was capable of being jumped up the tower by lifting-tackle attached to the tops of the columns at each stage of their erection, and was guided by sliding-devices attached to those columns. The width of the creeper was adjusted at each move in accor-

dance with the decreasing size of tower. In its highest position, hung from the last splice-point, the creeper erected the top sections of the columns and bracing, and the top strut. Fig. 11.5.

Low level erection of the tower was done by ground-based mobile cranes of barge-mounted booms. Fig. 11.6. After 9 weeks' work, the Halifax tower was topped off, the Canadian Bridge crews started to repeat the performance on the Dartmouth tower.

The cable-bents were erected first, the base plate set on canvas sooked with red lead on the dressed central areas of the pedestals and fully grouted as soon as the columns had been made plumb. The 3 ft. by 5 ft. rectangular box sections were shop welded and assembled on site. The construction procedure was similar to that of the main towers.

11.3 Approach Spans

By the time of stripping the last forms of the portal frame piers, the steel box girders and floor beams of both approach span had been delivered to the site. The box girders were shop welded and the double lines of Nelson studs were also welded to the top flanged of the girders. Fig. 11.7. Erection of the approach spans was started in May, 1968, and by the end of the same year the Dartmouth approach had been erected. The construction of Halifax approach span was slightly slow and all the steel work was furnished in the early spring of 1969. Fig. 11.8

Once the box girders and floor beams were in position, the placing of $8\frac{1}{2}$ in. reinforced concrete slab was immediately followed. After the $1\frac{1}{2}$ in. asphalt wearing surface was paved, it gave a total of 10 in. thick deck. The entire approach span on both sides were completed in fall of 1969.

11.4 Catwalks, Main Cables, Cable Bands, Suspender Ropes, and Sockets

11.4.1 Catwalks

The strand of catwalks for erection was the first of the bridge to link the two cities. The advantages in using of catwalks were that: they provided continuous access to all points of the cable and permitted detailed inspection. It could increase safety during the erection of the deck span.

The two catwalks extended for full length of the cables, being slung at elevation around three feet below those of the first cable-strands to be erected. Each was supported by 2 pre-stressed cable-strands, one under each side of the timber deck, the strands being hung from temporary brackets riveted to the steelwork at a convenient distance below the cable-saddles proper.

The strands for each catwalk were mounted on individual reels on a scow that was towed across the Narrows. The outer ends of the strands had been secured to one anchorage while the scow unrealed and laid the strands on the bottom of the riverbed. Upon arrival of the scow at the other shore, the strands were connected to the other anchorage and hoisted onto the temporary saddles.

The catwalks were formed of 2 by 10 planks to lie above the 4 by 8 struts which were tied to the 2 supporting-strands. Fig. 11.9. The handrail-posts of the 6 ft. wide catwalk were braced in two directions and the railing consisted of 5/8 in. wire-rope, bolted to every post. The catwalk-anchorage consisted of two long $3\frac{1}{2}$ in. rods set into the anchor-pier and connecting to two pairs of long 3 in. bolts. The sockets of the

strands in turn consisted with those bolts and were at first place as close to anchorage as the assembly permitted.

11.4.2 Main Cables

The 122 cable-strands, each on an individual wooden reel were shipped from Montreal to Halifax. For cable-erection, each reel in turn was fitted with a shaft and mounted on bearings behind and above the appropriate cable-anchor cavity. Fig. 11.10. Its outer socket was then hauled over the catwalk with a 5/8 in. line by means of a hoisting-engine established on the other anchorage-pier. At the tops of the tower, hardwood blocks were placed to receive the heavy pressure of the moving strands and to preserve the galvanizing, and wooden rubbing-stripe were provided wherever there was any possibility of the strands coming into contact with bolt-heads or other steelwork.

Upon the arrival of the leading socket at the other end of the cat-walk it was disconnected from the skid. The two sockets were then attached to the appropriate anchorage-buttons by the adjustable anchor-bolts. Fig. 11.11. The next step was to pick up the strand from the catwalk and lay it into the saddles. Great care was exercised to avoid damage to the strand by scraping the galvanizing or by abrupt bending.

The strands of each cable were arranged in nine horizontal layers, the lowest of which took its bearing directly onto the fluted invert of the saddle while the strands of other layer rest directly above the lower one. The lower half of the cable, including the bottom and adjacent four layers, is confined laterally by the sides of the saddle. Fig. 11.12. The remaining four upper layers are rendered stable by the strands of

each layer bedding into the hollows between the strands of the layer below, and they are further prevented from lateral movement by the cover slab. Fig. 11.13.

After the superstructure was completed, the main cables were rounded out with wooden filler blocks and then wrapped with galvanized wire to provide weather protection. Fig. 7.15

11.4.3 Cable Bands

The cable-bands were brought to the site in scows and delivered alongside the main piers, the two parts of each band having been previously bolted together. The bands were lifted to the tops of the towers and were distributed along the catwalk. The bands were positioned by reference to the painted works on the two outer strands of each cable, and were assembled onto the cable by hand. Fig. 11.14. The two halves of the saddle-groove were carefully aligned to prevent damage to the suspender-ropes, and the bolts were then tightened.

During the subsequent erection of the suspended structure, the increasing load on the cables caused then to decrease in diameter, owing to compaction of the 61-strand assembly. On this account, and to prevent slipping, the bolts were retightened to their original tension during the progress of the work. When all the dead loads were in place, a third and final tightening was carried out, under careful inspection.

After the cable-wrapping had been applied, the space at the upper junction of the two halves of each band was filled with oakum and then calked with lead wool. Small openings were left in the underside-caulking

of bands to permit the free drainage of any moisture that might accumulate inside the cables.

11.4.4 Suspender ropes and Sockets

The suspender-ropes were delivered alongside the main piers, hoisted to the tower-tops, and then assembled by hand. Fig. 11.15. Care was taken to place the marked center point of each rope exactly over the joint of the cable-band, and that position was maintained by the small keeper-castings. The sockets were left hanging freely in ready for assembly to the trusses.

Immediately before connection to the stiffening-truss, the suspender-sockets were rotated as required in order to bring the tell-tale paint-marks into alignment, and thus to ensure the correctness of the suspender-length. The galvanized ladder-rungs were assembled after the suspenders had received the greater part of their dead load. They were clinched onto the ropes by hand, with copper-headed hammers. The annular depression at the top of each socket was filled with a non-hardening putty (Tremco) to prevent the accumulation of moisture.

11.5 Orthotropic Deck Panels

The deck panels consisted of orthotropic deck plates, floor-beam trusses, stiffening trusses and bottom laterals. Deck erection commenced on the site by Canadian Bridge's crews in late July 1969.

The 44 preassembled panels in the main span were hoisted by means of twin high lines and a transverse lifting strut. On the side span, this technique was not applicable, because of access difficulties. However, each element was lifted in place and assembled in mid-air by the stiff-

leg derricks working from each cable-bent towards the main towers.

A special lifting beam was tightly bolted to each side of the completed deck panel.[17] This attachement carried the panel's load to a central lifting point at the centre of gravity where a lifting fall was attached to each side during erection. Two full sets of lifting-beam tackles were employed on the site such that while one was in use, crews might be ready in the next panel for lifting. As soon as the barge floated clear, the tugs towed it back to dockside so that another panel could be assembled on it.

The actual lifting was done by the twin 1-1/8 in. diameter falls which were controlled by a 2-drum synchronized hoist on the Halifax shore. It took 17 minutes for the 170 ft. vertical lift from the barge to the deck elevation. Fig. 11.16. Once the panel was in position, one end was loosely bolted to the adjoining panel already hanging in place while the other end was pinned to its suspension hanger on each side. Fig. 11.17

Travel of the strut back and forth, as well as up and down was guided by two high-lines - 1-7/8 in. diameter which were controlled by a 3-drum hoist near the Halifax cable bent. These high-lines, each with a capacity of 12 tons were strung across the Narrows on the same alignment, but well above the main suspension cables.

Upon the stringing of the main cables, erection of the bridge deck was started at the centre of the main span and progressed towards the towers. After the erection of about 1/10 of the main span, deck erection of both side spans was commenced at the cable bents and proceeded towards the towers simultaneously with the main span. This erection procedure

greatly reduced the hazard of over load in the main span portion without a counterbalancing load on the side spans.

Bolting of each deck panel following a lift was fairly loose so that joints might hinge and the desired parabolic vertical curvature in the completed deck be attained under the force of gravity. Final bolting of the bottom chord members, thereby forming a continuously stiffening deck truss, was done once the sag profile during erection coincided closely with the desired final geometry, which was when about 80% of the main span was erected. Fig 11.18. As soon as all the deck panels in place, access was available.

The verticality of the towers and the cable bents before and during erection was closely watched. To keep pace with the ever-changing leaning in both, the cable saddles atop each were offset shoreward 19 in. and those atop the cable bents moved a proportionately smaller distance. By the time nine panels were hung in place, deflecting the towers under the weight, the saddles were jacked back to be center atop the towers where they were bolted to prevent future movement. Once 30 panels were in place, the final jacking of the cable bent saddles took place.

11.6 Epoxy Asphalt Wearing Surface Paving

Concresive epoxy asphalt is a highly specialized product that differs entirely from conventional hot-mix asphalt. In order to obtain the best possible surface, the temperature conditions are the most crucial aspect and an ambient temperature of at least $50^{\circ}F$, with low humidity, was imperative during placement operations. This stipulation had already forced a postponement of the paving program from fall of 1969 to July, 1970, since

the steel deck erection phases were completed only after the cool temperature of autumn prevailed over the Halifax area.

The completed deck pavement is 52 ft. 6 in. in width and was laid in two 1 in. thick courses (i.e. a levelling course and a surface course). Successive passes were from 11 to $14\frac{1}{2}$ ft. wide atop sandblasted steel coated with an inorganic zinc primer. After all paint had dried for at least 24 hours, the area to be paced was washed with a detergent solution of 1% Triton in clean water to remove all oil and grease, zinc oxides, and any loose zinc paint. Finally, a bond coat was applied to the steel deck, to the surface of levelling course and to the pavement joints.

Sandblasting and priming, (a part of the deck was done in 1969), began during the warming days of spring 1970. Fig. 11.19. The first two week of June were designated as the time during which placement of the required 1,485 tons would proceed. Despite having showers throughout much of this period, thereby upsetting critical batching cycles, the paving crews sucessfully completed the project. Fig. 11.20.
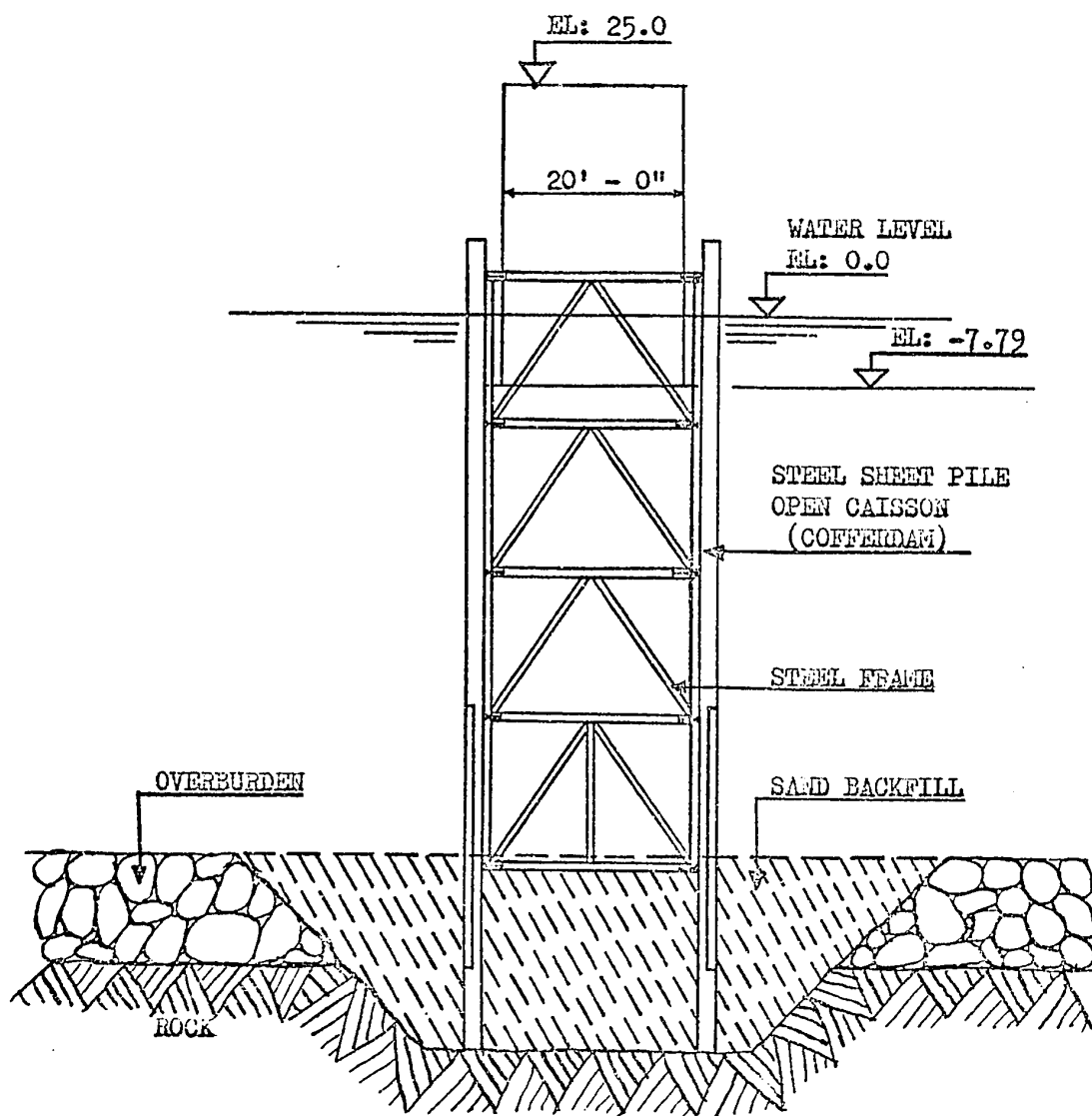
FIG. 11.1 CONSTRUCTION OF DARTMOUTH MAIN PIER

FIG. 11.2 ERECTION OF ANCHORAGE PIER
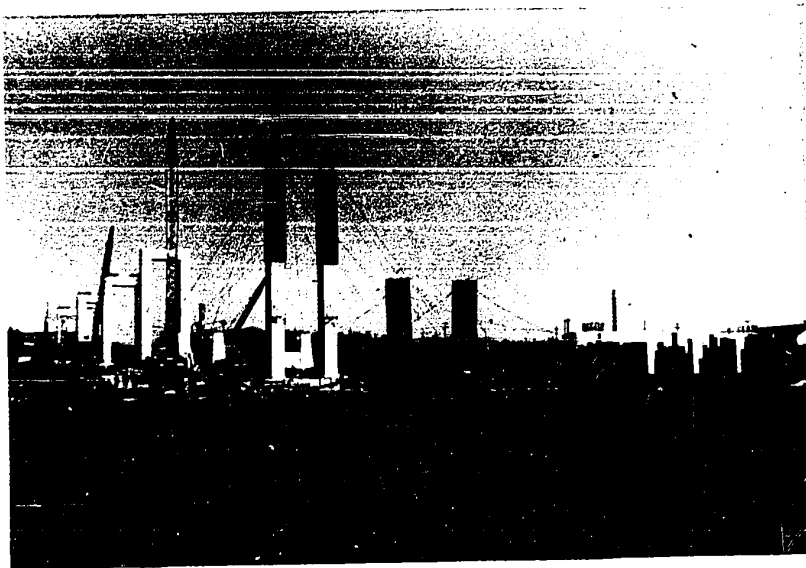
FIG. 11.3 PORTAL FRAME PIERS AT DARTMOUTH APPROACH
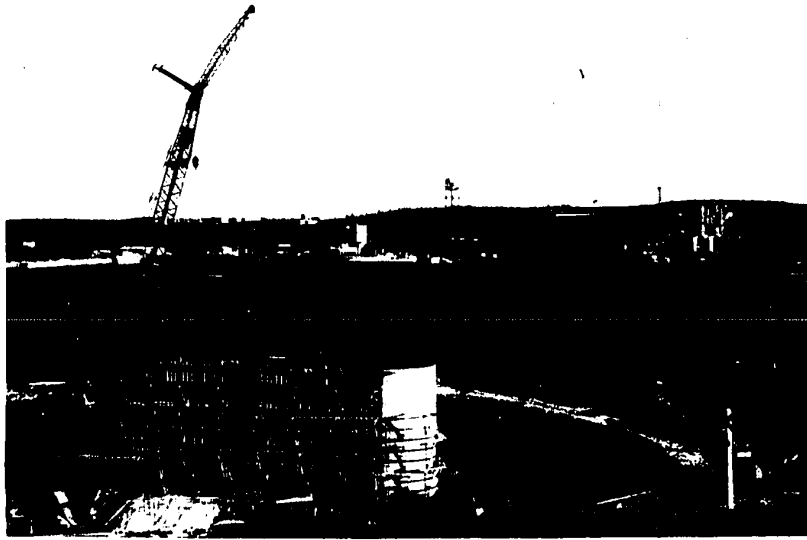
FIG. 11.4 HALIFAX MAIN TOWER PIER UNDER CONSTRUCTION IN DRY CONDITION

FIG. 11.5 ERECTION OF HALIFAX TOWER

FIG. 11.6 INSTALLATION OF BASE SECTION OF DARTMOUTH TOWER

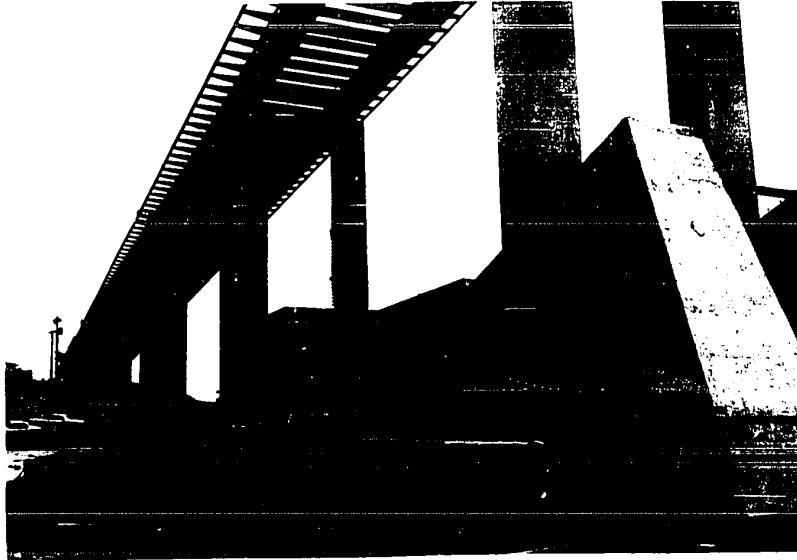FIG. 11.7 BOX GIRDERS AT DARTMOUTH APPROACH SPAN

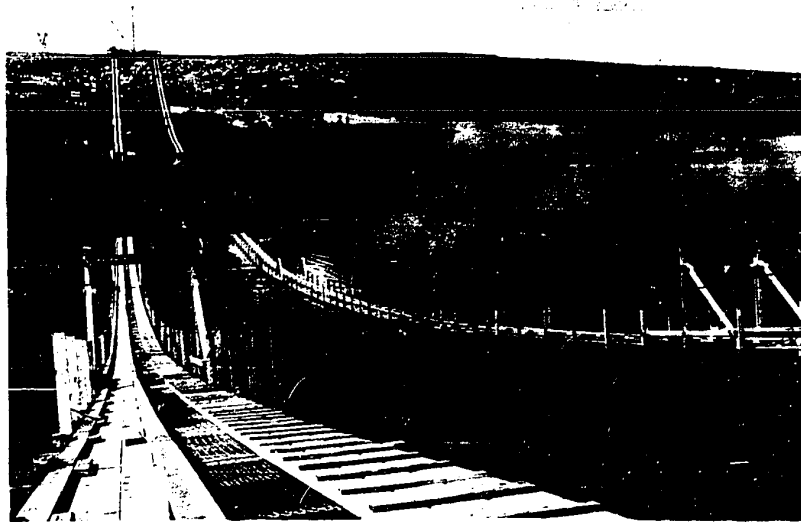FIG. 11.8 ANCHORAGE AND APPROACH SPAN AT HALIFAX SIDE
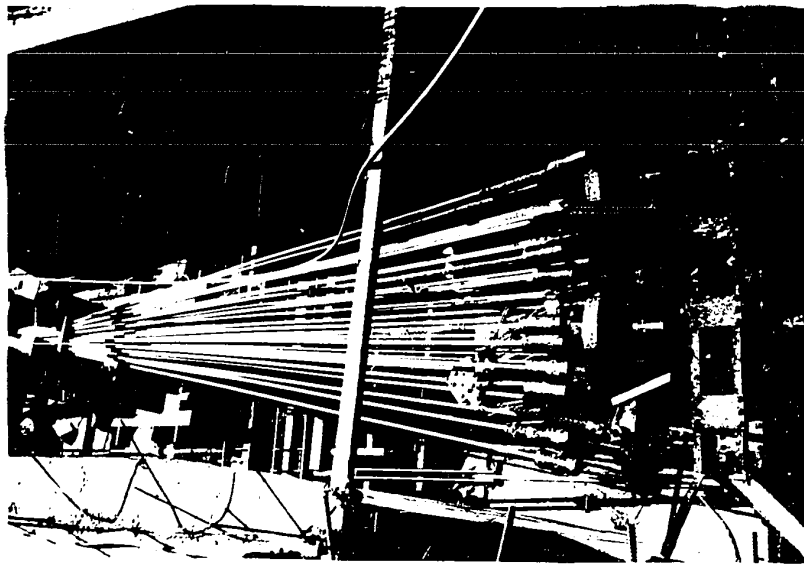

FIG. 11.9 ERECTION OF CATWALKS

FIG. 11.10 STEEL ANCHORS INSIDE THE CHAMBER OF ANCHORAGE

FIG. 11.11 MAIN CABLE STRANDS SOCKETED TO STEEL BUTTONS

FIG. 11.12 FIRST LAYER OF MAIN CABLE CROSS THE TOWER-SADDLE

FIG. 11.13 PLACING OF SADDLE-LID AT CABLE BENT
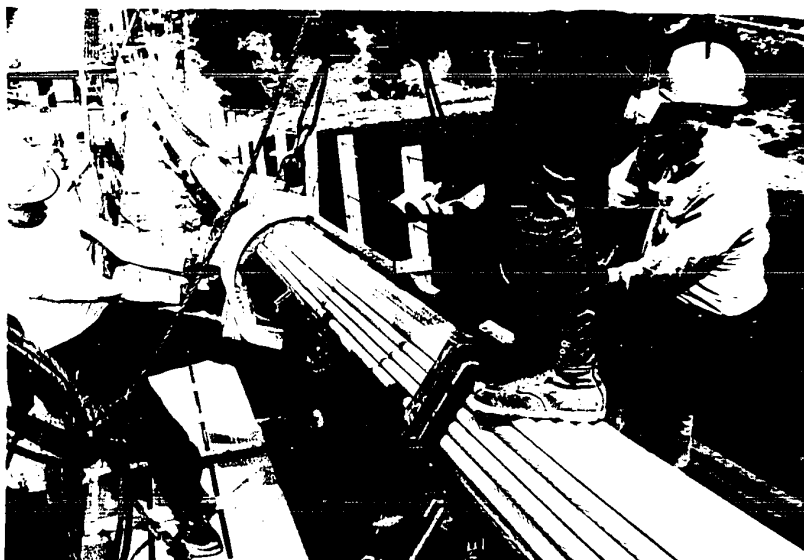
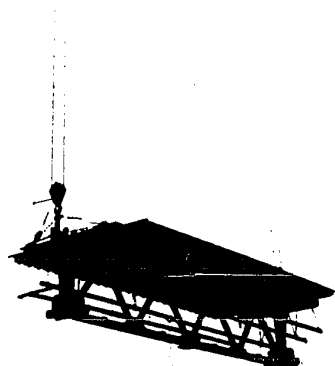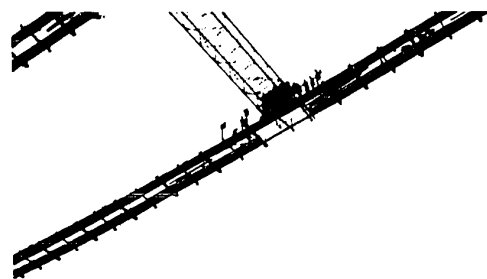FIG. 11.14 INSTALLATION CABLE BANDS AT MARKED LOCATION
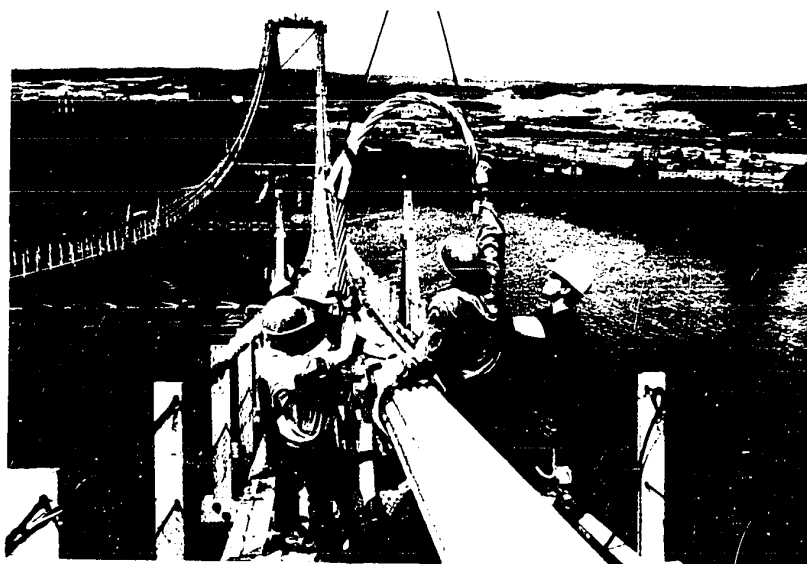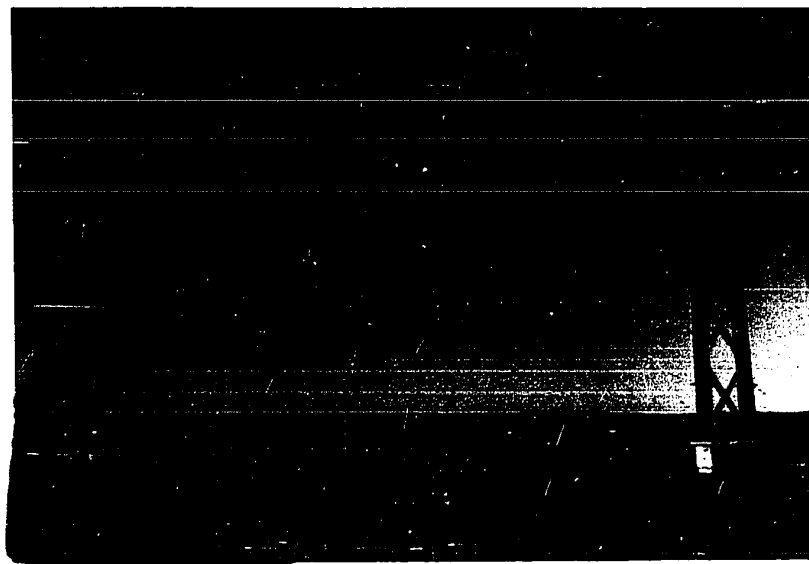

FIG. 11.15 ERECTION OF SUSPENDER ROPE

— A —

— B —

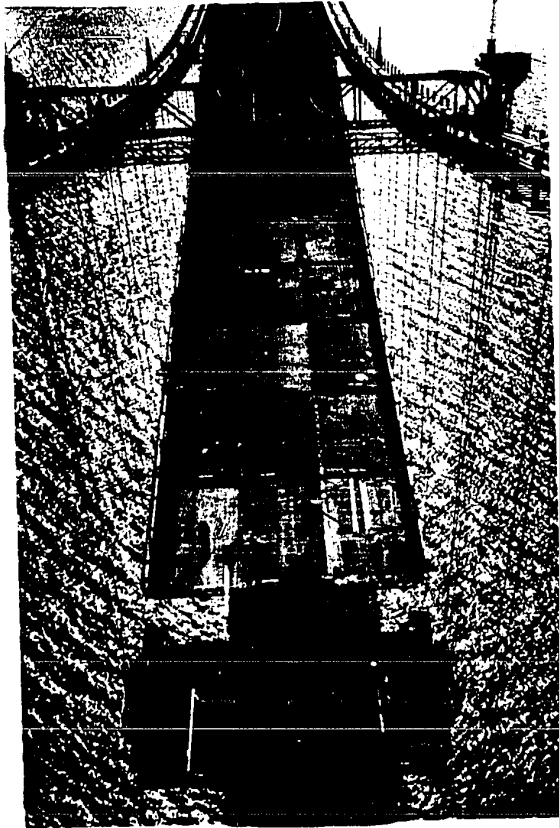FIG. 11.16 LIFTING THE PREASSEMBLED PANEL OF DECK AND TRUSS

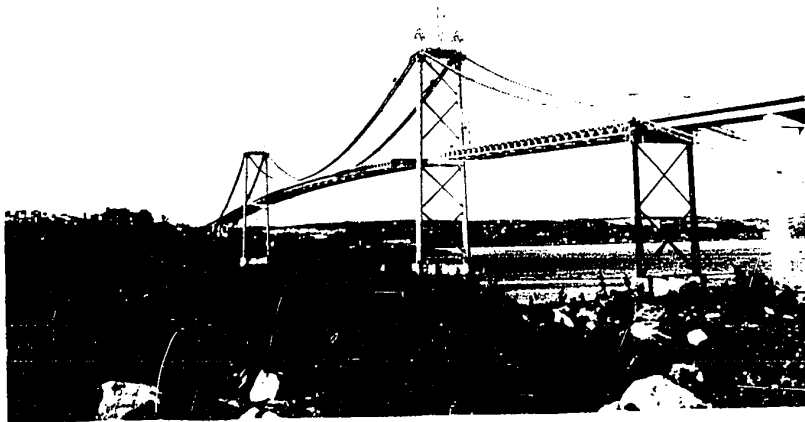FIG. 11.17 ASSEMBLY OF THE DECK

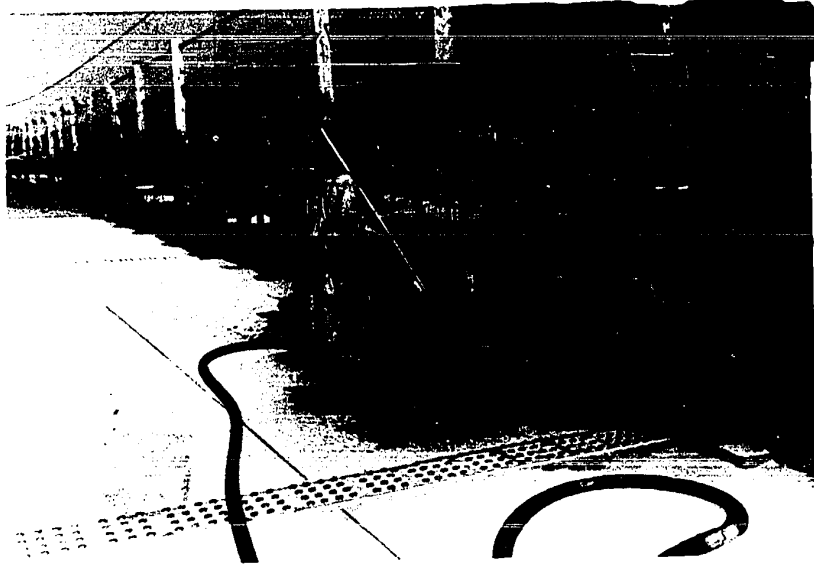FIG. 11.18 NEARLY COMPLETE OF THE SUPERSTRUCTURE

FIG. 11.19 SANDBLASTING BEFORE THE PAVEMENT OF EPOXY ASPHALT WEARING SURFACE

FIG. 11.20 THE COMPLETE VIEW OF THE A. MURRAY MACKAY BRIDGE

CHAPTER 12

COST AND WEIGHT

12.1 Final Cost and Weight

The cost of the whole project was $32,873,000 which included the construction of the bridge and approach roads in both cities. The cost of the substructure contract was $2,741,771 awarded to Robert McAlpine Ltd., Halifax. The construction of the substructure included cable anchorages, main piers, portal frame piers and abutments at approach spans. The cost of the superstructure contract was $8,394,552 awarded to Canadian Bridge Division of Hawker Industries Ltd. This contract included the construction of the orthotropic deck, main cables towers, steel works of the main and approach spans with concrete pavement. The 2 in. epoxy asphalt pavement on the orthotropic deck cost $323,815 and was applied by Adhesive Engineering Company, San Carlos, California, U.S.A.

The total cost of this suspension bridge with electrical contract is $11,988,334 while approach roads at each side share the rest of $32.9 million. The average cost for the suspension bridge is about $80 per sq. ft. of roadway surface. The steel weight in detail is shown in Table 12.1.

The whole project took 3 years to finish and involved more than 600 design, supervisory, and construction staff.

12.2 Conclusion

The development of orthotropic plate bridge decks is one of the most outstanding advances in bridge design and construction in recent

years. The use of an orthotropic steel deck gives a major reduction in weight by elimination of the usual heavy concrete slab. This reduces the size of the cable and anchorage. Since the dead load is significantly less, the steel required in the towers reduce to a minimum. Preliminary design studies indicated a saving in cost of 15% for the orthotropic deck type compared to the standard type with a concrete deck.

The usual stiffening truss depth for a bridge of this span would be 14 ft., but with the orthotropic deck acting with the trusses in bending the same stiffness was obtained with a truss depth of only 9 ft. 6 in., giving a more slender appearance. The orthotropic deck acts like a top lateral system in combination with the stiffening trusses and bottom laterals to form a box system of high torsional stiffness. The high torsional stiffness provided by the steel deck reduces the twisting of the deck due to live loading on one side of the bridge only, and also gives favourable aerodynamic characteristics by raising the natural frequency of vertical oscillation.

The orthotropic deck with closed ribs is more advantageous than open rib. Some preliminary studies in other bridges indicated that the critical stresses in orthotropic plates with open ribs are approximately 20 to 30% lower than those in orthotropic plate with closed ribs of equal cross-sectional area and moment of inertia. In most cases the use of closed ribs reduces the rib thickness by approximately 1/8 in. if rib length is maintained.

It is apparent that the development of the orthotropic deck is better than the other conventional bridge design, providing outstanding

advance in design and construction in the future.

Although this new technique is still subjected to intensive research, at this stage, it shows promise.

Generally, the design procedure has not been completely codified, so careful judgement is required in interpreting the results and establishing criteria of design.

TABLE 12.1 FINAL STEEL QUANTITIES OF THE BRIDGE

Main Span		Approach Span	
Item	Weight Tons	Item	Weight Tons
Main Towers	1687	Box Girders	1187
Cable Bents	222	Floor Beams	407
Stiffening Trusses	1352	Fascia Beams	47
Bottom Laterials	126	Traveller Beams	51
Floor Trusses	721	Catwalk	29
Orthotropic Deck	2260	Fence	63
Fence Curbs	177	Miscellaneous	24
Expansion Joints	23		
Cable Anchorage Anchors, Buttons Etc.	127		
Cable Saddles	50		
Cable, Suspenders, Bands	1283		
Erection	6		
Total	8034	Total	1808

BIBLIOGRAPHY

1. "A Policy on Geometric Design of Rural Highways", American Association of State Highway Officials, Washington, 1965.

2. Au, Tung, and Chang, Jerry C.L., "Fundamentals of Orthotropic Plate Design", Proceedings of the Conference on Orthotropic Plate Design and Construction, Pittsburgh, P.A. U.S.A., 1963

3. Troitsky, M.S., "Orthotropic Bridges Theory and Design", The James F. Lincoln Arc Welding Foundation, Ohio, 1968.

4. "Design Manual for Orthotropic Steel Plate Deck Bridges", American Institute of Steel Construction, New York, 1963.

5. Dorton, R.A., "Design of the Narrows Suspension Bridge, Halifax", The Engineering Journal, Engineering Institute of Canada, Vol. 51, pp 15-26, Dec. 1963.

6. Milek, W.A. Jr., "A.I.S.C. Orthotropic Plate Design Manual", Proceeding of the Conference on Orthotropic Plate Design and Construction, Pittsburgh, P.A. U.S.A. 1963

7. Tsien, Ling-Hi, "A Simplified Method of Analyzing Suspension Bridges", Transactions ASCE, Vol. 114, 1949.

8. "Aerodynamic stability of Suspension Bridges", Advisory Board on the Investigation of Suspension Bridges, Transactions ASCE, Vol. 120, 1955.

9. Bleich, F., "Dynamic Instability of Truss-Stiffened Suspension Bridge Under Wind Action", Transaction ASCE, Vol. 114, 1949.

10. Selberg, A., "Oscillation and Aerodynamic Stability of Suspension Bridges", Acta Polytechnica Scandinavia, Civil Engineering and Building Construction, Series No. 13, Trondheim, Norway, 1961.

11. Selberg, A., and Hjorth-Hansen, E., "Aerodynamic Stability and Related Aspects of Suspension Bridges", Proceeding of the International Symposium on Suspension Bridges, Lisbon, 1966.

12. Selberg, A., "Dampening Effect in Suspension Bridges", Publications of the International Association for Bridges and Structural Engineering, Vol. 10, Zurich, 1950.

13. Steinman, D.B., "Modes and Natural Frequencies of Suspension Bridge Oscillations", The Engineering Journal, Engineering Institute of Canada, Vol. 3, No. 2, pp 74-83, July 1959.

14. Frandsen, A. G., "Wind Stability of Suspension Bridges, Application of the Theory of Thin Airfoils", Proceedings of the International Symposium on Suspension Bridges, Lisbon, 1966.

15. Hirai, A., and Okubo, T., "On the Design Criteria Against Wind Effects for Proposed Honshu-Shikoku Bridges", Proceeding of the International Symposium on Suspension Bridges, Lisbon, 1966

16. Davenport, A.G., Isyumov, N., Fader, D.J. and Bowen C.F.P., "A study of Wind Action on A Suspension Bridge During Erection and on Completion: The Narrows Bridge, Halifax, Nova Scotia, Canada.", Research Report, The University of Western Ontario, London, Canada, BLWT-3-69, May 1969.

17. Rooke, W., "Lift Deck Truss Segments for Narrows Suspension Span", Heavy Construction News, Toronto, Canada, Vol. 13, No. 36, pp4-5, Sept. 8, 1969.